THE UNIVERSITY OF
SYDNEY

The vascular-endothelial protein tyrosine phosphatase:

a novel therapeutic target in the tumour vasculature

Shom Goel (B Med Sci, MBBS, FRACP)

- 2014 -

Thesis Title

Vascular-endothelial protein tyrosine phosphatase: a novel therapeutic target in the tumour vasculature

Candidate

Shom Goel (B Med Sci, MBBS, FRACP)

Primary Supervisor

Professor Jennifer Gamble, PhD

Wenkart Chair of the Endothelium

Centre for the Endothelium

Centenary Institute

University of Sydney

Secondary Supervisor

Professor Rakesh K. Jain, PhD

Director, Steele Laboratory for Tumour Biology

Massachusetts General Hospital

Andrew Werk Cook Professor of Tumour Biology

Harvard Medical School

Harvard University

Thesis submitted in fulfillment of the requirements for the Degree of Doctor of Philosophy in the Department of Medicine, The University of Sydney, March 2014.

Table of Contents

Preface

Contributions of the author

The research presented in this thesis is the original work of the author, Dr Shom Goel. The author generated all of the hypotheses presented, and designed all of the experiments. Furthermore, the author, with the following exceptions, performed all the experiments described:

1. The author and Dr Brian P Walcott (Massachusetts General Hospital, Boston MA) jointly conducted the zebrafish embryonic angiogenesis assays.
2. The author and Ms. Nisha Gupta (Massachusetts General Hospital, Boston MA) jointly performed the measurement of endothelial cell nitric oxide production *in vitro* using the 4,5-diaminofluorescein diacetate assay.
3. Histological assessment of murine lung tissue for pulmonary metastases was performed jointly by the author and two trained pathologists (Dr Rekha Samuel and Dr Matija Snuderl, of the Massachusetts General Hospital).
4. Ms Sylvie Roberge, Massachusetts General Hospital, provided technical assistance for the measurement of mouse blood pressure.

Statement of institutional approval

Animal experiments were all performed following the guidelines of Public Health Service Policy on Humane Care of Laboratory Animals and approved by the Institutional Animal Care and Use Committee of the Massachusetts General Hospital (Boston, MA – protocol number 2010-N0000133).

Inclusion of previously published work within this thesis

The concepts and data presented herein have, at the time of writing, largely been published in peer-reviewed scientific journals. Of note, vascular abnormalities within solid tumours and strategies of vascular normalization are comprehensively reviewed in the following publications:

1. Goel S, Duda DG, Xu L, Munn LL, Boucher Y, Fukumura D, Jain RK. Normalization of the vasculature in cancer and other diseases. **Physiological Reviews.** 2011 Jul;91(3):1071-121. [PMID: 21742796]
2. Goel S, Wong AH, Jain RK. Vascular normalization as a therapeutic strategy for malignant and nonmalignant disease. **Cold Spring Harbor Perspectives in Medicine**. 2012 Mar;2(3):a006486. [PMID: 22393532].
3. Goel S, Fukumura D, Jain RK. Normalization of the tumour vasculature through oncogenic inhibition: an emerging paradigm in tumour biology. **Proceedings of the National Academy of Sciences of the United States of America**. 2012 May 1. [PMID: 22550180]
4. Huang Y, Goel S, Duda DG, Fukumura D, Jain R.K. Vascular normalization as an emerging strategy to enhance cancer immunotherapy. **Cancer Research.** 2013 May 15;73(10):2943-8. [PMID 23440326].

In addition, the results of experiments presented within this thesis have been published as follows:

1. Goel S, Gupta N, Walcott B, Snuderl M, Kirkpatrick ND, Heishi T, Huang YH, Kesler CT, Martin JD, Ager E, Samuel R, Wang S, Yazbek J, Vakoc B, Peterson R, Duda DG, Fukumura D, Jain RK. Tie-2 activation by a vascular-endothelial protein tyrosine phosphatase inhibitor normalizes breast cancer vasculature. **Journal of the National Cancer Institute**. 2013 Aug 21;105(16):1188-201 [PMID: 23899555].

These publications are included as Appendices to this thesis.

List of Abbreviations

ABIN2	A20-binding inhibitor of nuclear factor-κB activation 2
Ang-1	Angiopoietin-1
Ang-2	Angiopoietin-2
bFGF	Basic fibroblast growth factor
BSA	Bovine serum albumin
CD31	Cluster of differentiation 31
CD45	Cluster of differentiation 45
DAF-2 DA	4,5-diaminofluorescein diacetate
DLAV	Dorsal longitudinal anastomotic vessel
DMEM	Dulbecco's modified eagle medium
EC	Endothelial cell
EDG1	Endothelial differentiation sphingolipid G-protein–coupled receptor 1
EGFR	Epidermal Growth Factor Receptor
EGM	Endothelial Growth Medium
EMT	Epithelial to mesenchymal transition
eNOS	Endothelial nitric oxide synthase
FAK	Focal adhesion kinase
FBS	Foetal bovine serum
GBM	Glioblastoma multiforme
GFP	Green fluorescent protein
GRB2	Growth factor receptor-bound protein 2
HCPTA	Human Cytoplasmic Protein Tyrosine Phosphatase
HEK	Human embryonic kidney
HER2	Human epidermal growth factor receptor-2
HIF-1a	Hypoxia-inducible factor 1-alpha
HMVEC	Human microvascular endothelial cell
Hpf	Hours post-fertilization
HPTP-epsilon	Human protein tyrosine phosphatase-epsilon
HUVEC	Human umbilical vein endothelial cell
ICAM-1	Intercellular adhesion molecule-1
IFN-beta	Interferon-beta
IFP	Interstitial fluid pressure
iNOS	Inducible nitric oxide synthase
ISV	Intersegmental vessel
IV	Intravenous
L-NMMA	N^G-Monomethyl-L-arginine
MKP1	mitogen-activated protein kinase phosphatase-1
MMP	Matrix metalloproteinase
nNOS	Neuronal nitric oxide synthase
NO	Nitric oxide
NRP1	Neuropilin-1
OFDI	Optical frequency domain imaging

PBS	Phosphate buffered saline
PDGF	Platelet derived growth factor
PDGFR	Platelet derived growth factor receptor
PHD2	Prolyl hydroxylase 2
PI3K	Phosphatidylinositol-4,5-bisphosphate 3-**kinase**
PlGF	Placental growth factor
PRL-3	Phosphatase of regenerating liver-3
PTP-mu	Protein tyrosine phosphatase-mu
PTP1B	Protein tyrosine phosphatase 1B
PTPRB	Protein tyrosine phosphatase, receptor type, B
PVC	Perivascular cell
RIPA	Radioimmunoprecipitation assay buffer
RT-PCR	Real-time polymerase chain reaction
S1P1	Sphingosine-1-phosphate-1
SEMA3A	Semaphorin 3A
sFlt1	Soluble vascular endothelial growth factor receptor 1
Shp1	Src homology region 2 domain-containing phosphatase-1
Shp2	Src homology region 2 domain-containing phosphatase-2
TBS	Tris buffered saline
TBST	Tris buffered saline with tween 20
TGF-beta	Transforming growth factor beta
TSP-1	Thrombospondin 1
VCAM-1	Vascular cell adhesion molecule 1
VE-Cadherin	Vascular endothelial cadherin
VE-PTP	Vascular endothelial protein tyrosine phosphatase
VEGF/VEGF-A	Vascular endothelial growth factor
VEGFR1	Vascular endothelial growth factor receptor 1
VEGFR2	Vascular endothelial growth factor receptor 2
VPF	Vascular permeability factor
VVO	Vesiculo-vacuolar organelle

Abstract

Background: The microvasculature of solid tumours is characterized by profound structural and functional abnormality, which mediates several deleterious aspects of tumour behavior. As such, the development of therapeutic strategies to mitigate vascular dysfunction within tumours is an important goal. The Vascular Endothelial Protein Tyrosine Phosphatase (VE-PTP) attenuates the activity of the endothelial cell (EC) Tie-2 receptor tyrosine kinase, a key mediator of vessel maturation. In this study, I aimed to determine the effects of pharmacological VE-PTP inhibition on EC Tie-2 receptor activation and the resultant impact on breast cancer angiogenesis, progression, metastasis and treatment.

Methods: AKB-9778 is a first-in-class VE-PTP inhibitor. I examined its effects on ECs *in vitro* and on embryonic angiogenesis *in vivo* using zebrafish assays. The impact of AKB-9778 therapy on the solid tumour vasculature was studied using orthotopic models of primary murine mammary carcinoma as well as both spontaneous and experimental models of metastasis. Finally, I used endothelial nitric oxide synthase (eNOS) deficient mice to establish the causal role of eNOS in mediating the effects of VE-PTP inhibition.

Results: AKB-9778 induced ligand-independent Tie-2 activation in ECs and impaired embryonic zebrafish angiogenesis. In mouse models of breast cancer, AKB-9778 (i) delayed the early phase of tumour growth by enforcing vascular maturity; (ii) slowed progression of micrometastases by preventing extravasation

of tumour cells into distant organs (prolonging survival); and (iii) stabilized established primary tumour vessels, enhancing tumour blood perfusion and radiation response. The effects of AKB-9778 on tumour vessels were mediated in part by eNOS activation.

Conclusions: The results demonstrate that pharmacological VE-PTP inhibition can normalize the structure and function of tumour vessels through Tie-2 activation. This vascular normalization delays tumour growth and metastasis, and enhances response to concomitant cytotoxic treatments.

1 Chapter One: Introduction

1.1 Introduction

The establishment of a mature, organized vascular network is fundamental for tissue homeostasis. Therefore, creation of new blood vessels, *angiogenesis*, plays a critical role in health and development. Angiogenesis is vital for successful embryogenesis and organ growth, and is also an important requirement for wound healing and tissue repair. In such situations, angiogenesis is a tightly regulated process, as its onset and offset are carefully controlled by a host of molecular and mechanical factors (Jain, 2003, Dvorak, 1986). This strict regulation results in a tissue-specific, structured, hierarchically organized vascular tree that is optimally positioned to meet the needs of the organ and of the body.

In contrast, many human diseases are associated with vascular dysfunction of some sort. When Celsus described the four cardinal features of inflammation – *tumour, rubor, calor, dolor* – in the First Century AD, he provided the first report of the phenotype associated with the microvascular dilation and hyperpermeability that is classical of several inflammatory diseases. In more recent times, increased attention has been given to disorders characterized not only by a dysregulation of vascular function, but also associated with uncontrolled angiogenesis. In such conditions, new blood vessel development occurs in a disorganized fashion (Jain, 2005, Mazzone et al., 2009, Morikawa et al., 2002, Hashizume et al., 2000, Gazit et al., 1997, Nagy et al., 2009). Solid

cancers are the prototypic example of a disease state associated with pathological angiogenesis, which has become a vibrant area of research. Other common and important diseases such as inflammatory disorders and atherosclerosis (Jain et al., 2007, Sidky and Auerbach, 1975, Leibovich et al., 1987, Orlandi et al., 1988, Bo et al., 1992), and more rare conditions such as certain benign tumours and age-related macular degeneration (Carmeliet and Jain, 2000) are other examples of diseases associated with an abnormal vasculature.

The concept that growing tumours have a rich vascular network first arose well over one hundred years ago, through observations by notable scientists such as Virchow (Ferrara, 2002), and was strengthened by the seminal work of Ide (Ide et al., 1939) and later Algire (Algire and Chalkley, 1945) who confirmed the importance of an abundant blood supply to tumour growth. In 1968, the hypothesis that tumours produce a diffusible factor that promotes angiogenesis was put forward (Greenblatt and Shubik, 1968, Ehrmann and Knoth, 1968), forming the foundation for Dr Judah Folkman's seminal paper in 1971 in which he suggested that the identification of key molecular players driving tumour angiogenesis could result in effective strategies to inhibit it, and hence "starve" a tumour to death (Folkman, 1971). Following this, Gullino demonstrated in 1976 that cells in pre-cancerous tissue acquire angiogenic capacity on their way to becoming cancerous, and suggested anti-angiogenesis as a strategy to prevent cancer (Gullino, 1978). Over the last four decades, these findings have spurred a very significant research effort, which has culminated in the introduction of

several anti-angiogenic medications into modern clinical practice. With this success came also very important questions related to the mechanism of action of antiangiogenic agents in patients.

Tumour angiogenesis is not simply the production of an increased number of blood vessels to serve a growing mass. Although the main purpose of tumour angiogenesis can be considered to maintain a cancer's blood supply, the process occurs in an unmitigated fashion and the resultant vessel network is highly abnormal. This stands in contradistinction to wound healing, in which angiogenesis is tightly regulated (Dvorak, 1986, Chung et al., 2010). Indeed, this relentless drive for angiogenesis led Dvorak to elegantly describe tumours as "wounds that do not heal" (Dvorak, 1986). This profoundly aberrant vasculature dramatically alters the tumour microenvironment, and influences heavily the ways in which cancers grow and progress, escape the host's immune system, metastasize, and respond to anticancer therapies.

In order to obtain nutrients for their growth and for dissemination to distant organs, cancer cells engulf existing blood vessels (*vascular co-option*) or form new blood vessels. The latter can take one of three forms: (i) new blood vessel sprouting from existing vessels (*angiogenesis*); (ii) recruitment of bone marrow derived endothelial progenitor cells to form new vessels (*postnatal vasculogenesis*); and (iii) *intussusception*, when a capillary wall extends into the lumen to split a single vessel into two (also known as splitting angiogenesis) (Patan et al., 1996, Carmeliet and Jain, 2000, Baum et al., 2010). Two further emerging mechanisms of vessel formation in tumours include *vasculogenic*

mimicry (the trans-differentiation of cancer cells) and *mosaic vessel formation* (the incorporation of cancer cells into the vessel wall) (Folberg et al., 1993, Ricci-Vitiani et al., 2010, Hammersen et al., 1985). All of these processes are driven by a number of molecular players. Of these, a critical factor is the Vascular Endothelial Growth Factor A (VEGF-A, also known as VEGF). VEGF was first discovered by Dvorak and colleagues as a "Vascular Permeability Factor" (VPF) in 1983 (Senger et al., 1983), and later by Ferrara and colleagues as the angiogenic endothelial mitogen (named VEGF) in 1989 (Leung et al., 1989). At the same time, it was reported that VPF and VEGF were the same molecule (Keck et al., 1989), and that the VEGF Receptor 2 (VEGFR2) (Terman et al., 1992) is the main endothelial cell mediator of VEGF's pro-angiogenic activities (Millauer et al., 1993). Since these landmark discoveries, a catalogue of other molecular players has been established in the process of tumour angiogenesis. The chronic imbalance of the pro- and anti-angiogenic signaling in tumours (ie. an excess of pro-angiogenic signaling, a deficiency of anti-angiogenic signaling, or both) leads to the development of the abnormal tumour vasculature.

1.2 The role of abnormal vasculature in tumour progression and treatment-resistance

1.2.1 The abnormal structure of the tumour vasculature

Overexpression of VEGF and other pro-angiogenic factors leads to formation of a new vasculature that is structurally abnormal at both macroscopic and microscopic levels (Fukumura et al., 2010, Gazit et al., 1997, Jain, 2003, Nagy et

al., 2002, Nagy et al., 2009). These abnormalities are exacerbated as a tumour continues to grow (Gazit et al., 1997). Anatomically, tumour microvessels are dilated, tortuous, and saccular with haphazard patterns of interconnection and branching (Kim et al., 2010, Jain, 2005, Less et al., 1991, Less et al., 1997). Of particular relevance to this thesis, this vessel phenotype has been observed in preclinical models of breast cancer (Tong et al., 2004, Yuan et al., 1996). Unlike the microvasculature of normal tissue, which has an organized and regular branching pattern, tumour vasculature is characterized by pockets of increased vessel density and others of reduced vessel density (Less et al., 1991, Less et al., 1997, Baish et al., 2011, Baish and Jain, 2000). There is also increased vascular shunting within tumours, caused by a loss of vascular diameter control, an increase in vascular reactivity, and a higher tendency for vessel growth (Pries et al., 2009, Pries et al., 2010).

At the cellular level, the endothelial cells (ECs) lining tumour vessels have an irregular, disorganized morphology. Mature, stable ECs are connected by adherens junctions including vascular endothelial-cadherin (VE-Cadherin) (Dejana et al., 2009). VE-Cadherin is a transmembrane receptor, the extracellular domain of which binds to other VE-Cadherin molecules on neighboring ECs. The intracellular domain of VE-Cadherin attaches to the EC cytoskeleton via the catenin family of proteins, acting as structural links but also effectors for downstream molecular signaling (Dejana et al., 2009). Downstream signaling from VEGF-VEGFR2 interactions promotes contraction of the endothelial cell cytoskeleton and weakening of VE-Cadherin junctions, and

hence a loosening of EC associations and EC migration (Dejana et al., 2009). As a consequence, ECs within tumours are often poorly connected or overlapping, with less VE-Cadherin and a branched phenotype with long cytoplasmic projections (Hobbs et al., 1998, Hashizume et al., 2000). At times, ECs might protrude into the capillary lumen, or conversely sprout into the perivascular tumour tissue (Hashizume et al., 2000). There is also an abundance of vesiculo-vacuolar organelles (VVOs) in tumour EC's, which have been associated with vascular permeability, however these do not explain the large gaps in the walls of tumour vessels (Hobbs et al., 1998, Qu et al., 1995).

In addition, perivascular cells (PVCs) – both pericytes and vascular smooth muscle cells – around tumour vessels demonstrate abnormal structural characteristics. These connective tissue cells normally surround and support the endothelium. Pericytes usually lie within the vessel basement membrane, and interact closely with ECs to prevent vessel leakage. They are normally recruited to stabilize vessels and hence envelop ECs in response to activation of a number of molecular pathways: (i) platelet-derived growth factor B (PDGF-B), which is secreted by ECs and facilitates pericyte recruitment to vessels through binding to the platelet-derived growth factor receptor-β (PDGFRβ) on pericytes; (ii) angiopoietin-1 (Ang-1), a vascular stabilizing factor that facilitates pericyte-EC connections; (iii) sphingosine-1-phosphate-1 (S1P1) and endothelial differentiation sphingolipid G-protein–coupled receptor 1 (EDG1); and (iv) transforming growth factor-β (TGF-β) (Jain, 2003).

Dysregulation of these vessel maturation pathways in tumours often results in

vessels with an absent or loose attachment of PVCs (Abramsson et al., 2003, Inai et al., 2004, Jain, 2003, Tong et al., 2004), including those of mammary carcinomas (Morikawa et al., 2002). PVC detachment is an early step in the process of tumour angiogenesis, and facilitates the movement of ECs into the surrounding matrix to form new vessels. Moreover, these PVCs are often abnormal in shape with bizarre cytoplasmic processes, irregularly scattered around the endothelium (Morikawa et al., 2002). The mechanisms for PVC detachment in tumours are multiple, but include a VEGF-mediated disruption of PDGFR-β activity (Greenberg et al., 2008), and overexpression of Ang-2, the endogenous "antagonist" of Ang-1 (Augustin et al., 2009). Moreover, detached PVCs become activated, releasing further VEGF and the basic fibroblast growth factor (bFGF), setting up a vicious cycle of continuous angiogenesis (Raza et al., 2010, Fukumura et al., 1998, Brown et al., 2003). Finally, the vascular basement membrane in tumour tissue is also abnormal: unusually thick in some tumours (eg. in the brain), or completely absent in others (Inai et al., 2004, Kamoun et al., 2009, Tong et al., 2004, Winkler et al., 2004).

1.2.2 Functional consequences of an abnormal tumour vasculature

The structural abnormalities of the tumour vasculature have far-reaching consequences for tumour pathophysiology, growth, metastasis, and response to anti-cancer therapies. Just as the aberrations in cancer cells promote their survival and resistance to treatments, the genetic and epigenetic abnormalities of the tumour microvasculature result in pathophysiological traits that are functionally advantageous for most cancers.

Firstly, the heterogeneity in vessel distribution and haphazard anatomical arrangement of the vasculature cause spatial and temporal heterogeneity in blood flow (Jain, 1988, Jain, 2005), with areas of hypervascularity adjacent to hypovascular ones (Baish et al., 2011, Tong et al., 2004). Furthermore, blood flow in solid tumours, including mammary carcinomas, is often redundant in closed or blind loops (Less et al., 1991, Less et al., 1997). Secondly, the structural abnormalities described above lead to a marked increase in vessel leakiness. Poorly connected ECs, loosely associated PVCs, and an increase in VVOs all contribute to this hyperpermeable phenotype, and hence intravascular fluids and plasma proteins can easily extravasate (Jain, 2005, Greenberg et al., 2008, Hamzah et al., 2008, Morikawa et al., 2002). As a consequence, there is a protein and fluid build-up in the tumour interstitium. This excess extravasation of proteins increases the extravascular oncotic pressure (osmotic pressure of plasma proteins), dragging further fluid into the interstitial space (Tong et al., 2004, Stohrer et al., 2000). Furthermore, there is an absence of functional intratumoural lymphatic vessels, resulting in the impaired clearance of extracellular fluid and hence interstitial hypertension within tumours. This elevated interstitial fluid pressure (IFP) has been documented within murine and human tumours, including breast, colorectal, and cervical cancer as well as melanoma and glioblastoma (Boucher et al., 1997, Boucher et al., 1990, Boucher et al., 1991, Lee et al., 2000, Less et al., 1992, Leunig et al., 1992, Roh et al., 1991, Willett et al., 2004, Willett et al., 2009). The raised intratumoural IFP reduces the hydrostatic pressure gradient between the intravascular and

extravascular compartments such that the two essentially equilibrate. Although this in itself is not sufficient to collapse tumour vessels, it does reduce transvascular flow (as per Starling's equation describing fluid movement across the vascular wall (Starling, 1896)). On the other hand, the mechanical stress from the solid mass of proliferating cancer cells and the matrix is able to collapse tumour vessels, closing their lumen through compressive forces (Padera et al., 2004). This combination of regional poor perfusion, raised IFP, and areas of vascular collapse produces regional hypoxia and acidosis within tumours (Helmlinger et al., 1997). Indeed, Vaupel and colleagues measured the partial pressure of oxygen in tumours using electrodes, and demonstrated the presence of hypoxia within several different human tumour types (Hockel et al., 1999, Hockel and Vaupel, 2001).

The anomalous tumour vasculature and the ensuing hypoxia have several consequences for tumours beyond promotion of angiogenesis. Firstly, because cancer cells are more resistant to hypoxia than normal cells, they undergo epigenetic changes in hypoxic conditions that promote their malignant phenotype and the epithelial-to-mesenchymal transition (EMT). This may result in a greater metastatic potential (Bottaro and Liotta, 2003, DeClerck and Elble, 2010, Hockel et al., 1999, Semenza, 2010a, Semenza, 2010b). For example, hypoxia induces HIF1a-mediated production of several growth factors in cancer cells (Harris, 2002), and the activation of oncogenes that promote invasive growth and metastasis (Pennacchietti et al., 2003). In addition, hypoxia can upregulate expression of VEGF-C in tumour cells, promoting lymphatic metastasis

(Morfoisse et al., 2014). Indeed, increased hypoxia also correlates with metastasis and reduced survival in patients (Hockel et al., 1999). Secondly, hypoxia and low pH also compromise the cytotoxic functions of immune cells that infiltrate a tumour, further enhancing the malignant phenotype (Ganss et al., 2004). Thirdly, aberrations in the tumour vasculature have great implications for tumour sensitivity to therapy. Hypoxia is a well-known mediator of cancer cell resistance to conventional radiotherapy and cytotoxics (Wouters and Brown, 1997, Teicher, 1996). Moreover, the poor blood supply and raised intratumoural IFP (leading to a reduction in transvascular flow) impair the delivery of systemically administered therapies to tumours such as conventional cytotoxics and monoclonal antibodies (Jain, 1989, Wildiers et al., 2003, Tong et al., 2004). Drugs become concentrated in regions that already have sufficient blood supply, and fail to enter inaccessible regions.

1.3 Vascular normalization – a therapeutic strategy in solid tumours

1.3.1 The Vascular Normalization hypothesis

Systemic anti-angiogenic therapy has been developed with the rationale that inhibiting blood vessel formation would cause profound vascular regression, essentially starving tumours to death or rendering them “dormant” (Folkman, 1971). Early preclinical studies provided support for this hypothesis. In various xenograft models, anti-VEGF monoclonal antibodies hindered tumour angiogenesis and delayed tumour growth (Kim et al., 1993, Warren et al., 1995).

Despite these promising preclinical results, the effects of anti-VEGF monotherapy in the treatment of human solid tumours have been generally underwhelming, with only modest objective response rates and a lack of meaningful survival benefits in phase 3 trials (Jain et al., 2006). In metastatic colorectal cancer, for example, an objective response rate of 3.3% was observed amongst chemotherapy-pretreated patients receiving monotherapy with bevacizumab, a monoclonal antibody against human VEGF (Giantonio et al., 2007). Similar results were observed in a breast cancer population (Cobleigh et al., 2003). Such data suggest that anti-VEGF therapy alone is unable to effectively induce sufficient vascular regression in the clinical setting to cause significant tumour shrinkage.

In contrast, large randomized phase 3 clinical trials of bevacizumab therapy *in combination with systemic chemotherapy* have demonstrated significant improvements in progression-free and overall survival when compared with systemic chemotherapy alone. Multiple clinical trials in the first- and second-line treatment of metastatic colorectal cancer have all confirmed that the addition of bevacizumab to standard first-line chemotherapy regimens significantly improves patient outcomes (Hurwitz et al., 2004, Tebbutt et al., 2010, Saltz et al., 2008). Trials of bevacizumab with chemotherapy as first-line treatment for metastatic non-small cell lung cancer have yielded similar results (Sandler et al., 2006, Reck et al., 2009). Additionally, initial studies in metastatic breast cancer suggested a significant improvement in progression-free survival from the addition of bevacizumab to standard cytotoxic chemotherapy (Miller et al., 2007). Although

in the case of breast cancer this did not translate into an improvement in overall survival (Miles et al, 2010, Brufsky et al, 2011, Robert et al., 2011), such data are intriguing, and collectively imply that anti-VEGF antibody therapy augments the efficacy of systemic chemotherapy but has limited action as a monotherapeutic. Taken together, there appears to be a synergistic effect upon combining anti-VEGF antibody therapy with chemotherapy.

These clinical results seem counter-intuitive. Anti-VEGF therapy is designed to promote vascular regression and tumour starvation, and yet the efficacy of chemotherapy depends on efficient tumour blood flow and hence drug delivery. Thus, vascular regression should theoretically dampen, rather than enhance, the effects of systemic chemotherapy. In addition, tumour hypoxia induced by the antivascular effects anti-VEGF therapy should also increase the metastatic proclivity of tumours and render them relatively chemoresistant (Pennacchietti et al., 2003). The trial results refute these hypotheses, however, and are further supported by the fact that no trial in patients with metastatic disease has demonstrated a significant detriment in overall survival from the addition of bevacizumab to systemic chemotherapy (Miles et al., 2011, Welch et al., 2010, Padera et al., 2008).

The “vascular normalization” hypothesis is an attempt to resolve this paradox (Jain, 2001, Jain, 2005). The hypothesis posits that rather than obliterating vessels, the judicious use of anti-angiogenic therapy reverts the grossly abnormal structure and function of the tumour vasculature towards a more normal state. In turn, this normalizes the tumour microenvironment.

1.3.2 Consequences of vascular normalization in tumours

The normalization hypothesis suggests that by correcting the abnormalities in structure and function of tumour vessels (rather than destroying vessels completely), we can rectify aberrations in the tumour microenvironment and ultimately control tumour progression and improve response to other therapies (Jain, 2001, Jain, 2005). This may occur via different physiological mechanisms. Firstly, increased homogeneity of functional vascular density and a more orderly arrangement of vessels could reduce heterogeneity in blood flow in different regions within a tumour. Secondly, improved connections between adjacent endothelial cells, an increased proportion of PVC-covered vessels, and a tighter association between PVCs and ECs would reduce vascular permeability, resulting in a drop in intratumoural IFP. While tumour vessels may never become completely "normal" the effect of these changes is a more even distribution of blood flow within a tumour, with a subsequent reduction in areas of hypoxia and acidosis. In turn, one would expect amelioration of the hypoxia-mediated increase in cancer cell metastatic potential, more uniform delivery of systemically administered anti-cancer therapies within a tumour, and enhanced radiosensitivity of tumours. This might serve to explain the seemingly paradoxical clinical trial data demonstrating synergism between anti-VEGF therapy and chemotherapy in the treatment of solid tumours.

1.3.3 Molecular mechanisms of vascular normalization

In normal tissues, the collaborative action of various proangiogenic factors (eg.

VEGF, basic fibroblastic growth factor [bFGF], angiopoietin-2 [Ang-2]) is in balance with the action of endogenous antiangiogenic and vascular stabilizing factors (eg. Thrombospondin-1 [TSP-1], Ang-1) (Goel et al., 2011, Winkler et al., 2004, Chae et al., 2010, Bocci et al., 2003, Watnick et al., 2003, Thurston et al., 1999, Maisonpierre et al., 1997, Relf et al., 1997). In pathological angiogenesis, an imbalance persists leading to the relentless development of aberrant vessels. By attempting to redress this imbalance, it is possible to normalize tumour vessels. One validated mechanism of vascular normalization is blockade of VEGF signaling. Inhibition of VEGF – a factor that promotes the survival and proliferation of ECs and increases vascular permeability – can transiently restore the balance between pro- and antiangiogenic signaling, shifting it back towards equilibrium.

Over time, a number of other key angiogenic molecules and genes have been directly implicated in the development of an abnormal tumour vasculature and the normalization process. In total, over three hundred original published manuscripts describe evidence of the normalization process as a result of inhibition of any of several different pro-angiogenic pathways, both preclinically and in patients. A detailed description of these is beyond the scope of this thesis, but they are summarized in Figure 1 and reviewed in Goel et al, 2011.

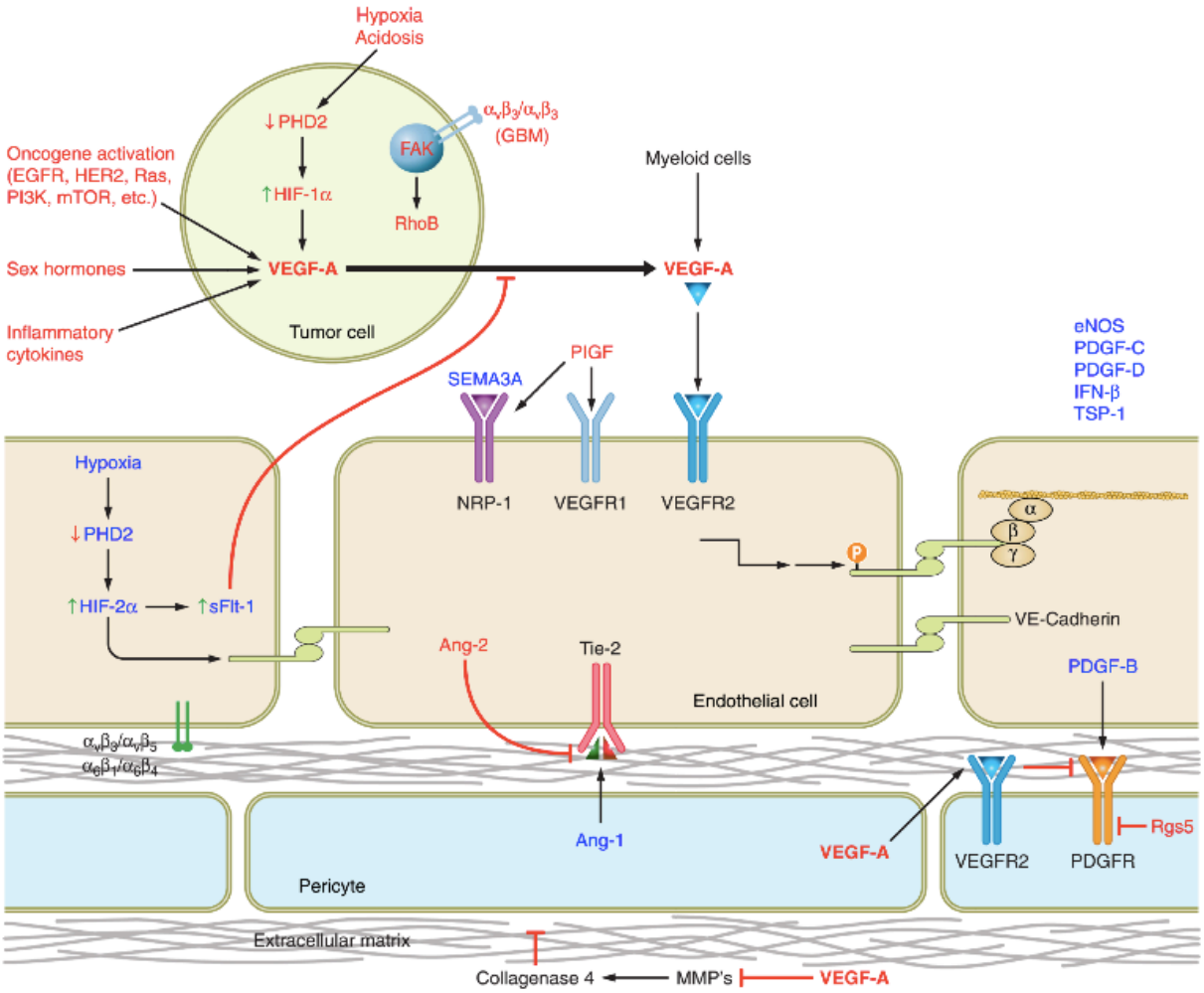

Figure 1: Factors shown to promote or inhibit the vascular normalization phenotype in tumours. This schematic depicts a tumour cell (green), endothelial cell (beige), pericytes (blue), and the extracellular matrix. Molecules that lead to characteristic vessel abnormalities are in red, and those that promote the normalization phenotype are in blue. The principal angiogenic molecule responsible for vascular abnormalities is VEGF-A. This is produced by tumour cells (in reponse to hypoxia via the PHD2/HIF pathway; or due upregulation by oncogenic activation (Izumi et al., 2002, Schnell et al., 2008, Cerniglia et al., 2009, Qayum et al., 2009), sex hormones (Jain et al., 1998, Hansen-Algenstaedt et al., 2000), inflammatory cytokines, etc.). VEGF-A may also be derived from tumour-infiltrating myeloid cells, pericytes, or released from the extracellular matrix, and acts primarily via VEGFR2 on ECs. In addition, VEGF-A stimulation of VEGFR2 on pericytes inhibits PDGFB-PDGFRβ mediated pericyte recruitment to ECs (Greenberg et al., 2008). In addition, PlGF may contribute to tumour vessel abnormalities (possibly by changing the number or phenotype of macrophages), potentially acting through the VEGFR1 or NRP1 (Mazzone et al., 2009). Other mediators of the abnormal vessel phenotype shown include Ang-2 (acting on the Tie-2 receptor – (Maisonpierre et al., 1997)), Rgs5 (which inhibits PDGFR-mediated pericyte recruitment – (Hamzah et al., 2008, Gunaje et al., 2011)), and tumour cell integrins (in the case of GBM). Factors that may restore tumour vessels toward a more normal phenotype include Ang-1 (derived primarily from perivascular cells and acting on Tie-2 – (Suri et al., 1996)), SEMA3A, PDGF-B, and other factors whose mechanism of action is less clear (eNOS, PDGF-C, PDGF-D, IFN-β, TSP-1). Importantly, the differential effects of hypoxia in the tumour cell and endothelial cell are to potentially "abnormalize" or normalize vessels, respectively. Ang, Angiopoietin; EGFR, epidermal growth factor receptor; eNOS, endothelial nitric oxide synthase; FAK, focal adhesion kinase; GBM, glioblastoma multiforme; HER2, human epidermal growth factor receptor 2; HIF, hypoxia inducible transcription factor; IFN, interferon; MMP, matrix metalloproteinase; NRP, neuropilin; PDGF, platelet-derived growth factor; PDGFR, platelet-derived growth factor receptor; PHD, prolyl hydroxylase domain protein; PI3K, phosphoinositide-3-kinase; PlGF, placental growth factor; Rgs5, regulator of G protein signaling 5; SEMA, semaphorin; sFlt1, soluble VEGFR1; TSP, thrombospondin; VE-cadherin, vascular-endothelial cadherin; VEGF, vascular endothelial growth factor; VEGFR, vascular endothelial growth factor receptor; α, β, and γ refer to alpha-, beta-, and gamma-catenin, respectively. (Adapted from Goel et al, 2011).

1.4 Sustained normalization: an elusive goal

Ideally, vascular normalization within tumours would be a sustained process, facilitating a constant improvement in perfusion and reduction in tumour hypoxia. Indeed, various genetic studies have achieved this goal. For example, tumours growing in mice haploinsufficient for PHD2, or in *Rgs5* null mice, show evidence of a sustained, normalized vessel phenotype characterized by improved perfusion, reduced hypoxia, and the attendant improved efficacy of concomitantly administered anti-cancer therapies (Hamzah et al., 2008, Mazzone et al., 2009).

Unfortunately, pharmacologically induced vascular normalization is transient, and characterized by a narrow "time window". This refers to the time period after commencement of anti-angiogenic therapy during which vessels demonstrate features of the normalization phenotype. Studies of murine and human tumours have identified the onset of normalization, typically 1-2 days after commencement of therapy, followed by an eventual "closure" of the normalization window, at which point features of normalization are lost (Kamoun et al., 2009, Winkler et al., 2004, Willett et al., 2004). This may relate either to excessively high or prolonged dosing of antiangiogenic therapy (ie. tipping the balance past equilibrium in favour of antiangiogenic molecules, leading to vascular pruning/regression), or to the development of resistance by activation of alternative proangiogenic pathways or modes of acquiring new vessels. Importantly, it has been shown that cancer cells are more vulnerable to cytotoxic therapies specifically whilst the window is open, and thus defining its timing in a variety of situations is of critical importance (Winkler et al., 2004). Given the tight

balance between excessive and insufficient angiogenesis within tumours, attainment of a sustained, pharmacologically induced vascular normalization has thus far proved an elusive goal. Indeed, the functional vascular phenotype seen following treatment with anti-angiogenic therapies for cancer is likely to reflect the balance between the degree of vascular regression and vascular normalization, both of which are likely to occur concurrently within the same tumour.

1.5 The Angiopoietin-Tie2 system: a key mediator of vascular abnormalities in tumours

After the VEGF-VEGFR system, the next best characterized molecular pathway involved in regulation of angiogenesis and vessel maturation is the Angiopoietin-Tie2 axis, which plays a key role in regulating both physiological and pathological angiogenesis (Huang et al., 2010, Suri et al., 1996).

Ang-1 and Ang-2 bind to their cognate receptor tyrosine kinase Tie-2 on the EC surface. Ang1 is synthesized by PVCs and serves as a Tie-2 agonist. Activated Tie-2 binds to and activates a number of downstream effector molecules within ECs, including endothelial nitric oxide synthase (eNOS), the PI3-Kinase catalytic complex, growth factor receptor-bound protein 2 (GRB2), and A20-binding inhibitor of nuclear factor-κB activation 2 (ABIN2) (Huang et al., 2010). Ultimately, this promotes EC survival, inhibits EC apoptosis, and supports endothelial quiescence. The resultant phenotype is one of vascular stability, maturity, and integrity (Augustin et al., 2009). In keeping with this, Tie-2 activation by Ang-1 has been shown to reduce vascular permeability (Thurston et

al., 1999, Thurston et al., 2000, Wong et al., 1997, Gamble et al., 2000), and also increases vessel diameter and hence blood flow (Suri et al., 1998).

In contrast, Ang-2 is synthesized primarily by ECs, and normally antagonizes the actions of Ang-1 (Maisonpierre et al., 1997). It is the ratio of Ang-1/Ang-2 that determines their ultimate effects. In contrast to Ang-1, Ang-2 destabilizes vessels, promotes PVC detachment from ECs, and drives (especially in concert with VEGF) the process of pathologic angiogenesis. In reality, the effects of Ang-2 are more complex and in certain circumstances it can also serve as a Tie-2 agonist (Daly et al., 2006).

Typically, Ang-1 is constitutively expressed within normal tissues, and plays a key role in maintaining vessel integrity. Conversely, Ang-2 is primarily produced at times when active angiogenesis or vessel remodeling is occurring (of note, Ang-2 is also critical in the regulation of lymphatic vessel development {Zheng et al, 2014)). In both solid tumour growth and metastasis, Ang-1 levels are relatively constant but levels of Ang-2 are higher than those of normal tissue (Holash et al., 1999, Koh et al., 2010). In various stages of tumour development, this increased production of Ang-2 facilitates vessel destabilization and hence encourages tumour growth.

In the earliest phases of primary tumour growth, tumour cells co-opt normal host vessels, leading them to upregulate Ang-2 production. This in turn facilitates the earliest steps that permit the onset of sprouting angiogenesis (Holash et al., 1999), and the beginnings of an abnormal vasculature. Similarly, when tumour

cells circulate and lodge within the vessels of distant organs, it is the production of Ang-2 by these vessels that destabilizes them and permits tumour cell extravasation and tumour cell colonization (Holash et al., 1999, Holopainen et al., 2012, Avraham et al., 2014, Rodriguez et al., 2014). Finally, in established primary tumours, levels of Ang-2 continue to rise as tumours enlarge, and in concert with VEGF drive the abnormal, immature vessel phenotype (Koh et al., 2010). Consistent with this, recent data also suggests that Ang-2 may serve as a direct mediator of resistance to anti-VEGF therapy in mammary carcinomas (Rigamonti et al., 2014), with Ang-2 levels rising in direct response to VEGF blockade.

The Angiopoietin-Tie2 system has been studied using genetic approaches, and evidence supports previously established notions that EC-derived Ang-2 is an important “abnormalizing” factor. When Ang-2 knockout mice are implanted with syngeneic carcinoma or melanoma, the resultant tumours show various features similar to those reported with pharmacological anti-Ang2 therapy (Falcon et al., 2009, Nasarre et al., 2009), including a reduction in vessel diameter, an increase in tumour perfusion and a more mature PVC profile.

Furthermore, Ang-1 is required for the establishment of a stable, normalized vasculature in the face of VEGF pathway blockade (Winkler et al., 2004), and an excess of Ang-2 compromises this process (Chae et al., 2010).

Therefore, a reduced Ang-1:Ang-2 ratio, and the consequent decline in Tie-2 activity, is an important determinant of tumour vessel abnormalities.

1.6 Targeting the Angiopoietin-Tie2 system in solid tumours

In recent years, a number of pharmacologic agents have been developed to target the abnormal tumour vasculature caused by excessive Ang-2 activity (Huang et al., 2010). Several preclinical studies using these agents have shed further light on the role of the Ang-Tie2 axis in tumour vasculature.

A study using specific pharmacological blockade of Ang-1 and Ang-2 (Falcon et al., 2009), highlighted the requirement of Ang-1 for vascular normalization and the contribution of Ang-2 to vascular abnormalities. Nude mice bearing colon cancer xenografts were treated with ML4-3 (a peptibody specifically neutralizing Ang-1), Li-7 (a peptibody specifically neutralizing Ang-2), or their combination. Treatment with ML4-3 alone did not affect tumour growth or vascular morphology, and vessels remained immature and disorganized as evidenced by faint, irregular deposition of VE-Cadherin. Neutralization of Ang-2 with Li-7 normalized vessels. In particular, vessels were narrower and more uniform in morphology with less tortuosity. In addition, increased pericyte coverage was observed and there was a tightening of association between pericytes and ECs, which showed uniform linear deposition of VE-Cadherin. Finally, when tumours were subjected to combined Ang-1 and Ang-2 blockade, vessel density reduced but vessels remained disorganized with irregular VE-Cadherin staining. These data are consistent with those seen after anti-VEGFR2 treatment of glioblastomas (Chae et al., 2010, Winkler et al., 2004).

Recently, a number of reports detailing the effects of other anti-Ang-2 strategies (including anti-Ang-2 antibodies) in solid tumours and inflammatory diseases have been reported (Brown et al., 2010, Tabruyn et al., 2010, Huang et al., 2011, Zheng et al, 2014). Together, they show inhibition of tumour growth, reduction in tumour vessel density, and remodeling of the vasculature suggesting that targeting Ang-2 may prove a valuable method to exploit the benefits of vascular normalization. Of relevance to this thesis, it is noteworthy that the ongoing I-SPY2 clinical trial is studying the effects of an anti-angiopoeitin 1/2 "peptibody" - AMG-386 – as neoadjuvant therapy for breast cancer (Barker et al., 2009).

In addition, a dual pharmacological inhibitor of VEGF and the angiopoietins (named the "Double anti-angiogenic protein", DAAP) has been developed and studied preclinically (Koh et al., 2010). DAAP, a chimeric decoy receptor that simultaneously binds VEGF and Ang1/2, was shown to inhibit the growth of several murine tumours, and in the case of implanted ovarian carcinoma, resulted in a normalization of vessels in the peritoneum – characterized by reduced vessel diameter and a more organized vascular hierarchy. These effects are likely mediated by suppression of the activities of VEGF and Ang-2, given their propensity to promote tumour angiogenesis (Koh et al., 2010).

In general, agents targeting this axis are designed to shift the Ang1:Ang2 ratio in favor of Ang1, hoping to diminish Ang-2-mediated angiogenesis and stabilize vessels. Intriguingly, a recent clinical study has provided preliminary data suggesting that patients with higher levels of circulating Tie2 have an improved outcome after neoadjuvant chemotherapy for breast cancer, further supporting

the importance of the angipoeitin-Tie2 axis as a mediator of tumor behavior and potentially patient prognosis (Makhoul et al., 2014).

1.7 The Vascular Endothelial Protein Tyrosine Phosphatase: an important regulator of Tie2 activity

1.7.1 VE-PTP is essential for vascular development

In 1999, Fachinger et al provided the first report of a receptor tyrosine phosphatase that is expressed exclusively in endothelial cells (Fachinger et al., 1999). This phosphatase was named the Vascular-Endothelial Protein Tyrosine Phosphatase (VE-PTP, human orthologue protein tyrosine phosphatase receptor type B, PTPRB).

In subsequent years, work from the laboratory of Dietmar Vestweber has begun to characterize the structure and function of VE-PTP (Nawroth et al., 2002, Baumer et al., 2006, Broermann et al., 2011, Nottebaum et al., 2008, Winderlich et al., 2009). VE-PTP is a membrane-spanning receptor tyrosine phosphatase, and is so far the only known phosphatase expressed exclusively in the endothelium (Kuppers et al., 2014). Structurally, VE-PTP comprises a cytosolic phosphatase domain, a transmembrane domain, and an extracellular portion comprised of 17 fibronectin-like domains (Nawroth et al., 2002).

The critical role of VE-PTP in endothelial function is clear, given that is essential for successful embryogenesis. Two different VE-PTP deficient mouse models both show embryonic lethality (Baumer et al., 2006, Dominguez et al., 2007). In both models, vasculogenesis occurs normally (and VE-PTP is not expressed at

this early stage), but there are severe defects observed due to failed angiogenesis – namely failure of the yolk sac vasculature to form a organized vascular tree, and development of large, saccular vessels (Dominguez et al., 2007, Baumer et al., 2006). Further supporting a role for VE-PTP in vascular development, Shen et al. recently showed that VE-PTP is upregulated in endothelial cells in response to hypoxia (Shen et al., 2014).

1.7.2 VE-PTP is a negative regulator of Tie-2 activity

In recent years, some of the molecular interactions of VE-PTP have been elucidated. Importantly, the initial report describing VE-PTP showed that it binds directly to the Tie-2 receptor tyrosine kinase, but not VEGFR2 (Fachinger et al., 1999). Further work has clarified the nature of this interaction: Tie-2 and VE-PTP are associated through their cytoplasmic domains, and VE-PTP directly dephosphorylates tyrosine residues on Tie-2 (Winderlich et al., 2009). Elegant work by Winderlich at al has shown that inhibition of VE-PTP expression by antibodies, siRNA, or gene disruption triggers Tie-2 tyrosine phosphorylation, and that by dephosphorylating Tie-2, VE-PTP serves as an important regulator of Tie-2 activity (Winderlich et al., 2009). Furthermore, Ang-1 stimulation of Tie-2 heightens the association of Tie-2 and VE-PTP. As such, Vestweber's team have posited that VE-PTP serves as a negative feedback control mechanism to limit the extent of Tie-2 activation by Ang-1 (Winderlich et al., 2009).

The primary vascular defect in the VE-PTP knockout mouse is that of enlarged, saccular vessels that fail to form correct branch points (Baumer et al., 2006,

Dominguez et al., 2007). Through culture of allantois explants from *VE-PTP* null mice, it has been shown that this enlarged vessel phenotype occurs directly through hyperactivation of Tie-2 (Winderlich et al., 2009).

1.7.3 Interactions between VE-PTP and VE-Cadherin

Beyond Tie-2, VE-PTP has also been found to physically interact with the central EC junction adhesion molecule, VE-Cadherin. VE-PTP and VE-Cadherin can be co-immunoprecipitated from EC lysates (Nawroth et al., 2002).

The interaction between VE-PTP and VE-Cadherin seems to play an important role in regulating endothelial barrier integrity. Loss of VE-PTP in EC's is associated with loss of endothelial barrier function *in vitro,* and overexpression of VE-PTP in ECs has the opposite effect (Nawroth et al., 2002). Furthermore, endothelial exposure to VEGF, lipopolysaccharide (LPS), neutrophils, or lymphocytes triggers dissociation of VE-PTP from VE-Cadherin, increased VE-Cadherin phosphorylation, and an associated increase in endothelial layer permeability (Nottebaum et al., 2008, Broermann et al., 2011).

The overexpression of VE-PTP in VE-Cadherin-transfected cells is associated with decreased tyrosine phosphorylation of both VE-Cadherin and also plakoglobin (gamma-catenin), another important component of the EC junctional complex. At first glance, this would suggest that VE-PTP directly dephosphorylates VE-Cadherin and plakoglobin, in a similar fashion to Tie-2. However, overexpression of a catalytically inactive mutant form of VE-PTP has the precise same effect as expressing wild-type VE-PTP (Nawroth et al., 2002),

implying that it is in fact the interaction of the extracellular domains of VE-PTP and VE-Cadherin, rather than the activity of the VE-PTP phosphatase, that somehow regulates VE-Cadherin phosphorylation and EC barrier integrity. In further support of this notion, Wessel et al recently reported that it is the dissociation of VE-PTP and VE-Cadherin that precedes tyrosine phosphorylation at its Tyr685 residue (Wessel et al., 2014)

To summarize, the currently available data suggests that VE-PTP negatively regulates Tie-2 activity through its phosphatase activity, and heightens EC barrier function through its extracellular interaction with VE-Cadherin.

1.7.4 VE-PTP in the tumour endothelium

Unlike the angiopoietins, the role of VE-PTP in the solid tumour endothelium has been essentially unexplored. In one report, implantation of murine lung carcinoma cells subcutaneously resulted in rapid overexpression of VE-PTP in host endothelial cells (Dominguez et al., 2007). This observation leads one to speculate that VE-PTP activity, possibly by deactivating Tie-2, might play a role in the initial destabilization of tumour vessels. This remains to be proven, however.

1.8 AKB-9778 – a first-in-class inhibitor of the VE-PTP catalytic domain

AKB-9778 (Aerpio Therapeutics, Cincinnati OH) is a novel, first-in-class small molecule inhibitor of the VE-PTP phosphatase domain. AKB-9778 was developed through structural modifications of 1,2,3,4-tetrahydroisoquinolinyl

sulfamic acids. These acids are phosphotyrosine mimetics, and act competitively to prevent phosphatases from dephosphorylating their endogenous targets. Coupling 1,2,3,4-tetrahydroisoquinolinyl sulfamic acids to a malonate template yields selective and potent inhibitors of VE-PTP (Amarasinghe et al., 2006). The phenylsulfamic acid moiety acts as a general phosphotyrosine mimetic "warhead", and surrounding moieties were optimized as part of an extensive structure-based drug design program (Shen et al., 2014).

In vitro enzyme kinetic studies show that AKB-9778 is a selective inhibitor of VE-PTP, with over 7000-fold higher potency for VE-PTP that the generic intracellular phosphatase PTP1B. Furthermore, it is over 5000-fold more selective for VE-PTP than other phosphatases including HPTP-epsilon, CD45, Shp1, Shp2, MKP-1, HCPTA, PTP-mu, PRL-3, VHR, PTEN, and alkaline phosphatase (Shen et al., 2014).

As described earlier, the central bona fide function of the phosphatase domain of VE-PTP appears to be dephosphorylation of Tie-2. Therefore, it is plausible that by inhibiting VE-PTP, AKB-9778 might serve to enhance Tie-2 signaling within ECs. Consistent with this hypothesis – and published after the experiments in this thesis were completed – a report from Shen et al. has recently demonstrated that through Tie-2 activation, AKB-9778 stabilizes retinal vessels in mice with neovascular macular degeneration (Shen et al., 2014), reducing permeability and inhibiting pathological vascularization. Indeed in this light, AKB-9778 has now entered clinical trials for patients with diabetic macular oedema, and unpublished

data demonstrate a significant reduction in retinal oedema in a proportion of patients (Aerpio Therapeutics, 2014).

The neovasculature of the diabetic eye is often compared to the vasculature of solid tumours, and the results above therefore provide further support for study of AKB-9778 as a promoter of vascular stability within tumours.

1.9 The current study

The present study has two central aims.

The first is to characterize the effects of AKB-9778 as an inhibitor of the VE-PTP catalytic domain. We speculated that by reducing Tie-2 dephosphorylation, AKB-9778 might mediate an enhancement of Tie-2 signaling in EC's.

The second, and most important, is to describe the effects of AKB-9778 therapy on the solid tumour vasculature, tumour growth, and metastasis. We hypothesized that as an activator of endothelial Tie-2 signaling, AKB-9778 might promote the development of a more mature, stable, functionally normalized vasculature within solid tumours – mitigating some of the adverse consequences associated with vessel abnormalities. We specifically explored this in three settings: i) the earliest phases of tumour growth when Tie-2 deactivation promotes the onset of sprouting angiogenesis; ii) the earliest stages of metastatic colonization, with Tie-2 deactivation facilitates circulating tumour cells' extravasation into distant organs; and iii) during the growth of established primary tumours, where vascular immaturity promotes tumour hypoxia and impairs the response to concomitantly administered cytotoxic therapies.

2 Chapter Two: Materials and Methods

2.1 In vitro and molecular biology studies

2.1.1 Cell lines and cell culture

Human umbilical vein endothelial cells (HUVECs) were obtained from the Center for Vascular Excellence at the Brigham and Women's Hospital (Boston, MA). HUVECs were received at passage zero, and all experiments were performed at passage numbers less than or equal to four. HUVECs were cultured in 100mm tissue culture dishes coated with 0.1% gelatin (ATCC, Manassas, VA) in Endothelial Growth Medium (EGM, Lonza, Mapleton, IL) containing all manufacturer-supplied supplements.

Human microvascular endothelial cells (HMVECs) were dermal microvascular endothelial cells purchased from Lonza (CC-2811 line) and were cultured in EGM with all manufacturer supplements on tissue culture dishes coated with 0.1% gelatin.

The 4T1 murine mammary carcinoma line was purchased from ATCC and was cultured in Dulbecco's Modified Eagle Medium (DMEM) with 4.5 g/L glucose, L-glutamine, and sodium pyruvate (Cellgro, Manassas, VA), supplemented with 10% fetal bovine serum (FBS) (Sigma-Aldrich, St Louis, MO) and 1% MEM non-essential amino acids (Invitrogen, Grand Island, NY). The E0771 murine mammary carcinoma cell line was originally established by Dr Sirotnak (Memorial Sloan Kettering Cancer Center, New York) and were provided as a generous gift

by Dr Mihich (Roswell Park Cancer Institute, Buffalo, NY). E0771 was cultured in DMEM (ATCC) supplemented with 10% FBS and 1% HEPES buffer (Invitrogen). The 4T1 and E0771 cell lines were subcultured upon reaching 70-80% confluence at a ratio of 1:5.

The *MMTV-PyVT* tumour cell line was derived as follows: spontaneously arising mammary tumours were resected from FVB/N-Tg(*MMTV-PyVT*) 634Mul/J mice (Jackson Laboratories, Bar Harbor, ME). Tumours were cut into 1mm pieces under sterile conditions, and then digested at 37^{o}C for 45 min in DMEM containing 10% fetal bovine serum, collagenase type 1A (1500 U/ml), hyaluronidase (1000 U/ml) and DNase (2 mg/ml) (all from Sigma). The digestion mixtures were filtered through 70 μm cell strainers. Cells were then cultured in DMEM media containing 10% fetal bovine serum and passaged ten times, until a homogenous tumour cell population was obtained.

Human Embryonic Kidney (HEK) 293T cells were utilized for generation of lentiviral particles, were purchased from ATCC, and were cultured in DMEM with 10% FBS.

All cells were incubated continuously at 37^{o}C in a humidified incubator with 5% carbon dioxide, and cell manipulation was performed under sterile conditions in a biosafety hood.

2.1.2 In vitro studies of AKB-9778 using endothelial cell lines

The vascular-endothelial protein tyrosine phosphatase inhibitor AKB-9778 was provided under a Material Transfer Agreement with Akebia Therapeutics (Cincinatti, OH), the manufacturer of this compound. For in vitro experiments, AKB-9778 was dissolved in a sterile solution of 5% dextrose.

HUVECs or HMVECs were grown to confluence in 100mm cell culture dishes pre-coated with 0.1% gelatin. Media was refreshed, AKB-9778 was added directly to the medium at a concentration of 10μM. Cells were then incubated in AKB-9778 for varying lengths of time, as indicated within each experiment. When indicated, recombinant human angiopoietin-1 (500ng/mL, R&D Systems, Minneapolis, MN) and/or recombinant human angiopoietin-2 (500ng/mL, R&D Systems) was also added to the cell culture medium. For angiopoietin-1 treatment of cells, a mouse anti-polyHistidine monoclonal antibody (5 mg/mL, R&D Systems) was added with Ang-1 to facilitate multimerization (Kim et al., 2005).

After treatment, media was aspirated and cell dishes placed immediately on ice. Cells were then washed with ice-cold phosphate-buffered saline (PBS) and then lysed with RIPA buffer (Boston Bioproducts, Ashland, MA) supplemented with protease inhibitors (Complete Ultra, Roche, Indianopolis, IN) and phosphatase inhibitors (Phostop, Roche). Cell lysates were sonicated at 4ºC for 20 minutes and then centrifuged at 4ºC at 25,000xg for 20 minutes. The supernatant was then collected, and the lysate protein concentration was determined using the

Bradford Quick Start Protein Assay Kit (Bio-Rad, Hercules, CA). Lysates were then diluted to a final concentration of 1ug/uL in RIPA buffer and a 4X sodium dodecyl sulfate buffer (Boston Bioproducts), before denaturing at 95^{o}C for 5 minutes. Denatured lysates were then subjected to Western Blotting as described below.

2.1.3 Immunoprecipitation

To assess tyrosine phosphorylation of Tie-2, VE-Cadherin, and plakoglobin in both endothelial cell lines and murine tissue, protein lysates were subject to immunoprecipitation of the protein in question prior to blotting with an anti-phosphotyrosine antibody.

Cell lysates were prepared as described above. Protein lysates from murine tissue was obtained by cutting the tissue into 1-2mm pieces on ice, before immediately homogenizing the tissue in RIPA buffer containing protease and phosphatase inhibitors, sonicating the resultant lysate at 4^{o}C for 20 minutes, and then centrifuging the lysate at 25,000xg for 20 minutes at 4^{o}C.

The primary immunoprecipitating antibody was then added to 200uL of the protein lysate. Antibodies used for immunopreciptation were as follows:

Antibody	Manufacturer	Concentration	Catalog Number
Tie-2	Santa Cruz Biotechnology (Santa Cruz, CA)	1:50	sc-324

VE-Cadherin	Abcam (Cambridge, MA)	1:50	ab7047
Plakoglobin	Cell Signaling (Beverley, MA)	1:100	2309

The antibody-lysate mixture was then incubated with gentle rocking overnight at 4^{o}C. The following day, 20uL of a fifty percent slurry of Protein A Sepharose beads (GE Healthcare Lifesciences, Pittsburgh, PA) was added and the mixture was incubated with gentle rocking at 4^{o}C for 3h. Samples were then centrifuged for 30 seconds at 4^{o}C, and then washed five times with 500uL of RIPA buffer. After the fifth wash, the bead pellet was resuspended in 20uL of 3X SDS buffer, vortexed, and then microcentrifuged for 30 seconds. Samples were then boiled at 95^{o}C for 5 minutes, and microcentrifuged at 14,000g for 1 minute. The supernatant was aspirated and subjected to Western Blotting for phosphorylated tyrosine residues as described below.

2.1.4 Western Blotting

Western Blots to assay protein and phospho-protein levels were performed using the Bio-Rad Mini Trans-Blot Cell, according to manufacturer's instructions. Protein lysates were prepared and denatured as described above. 40ug of lysate (or the entire sample in the case of immunopreciptated proteins) was loaded into a polyacrylamide gel containing a percentage of acrylamide suitable for detecting the protein of interest (according to size). Electrophoresis was

performed at 80 volts until lysate was seen to have entered the separating gel, at which time the voltage was increased to 100V.

At completion of gel electrophoresis, protein was transferred to a nitrocellulose membrane at 4^{o}C, using a Tris-glycine transfer buffer supplemented with 20% methanol. Transfer was performed under a fixed voltage of 100V for 90 minutes. Membranes were washed in Tris-buffered saline (TBS) three times for five minutes, and then blocked in a solution of 5% dry non-fat milk (BioRad) in TBS for 1h at room temperature, with gentle rocking.

Membranes were then washed again in TBS three times for five minutes, before being incubated in primary antibody overnight at 4^{o}C, with gentle rocking. All primary antibodies were prepared in a solution of 5% bovine serum albumin (BSA) in TBS supplemented with Tween-20 at 0.05% (TBST). The primary antibodies used are listed below:

Antibody	**Manufacturer**	**Concentration**	**Catalog Number**
Beta-tubulin	Millipore (Billerica, MA)	1:2000	05-661
Phospho-tyrosine	Millipore (Billerica, MA)	1:100	05-321
Tie-2	Santa Cruz Biotechnology	1:500	sc-324
p-AKT (ser 473)	Cell Signaling	1:1000	9271
Total AKT	Cell Signaling	1:1000	9272
p-eNOS (ser1177)	Abcam	1:1000	ab75639
p-eNOS (Thr495)	Cell Signaling	1:1000	9574

Total eNOS	Abcam	1:1000	ab5589
VE-Cadherin	Abcam	1:500	ab7047
Plakoglobin	Cell Signaling	1:1000	2309
Na-K-ATPase α1 isoform	Cell Signaling	1:1000	3010

The following day, membranes were washed in TBST three times for ten minutes, before incubation in secondary antibody for 1h at room temperature.

Secondary antibodies for Western Blotting included anti-rabbit HRP (Cell Signaling) and anti-mouse HRP (GE Healthcare), and were suspended in a solution of 1% dry non-fat milk and 5% BSA in TBST. Membranes were then washed three times for 10 minutes in TBS, and then incubated in the chemiluminescent ECL Plus Substrate (Thermo Scientific, Rockford IL) and developed in a dark room onto CL-XPosure Film (Thermo Scientific).

2.1.5 Lentiviral production and infection of endothelial cells

For gene silencing of Tie-2 in HUVECs, a lentiviral target gene set to *TEK* (Accessions NM_000459, AB208796, BC035514, and L06139) was purchased from Thermo Scientific and screened for Tie-2 silencing efficiency. Lentiviral particles were generated by co-transfection of pLKO.1-sh*TEK* (10ug), pDelta8.9 (5ug) and pVSVG (1ug) plasmids into 100mm dishes of HEK293T cells at 80% confluency. Transfection was performed using the Fugene-6 transfection reagent (Roche) according to manufacturer's instructions, using a Fugene:pLKO.1-sh*TEK* ratio of 3:1. HEK293T cell supernatant containing lentivirus was collected at 24

and 48h post-transfection, filtered through a 0.25um filter, and applied directly to low passage HUVECs at 70% confluence in 6 well plates, together with polybrene at a concentration of 8ug/mL. HUVECs were transduced for 24 h after which they were subjected to antibiotic selection with 2ug/ml puromycin for an additional 24-48h prior to seeding for indicated experiments. The silencing efficiency of TEK was determined in primary endothelial cells by western blotting, and clone ID TRCN0000000415 was chosen for these studies. Lentiviral particles containing a scrambled shRNA sequence were used as a control (Sigma).

2.1.6 Fractionation of cells into membranous and non-membranous compartments

For experiments quantifying the amount of membranous versus non-membranous VE-Cadherin in HUVECs, cells were lysed and processed using the Mem-PER Plus Membrane Protein Extraction Kit (Thermo Scientific). This kit contains a cell wash solution, permeabilization buffer, and solubilization buffer and uses a mild detergent-based selective extraction protocol. Cells are first permeabilized with a mild detergent, allowing the release of soluble cytosolic proteins, after which a second detergent solubilizes membrane proteins. Membrane proteins with one or two transmembrane domains are typically extracted with an efficiency of up to 90%, and cross-contamination of cytosolic proteins into the membrane fraction is usually less than 10%.

HUVEC membrane and non-membrane fractions were prepared according to manufacturer's instructions.

2.1.7 *In vitro* detection of nitric oxide production in HUVECs using DAF-2 DA

4,5-diaminofluorescein diacetate (DAF-2 DA) stock solution (5mM in DMSO) (Enzo Life Sciences Inc., Farmingdale, NY) was aliquoted and stored at -20^{o}C in darkness under inert gas. The DAF-2 DA working dilution was prepared just before use. HUVECs were grown to confluence in EGM (with all manufacturer-supplied supplements) on gelatin-coated and 0.5% glutaraldehyde cross-linked 8-chamber culture slides (BD Biosciences). After washing with PBS, medium was changed to phenol red-free endothelial growth medium (Lonza) with manufacturer-supplied supplements and 0.5mM L-arginine (adjusted to pH 7.4). After 105 minutes, 100uM N^{G}-Monomethyl-L-arginine (L-NMMA, Sigma-Aldrich) was added to indicated wells for 15 min, followed by a PBS wash. HUVECs were then loaded with 10 μM DAF-2 DA in HEPES buffered saline (pH 7.4) for 45 min at 37^{o}C in darkness, with or without 16uM AKB-9778. 100 μM L-NMMA was again added for the negative controls. Cells were then washed with PBS, incubated with fresh phenol red free EGM (with manufacturer-supplied supplements) for 30 min at 37^{o}C, PBS washed, fixed with 4% formaldehyde for 5 min and mounted with Vectashield Mounting Medium for fluorescence with DAPI (Vector Laboratories Inc., Burlingame, CA). Cells were imaged using an Olympus Fluoview FV 1000 confocal microscope and nitric oxide (NO) production measured by the ratio of FITC signal to DAPI signal, quantified using the ImageJ image analysis software (National Institutes of Health, Bethesda, MD).

2.2 Zebrafish studies

2.2.1 Embryonic angiogenesis assays

Flk-1:GFP transgenic zebrafish were obtained from the Cardiovascular Research Center, Massachusetts General Hospital (Charlestown, MA). Fertilized eggs were incubated either in E3 fish water (control) or E3 fish water supplemented with AKB-9778 (dissolved in DMSO) at the concentrations indicated. E3 fish water was made as a 60x stock solution (34.4 g NaCl, 1.52 g KCl, 5.8 g $CaCl_2.2H_2O$, 9.8 g $MgSO_4.7H_2O$, made up to 2L with 18 mOhm double distilled water. The final DMSO concentration in both control and treatment groups in the fish water was 1%. Embryos were examined under an epifluorescent stereomicroscope at 48h post-fertilization. Digital images were obtained and then analyzed by manually counting the number of intersegmental vessels seen to reach the dorsal longitudinal anastomotic vessel (DLAV) in each embryo.

2.2.2 Zebrafish xenograft assays

Fertilized *Flk-1:GFP* transgenic zebrafish eggs were incubated at 28ºC for 24h in E3 fish water. At 24h post-fertilization, embryos were manually dechorionated with forceps and then placed into incubation medium containing 75uM propythiouracil (Sigma) in E3 fish water. At 48h post-fertilization, embryos were anesthetized with 0.02mg/mL tricane and then aligned in the lateral decubitus position on an agarose-modified Petri dish. 4T1-dsRed tumour cells were suspended in growth factor reduced Matrigel (BD Bioscience, San Jose, CA) diluted with PBS to a protein concentration of 8.25mg/mL, at a density of $5x10^6$

cells/60uL Matrigel. A hand-pulled borosilicate needle was loaded with 10uL of tumour cell suspension. Using a microinjector under 50 X stereomicroscopic magnification, the needle tip was introduced into the perivitelline space in proximity to the developing sub-intestinal vein plexus. 10nL of tumour cell suspension was injected per embryo. The injections were performed by Dr Brian Walcott (Massachusetts General Hospital, MA). Embryos were then recovered in fresh E3 fish water for 1h and then either maintained in E3 fish water or in AKB-9778 (100mM in DMSO). Embryos were fixed with 4% paraformaldehyde in PBS for 2h, 48h post-xenografting. Tumour neovascularization was examined using a confocal microscope – axial sections were obtained through the entire tumour mass and five sections analyzed per embryo. Neovascularization was quantified by the ratio of GFP-positive area (endothelial cells) to dsRed positive area (tumour mass) using ImageJ software.

2.3 Murine studies

All animal procedures were performed following the guidelines of Public Health Service Policy on Humane Care of Laboratory Animals and approved by the Institutional Animal Care and Use Committee of the Massachusetts General Hospital, Boston MA. Mice were bred and maintained in a gnotobiotic (defined flora) animal facility in the Edwin L. Steele Laboratory within the Massachusetts General Hospital. NCr/Sed Nude mice (nu/nu), C57BL6/J mice, and FVB/N-Tg(MMTV-PyVT)634Mul/J mice were originally obtained from Jackson

Laboratories (Bar Harbor, ME). FVB/N mice originally were obtained from Taconic Farms (FVB/NTac; Germantown, NY) in July 1999. *Nos3*$^{-/-}$ *(eNOS*$^{-/-}$*)* mice were obtained from Dr. Paul Huang (Massachusetts General Hospital, Boston MA).

2.3.1 Murine models of mammary carcinoma

To establish 4T1 primary tumours, 4T1 tumour cells were harvested at 80% confluence, and resuspended in PBS. Mice were first anaesthetized by intraperitoneal injection of ketamine (150mg/kg) and xylazine (10mg/kg). For early tumour growth studies, 2 x 10^4 4T1 cells (suspended in 50uL of PBS) were injected into the left third mammary fat pad of female nude mice aged 6-8 weeks. For studies of established tumours, 5 x 10^4 tumour cells into the left third mammary fat pad of female nude mice aged 6-8 weeks.

To establish E0771 primary tumours, E0771 tumour cells were harvested at 80% confluence, resuspended in PBS, and injected into the left third mammary fat pad of anaesthetized female C57BL6/J mice aged 6-8 weeks (2 x 10^5 tumour cells in 50uL of PBS).

The P0008 mammary carcinoma was derived in the laboratory of Rakesh K. Jain from a spontaneously occurring mammary carcinoma in a female mouse with an FVB/N background (Huang et al., 2008). In the present study, P0008 tumours were established by implanting 1-2mm viable fragments of tumour tissue from P0008 tumour-bearing FVB/N mice directly into the left third mammary fat pads of 6-8 week old female FVB/N mice. Mice were first anaesthetized with ketamine

and xylazine, and then shaved to expose the skin around the left third nipple. A 3-4mm cutaneous incision was made 5mm inferior to the nipple, and a small tumour fragment inserted through this incision into a subcutaneous pocket directly below the nipple. The incision was then closed with a single nylon suture.

For *MMTV-PyVT* tumour growth experiments, we monitored *MMTV-PyVT* mice for the appearance of spontaneous tumours and commenced treatment when the largest palpable tumour reached 3mm diameter. Although *MMTV-PyVT* mice develop multiple spontaneous tumors, only this tumour was measured and analyzed during treatment.

Tumours were measured daily with calipers except where otherwise specified. Tumour volume was calculated as Volume = 4/3 x π x (long axis/2) x (short axis/2)^2.

2.3.2 Drug treatment of mice

AKB-9778 was injected at a dose 40 mg/kg subcutaneously every 12h. AKB-9778 was dissolved in 5% dextrose, except where otherwise specified. Control vehicle was the same volume of 5% dextrose. Doxorubicin was administered at 2.5 mg/kg via intraperitoneal injection every 72h.

2.3.3 Measurement of tumour hypoxia

To assess hypoxia, tumour-bearing mice were injected with pimonidazole hydrochloride (Hypoxyprobe, Burlington MA) at a dose of 60mg/kg

intraperitoneally, 1h before sacrifice. At the time of sacrifice, mice were anaesthetized with ketamine and xylazine, after which tumours were surgically excised and fixed according to protocols described below. 20um thick frozen sections were prepared, and stained with the Hypoxyprobe monoclonal antibody using a mouse-on-mouse staining kit (Vector Laboratories, Burlingame, CA). Sections were analyzed using confocal microscopy as described in section 2.5.

2.3.4 Measurement of tumour perfusion

To assess perfusion, 100mg of biotinylated tomato lectin (Vector Laboratories) was injected into the lateral tail vein of anesthetized, tumour-bearing mice 5 minutes before sacrifice. After 5 minutes, tumours were excised, fixed, and 20um frozen sections were prepared. Immunofluorescent staining for the presence of biotinylated lectin was then performed using the AlexaFluor 546-streptavidin conjugate (Invitrogen). Details of immunofluorescent staining techniques are provided below.

2.3.5 Intravital microscopy and assessment of tumour vessel permeability in vivo

Tumours were implanted in the mammary fat pad of female mice and a mammary fat pad chamber placed over the tumour once it reached diameter 2-3mm, as previously described (Vakoc et al., 2009). To measure effective vascular permeability, mice were anesthetized with inhaled isoflurane and injected via retro-orbital injection with tetramethylrhodamine labeled BSA (Invitrogen) for baseline images and AlexaFluor-647 BSA (Invitrogen) at the post-

treatment time point (to avoid inadvertent imaging of tetramthylrhodamine-BSA at the second time point). At each time point, two distinct regions within the tumour were selected and a 200um image stack recording BSA fluorescence was taken through each region every ten minutes for 1h, using a multiphoton laser-scanning microscope. The analysis approach involved three-dimensional vessel tracing to create vessel metrics and a three-dimensional map of voxel intensity versus distance to the nearest vessel over time. Images were also corrected for sample movement over time with three-dimensional image registration. The normalized transvascular flux was calculated using

$$\frac{J_t}{S_v(C_v - C)} = P_{eff} = \lim_{t \to 0} \frac{\partial}{\partial t} \frac{\int_{r=R}^{\infty} C(r) r \partial r}{(C_v - C)R}$$

where J_t is the transvascular flux, S_v the vessel surface area, C_v the concentration of the probe in the vessel, C the concentration of the probe immediately extravascular, P_{eff} the effective permeability, t time after the initial image, r the distance from the vessel central axis, and R the vessel radius at that point along the vessel. The calculation was made as an average over the entire imaged volume for each tumour.

Optical frequency domain imaging (OFDI) of tumour perfusion was performed using orthotopic 4T1 carcinomas under mammary fat pad windows, as previously described (Vakoc et al, 2009). Briefly, tumours were implanted in the mammary fat pad of female mice as described above, and a mammary fat pad chamber placed over the tumour once it reached diameter 2-3mm. The OFDI microscope

and image analysis were built and designed at the Wellman Center for Photomedicine at the Massachusetts General Hospital. Pre-designed software and image processing algorithms were available at the time that OFDI experiments were performed, and are the subject of a previously published report (Vakoc et al., 2009).

2.3.6 Metastasis assays

Studies of spontaneous pulmonary metastasis were performed using the 4T1 tumour model in female nude mice, designed to model the effects of adjuvant therapy. Tumours were implanted into the mammary fat pad as described above.

It was initially determined through a series of pilot experiments that micrometastatic tumour cells were first consistently apparent within the lungs of 4T1 tumour-bearing mice once primary tumours reached 5mm in diameter. In experiments presented here, tumours were therefore resected from the mammary fat pad once they reached a diameter of 5mm. This was performed as a survival surgery: mice were anaesthetized with ketamine and xylazine, and the region around the tumour cleaned with 70% ethanol. The mammary tumour was then gently lifted away from the thoracic cage with sterile forceps, and the skin around the tumour was cut with surgical scissors until the entire tumour was excised. The resultant skin deficit was closed with nylon sutures.

24h after surgery, therapy was begun with either AKB-9778 or control vehicle, and the effects of therapy on the progression of lung metastases as well as metastases in other organs were studied.

Mice were sacrificed at a series of different time points: examination of the lungs after two weeks of therapy was performed to study metastases histologically: lungs were resected, tissue was fixed in 4% formaldehyde, and 5um paraffin-embedded sections were prepared at 100um intervals throughout all lobes of all lungs. These were stained with hematoxylin and eosin and metastases identified and counted by a trained pathologist. Metastases were photographed digitally and their area determined using ImageJ software.

To examine for macroscopic metastases, lungs were resected after 3 weeks of treatment and immersed in Bouin's solution (Sigma). After 24h, tissues were examined under a stereomicroscope at 4x magnification and all metastases visible on the lung surface were counted. Metastases were seen clearly as white nodules on the background of yellow normal lung tissue. In these studies, full necropsy was also performed on all mice, and metastases macroscopically evident in liver, bone, lymph nodes, or soft tissues were documented.

For survival studies, mice were treated either with doxorubicin chemotherapy alone after resection of primary tumours (2.5mg/kg intraperitoneally every 72h) or with doxorubicin in addition to AKB-9778. Mice were sacrificed by carbon dioxide inhalation if they appeared moribund, were unable to eat or drink, or had lost over 10% of bodyweight.

For experimental micrometastasis assays, 4T1 (1 x 10^6), E0771 (5 x 10^5), or *MMTV-PyVT* (5x10^5) tumour cells were injected into the tail vein of nude, C57BL/J, and FVB/N mice respectively, and treatment with AKB-9778 or control vehicle was commenced 12h later. Treatment was continued for 5 days for the E0771 and *MMTV-PyVT* experiments, and for 8 days for the 4T1 experiments. At the end of treatment, the lungs of anesthetized mice were fixed by intra-tracheal instillation of 4% paraformaldehyde. A minimum of 3 representative 5uM sections (at least 100uM apart) through each lobe of each lung were stained with hematoxylin and eosin and analyzed by two investigators including a trained pathologist. The number of metastatic foci was counted for each lung section. Each tumour focus was graded as intra- or extravascular and number of cell nuclei visible at 400x magnification in each focus was counted as a marker of tumour size.

2.3.7 In vivo assays of Tie-2 phosphorylation

For in vivo assessment of Tie-2 phosphorylation, mice received a single dose of AKB-9778 40 mg/kg in 5% dextrose intravenously. Lungs or tumours were resected 1h later and immediately frozen in liquid nitrogen. Tissues were later homogenized in RIPA buffer supplemented with protease inhibitors and phosphatase inhibitors (as described in section 2.1.2) before immunoprecipitation for Tie-2 and western blotting for phospho-tyrosine as described above.

2.3.8 Delivery of external beam radiotherapy to murine mammary tumours

Tumour-bearing mice were anesthetized with a combination of ketamine and xylazine via intraperitoneal injection. Mice were secured in the supine position on a supportive plastic platform using adhesive tape. A 15mm lead collimator of 6mm thickness was placed over the mammary fat pad tumour, and the mouse placed into the irradiator (XRAD 320, Precision X-Ray Inc., North Branford, CT). Radiation was directed at 3.52 Gy/min to a total of 20 Gy through the collimator aperture.

2.3.9 Miles assay

The Miles assay was used to measure changes in the permeability of normal murine skin vessels in response to AKB-9778 therapy. Mice were treated with AKB-9778 or vehicle control for 24h. One hour after the last dose, mice were anesthetized with ketamine/xylazine at doses described above, and Evan's Blue dye (Sigma) was injected intravenously via the lateral tail vein (100uL of a 1% solution in PBS). Thirty minutes later, bilateral 7mm skin punch biopsies were taken and snap frozen in liquid nitrogen. At the time of analysis, tissue was thawed to room temperature, weighed, and incubated in 1mL of formamide overnight at 55^{o}C. Evan's blue content was then assessed by spectrophotometric measurement of formamide containing eluted Evan's Blue at a wavelength of 620nm, and was normalized for the weight of each tissue fragment analyzed.

2.3.10 Measurement of mouse blood pressure

Mice were anaesthetized with ketamine/xylazine (dose normalized to body weight) and positioned in the supine position. Cannulation of the carotid artery was performed as previously described (Duyverman et al., 2012) by Ms Sylvie Roberge (Massachusetts General Hospital, MA). The arterial pressure waveform was obtained by connecting a carotid artery cannula to a pressure transducer via heparin-filled PE10 tubing. Mean arterial pressure was calculated as MAP = ((diastolic BP x 2) + systolic BP))/3.

2.4 Tissue processing, immunofluorescence, and immunohistochemistry

2.4.1 Fixation and processing of tissues for histologic analysis

Excised murine tissue (mammary tumours, lungs) was fixed by immersion in 4% formaldehyde in PBS (time of fixation (h) = diameter of tissue fragment (mm)/2).

To prepare tissue for frozen sections, this was followed by 3 washes in PBS and then dehydration in 30% sucrose in PBS overnight at 4ºC. Tissue was subsequently mounted in freezing media (OCT, Tissue-Tek, Torrance, CA). 20um frozen sections were prepared for immunofluorescent staining. To prepare tissue for paraffin embedding, it was washed three times after fixation and then stored in 70% ethanol. Tissue processing, cassetting, and embedding was then performed by the Department of Pathology at the Massachusetts General Hospital.

2.4.2 Immunofluorescent staining of frozen tissue sections

20um frozen sections were cut, placed onto glass microscope slides, and stored at -80°C. At the time of staining, sections were air-dried at room temperature for 1h, post-fixed in acetone at -20°C for 5 minutes, and then washed in PBS. Five percent normal horse serum (Jackson Immunoresearch, West Grove, PA) was used for blocking (1h at room temperature) and for diluting primary antibody (overnight at 4°C) and secondary antibody (1h at room temperature in darkness). Primary antibodies for immunofluorescent staining were as follows:

Antibody	**Manufacturer**	**Concentration**	**Catalog Number**
CD31	Millipore	1:200	1398
NG2	Millipore	1:1000	5320
Desmin	R&D Systems	1:50	AF3844
VE-Cadherin	Abcam	1:50	ab7047

Secondary antibodies for immunofluorescence (Cy3-Donkey anti-Rabbit, DyLight-649–Goat anti-Armenian Hamster, and Cy3-Donkey anti-Goat) were purchased from Jackson Immunoresearch and used at a concentration of 1:200. After incubation in secondary antibody, sections were washed three times in PBS and then mounted with 4'-6-diamidino-2-phenylindole (DAPI)–containing mounting media (Vectashield, VectorLabs, Burlingame, CA) for confocal microscopy.

2.4.3 Immunohistochemical staining of paraffin-embedded tissue sections

5um sections were cut from tissue previously fixed and embedded in paraffin blocks. Slides were then deparaffinized by washing sequentially in 100% xylene, 100% ethanol, 95% ethanol, 70% ethanol, and then demineralized water (two five minute washes in each solution). Slides were then subject to antigen retrieval using a citric acid based antigen unmasking solution (Vector Laboratories) in a conventional microwave. After cooling in antigen retrieval solution for 20 minutes, slides were washed twice in PBS (3 minutes each), then blocked in 5% horse serum for 1h at room temperature. Slides were then incubated in primary antibody overnight at 4^{o}C (Collagen IV antibody, Abcam catalog number ab6586 at concentration 1:1000). The following day slides were washed three times in PBS, and then soaked in 3% hydrogen peroxide for 10 minutes to quench endogenous peroxidase activity. After further washes in PBS, slides were incubated in secondary antibody (Biotin-SP-AffiniPure Donkey Anti-Rabbit IgG, Jackson Immunoresearch catalog number 711-065-152 at concentration 1:200) for 1h at room temperature. After three further PBS washes, slides were developed using a standard streptavidin-biotin-horseradish peroxidase-diaminobenzidine protocol (VECTASTAIN Elite ABC Kit, Vector Laboratories, and Immpact Kit Dab, Thermo Fisher Scientific, according to manufacturer's instructions). The peroxidase reaction was stopped by soaking slides in demineralized water, before counterstaining with hematoxylin, dehydration to xylene, and application of mounting media (Permount, Thermo Fisher Scientific) and coverslips.

2.5 Confocal microscopy and image analysis

For analysis of vascular parameters in frozen sections stained with immunofluorescence, an Olympus FV1000 confocal microscope was used. Multi-area time-lapse imaging was performed such that the entire tumour cross-section was visualized over its entire thickness, and the compiled three-dimensional image stack was used included for image analysis. Quantification of the stained area was performed using an in-house segmentation algorithm (MATLAB, The Mathworks, Natick, MA). Analysis of vessel diameter and vessel density was performed using an in-house MATLAB algorithm which skeletonized the entire tumour vasculature before determining the mean diameter of each vessel segment and hence the mean vessel diameter for each tumour. Analysis of pericyte-endothelial cell proximity was performed by fitting the intensity profile around the vessels (determined by CD31 staining) to an exponential function ($I = Ae^{-x/L} + C$), where I = pixel intensity, x = distance from vessels (1 to 10um), and L = characteristic length.

2.6 Statistical Methods

All animal experiments were designed after consultation with a statistician. Statistical analysis was performed using GraphPad Prism Software version 5.0 (GraphPad Software, Inc). Unless otherwise specified, statistical comparisons between experimental groups were made using the unpaired t-test. The chi-squared and Fisher's exact tests were used as indicated to compare the relative

distribution of metastatic events (by size or location). Repeated measures one-way analysis of variance (ANOVA) was used for the analysis of primary tumour growth curves. Survival analysis was performed using the Log-rank (Mantel Cox) test. All statistical tests were two-sided. Differences were considered statistically significant at a *p* value less than 0.05.

3 Chapter Three: The effects of AKB-9778 on Tie-2 activation and endothelial cell junctional proteins

3.1 The effects of AKB-9778 on endothelial cell Tie-2 signaling *in vitro*

Data provided by Akebia Therapeutics (manufacturers of AKB-9778, unpublished) suggest that AKB-9778 is a potent and specific inhibitor of the Vascular Endothelial Protein Tyrosine Phosphatase (VE-PTP). Given that VE-PTP is known to dephosphorylate (and hence inactivate) the endothelial cell (EC) Tie-2 kinase, the capacity for AKB-9778 to activate Tie-2 signaling in ECs was determined.

Human umbilical vein endothelial cells (HUVECs) and human microvascular endothelial cells (HMVECs) were treated with AKB-9778 *in vitro* for 15 or 30 minutes. In both cases, immunoprecipated Tie-2 from cell lysates showed a marked increase in tyrosine phosphorylation after AKB-9778 exposure (Fig 2 & 3).

To determine if this increase in Tie-2 phosphorylation was associated with activation of Tie-2 signaling, assays for changes in the phosphorylation of known effector molecules lying downstream of Tie-2 in EC's were performed. In both HUVECs (Fig 4) and HMVECs (Fig 5), short-term exposure to AKB-9778 led to a rapid and potent increase in phosphorylation of AKT (serine 473 residue) and endothelial nitric oxide synthase (eNOS, serine 1177 residue). These results strongly suggest that AKB-9778 activates Tie-2 signaling within ECs.

Given that AKB-9778 is a phosphatase inhibitor, it is possible that the changes observed above could be the result of non-specific EC phosphatase inhibition rather than a specific effect of VE-PTP inhibition and thus Tie-2 activation. To address this possibility, a *Tie2-shRNA* construct to knockdown the expression of Tie-2 within HUVECs was used (Figure 6, left). *Tie-2-shRNA HUVECs* and *scrambled-shRNA* HUVECs were treated with AKB-9778. HUVECs with diminished Tie-2 expression showed a marked abrogation of AKT and eNOS phosphorylation in response to AKB-9778, establishing the target specificity of AKB-9778 (Figure 6, right).

3.2 The effects of AKB-9778 on Tie-2 activation *in vivo*

Tie-2 phosphorylation after AKB-9778 exposure *in vivo* was determined next. Female nude mice were injected with a single dose of AKB-9778 intravenously (IV), and the lungs removed after 1h. Tie-2 was then immunoprecipitated from whole lung lysates, and blotted for phospho-tyrosine. AKB-9778 induced strong phosphorylation of Tie-2 tyrosine residues (Fig 7, left). The same experiment was repeated in female nude mice bearing orthotopic 4T1 mammary tumours. One hour after IV injection of AKB-9778, an increase in Tie-2 phosphorylation within tumour lysates was seen (Fig 7, right).

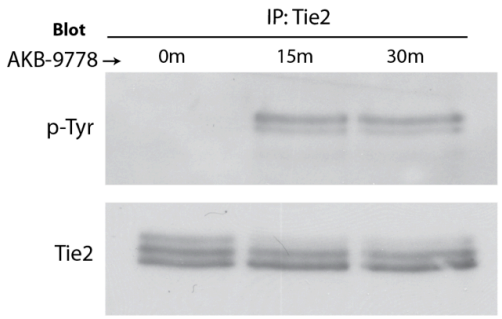

Figure 2: Tie-2 tyrosine phosphorylation in human umbilical vein endothelial cell (HUVEC) lysates after AKB-9778 treatment. Experiments were repeated in triplicate, with similar results (p-Tyr:Tie2 band intensity ratio is 0.24, 0.88, and 0.84 for 0m, 15m, and 30m respectively).

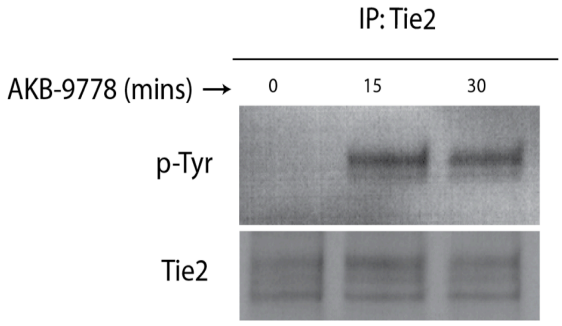

Figure 3: Tie-2 tyrosine phosphorylation in human microvascular endothelial cell (HMVEC) lysates after AKB-9778 treatment. Experiments were repeated in duplicate, with similar results (p-Tyr:Tie2 band intensity ratio is 0.24, 0.88, and 0.84 for 0m, 15m, and 30m respectively).

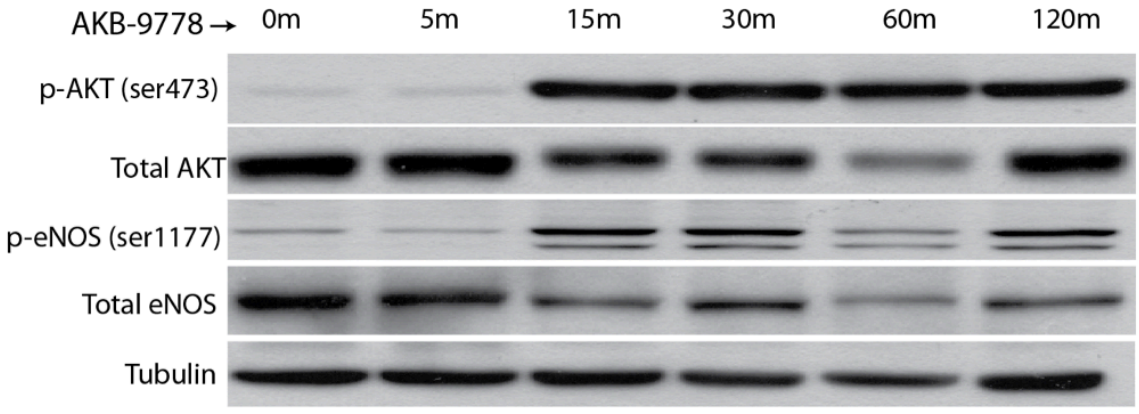

Figure 4: Levels of phosphorylated AKT (ser 473), total AKT, phosphorylated eNOS (ser 1177), and total eNOS in HUVEC lysates after treatment with AKB-9778. Experiments were repeated in triplicate, with similar results (Ratio of band intensities p-AKT:total AKT is 0.28, 0.30, 1.05, 1.13, 1.47, and 0.91 for 0m, 5, 15m, 30m, 60m, and 120m respectively. Ratio of band intensities p-eNOS:total eNOS is 0.38, 0.39, 1.05, 1.13, 1.47, and 0.91 for 0m, 5, 15m, 30m, 60m, and 120m respectively

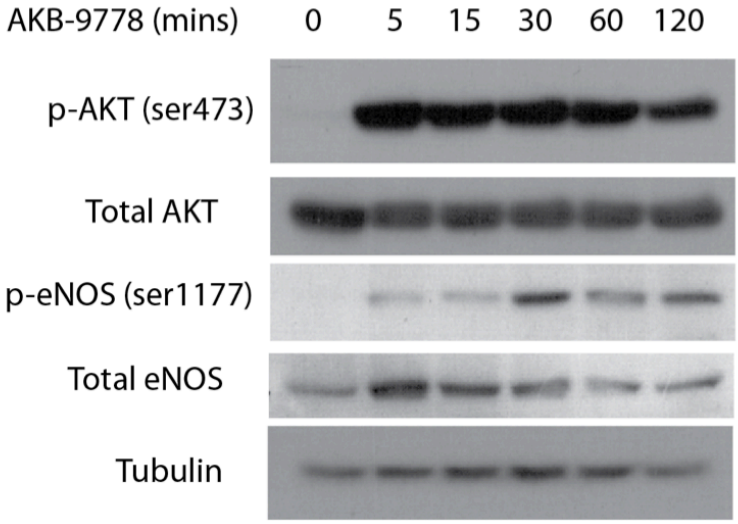

Figure 5: Levels of phosphorylated AKT (Ser473), total AKT, phosphorylated eNOS (Ser1177), and total eNOS in HMVEC lysates after treatment with AKB-9778. Experiments were repeated in duplicate, with similar results.

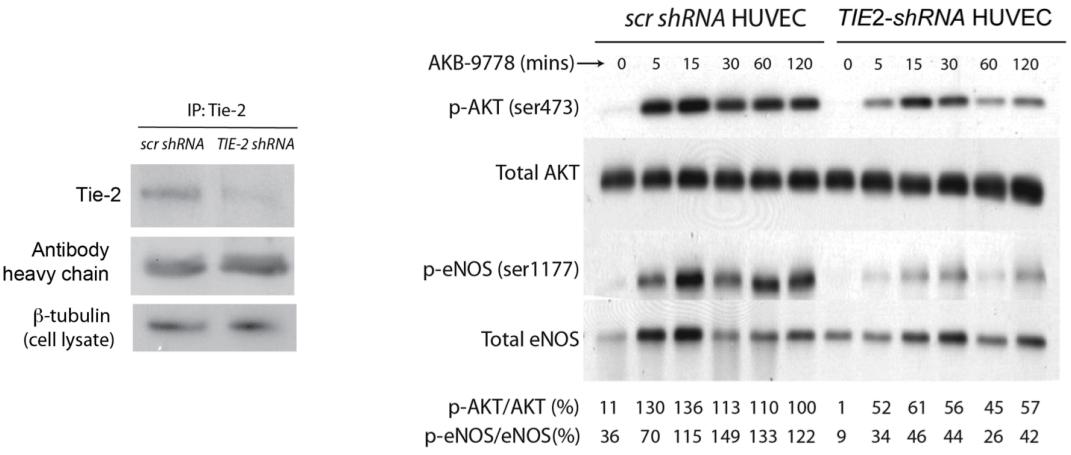

Figure 6: Left, Confirmation of *TIE-2* knockdown after *TIE-2 shRNA* transduction to HUVECs (densitometry confirms knockdown of 75% at protein level). Right, Phosphorylated AKT (ser 473 residue), total AKT, phosphorylated eNOS (ser 1177 residue), and total eNOS levels in HUVEC lysates or *Tie2-shRNA* HUVEC lysates after exposure in vitro to AKB-9778. Experiments were repeated in triplicate, with similar results.

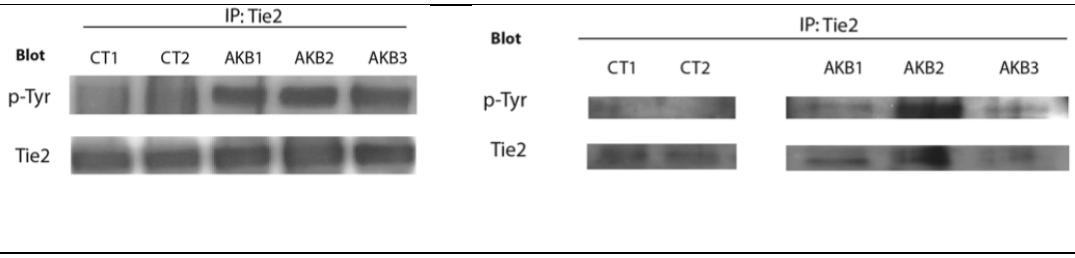

Figure 7: Left, Tie-2 tyrosine phosphorylation in murine whole lung lysates 1h after intravenous injection of AKB-9778 or control vehicle. Experiment was repeated in duplicate, with similar results. Right, Tie-2 tyrosine phosphorylation in murine orthotopic 4T1 mammary carcinoma lysates 1h after intravenous injection of AKB-9778 or control vehicle. CT1 and 2, and AKB1, 2, and 3 represent tumor samples from individual mice from the same experiment. Experiment was performed once only.

3.3 The impact of AKB-9778 Tie-2 activity in different ligand contexts

The effect of Tie-2 ligands angiopoietin-1 (Ang-1) and angiopoietin-2 (Ang-2) upon AKB-9778-induced Tie-2 activation was next determined. *In vitro,* Ang-1 acts as a potent Tie-2 agonist and in keeping with this, was found to activate the Tie-2 pathway in HUVECs (Fig 8). Ang-2 can demonstrate mixed agonistic/antagonistic effects on Tie-2, and in our experiments we found minimal change in Tie-2 signaling in HUVECs after Ang-2 treatment. Importantly, AKB-9778 induced similar levels of Tie-2 pathway activation (measured by p-AKT and p-eNOS) in the presence of Ang-1, Ang-2, both, or neither (Fig 8). This ligand-independent activation of Tie-2 suggests that it could stimulate Tie-2 activity regardless of ligand levels in the local microenvironment.

3.4 Effects of AKB-9778 on endothelial cell junctional proteins

In addition to Tie-2, the EC-EC adhesion molecule VE-Cadherin has also been reported to interact with VE-PTP, either directly or indirectly though phosphorylation of plakoglobin (gamma-catenin). Therefore, the effects of AKB-9778 on VE-Cadherin and plakoglobin phosphorylation within HUVECs were examined. AKB-9778 treatment of HUVECs induced tyrosine phosphorylation of both of these EC junctional proteins (Fig 9 a,b). Importantly, AKB-9778 did not induce phosphorylation of serine residues on VE-Cadherin (a key determinant of VE-Cadherin internalization and degradation, Fig 9c). Furthermore, the total amount of membrane-associated VE-Cadherin after AKB-9778 treatment did not

change, whether assessed by western blot of fractionated cell lysates (Fig 9d, f) or immunofluorescence (Fig 9e).

Collectively the data presented in Chapter Three shows that AKB-9778 is a potent inhibitor of VE-PTP that induces Tie-2 activation in ECs in a ligand-independent fashion. Furthermore, although VE-Cadherin phosphorylation is also increased by AKB-9778, there is no change in VE-Cadherin subcellular localization.

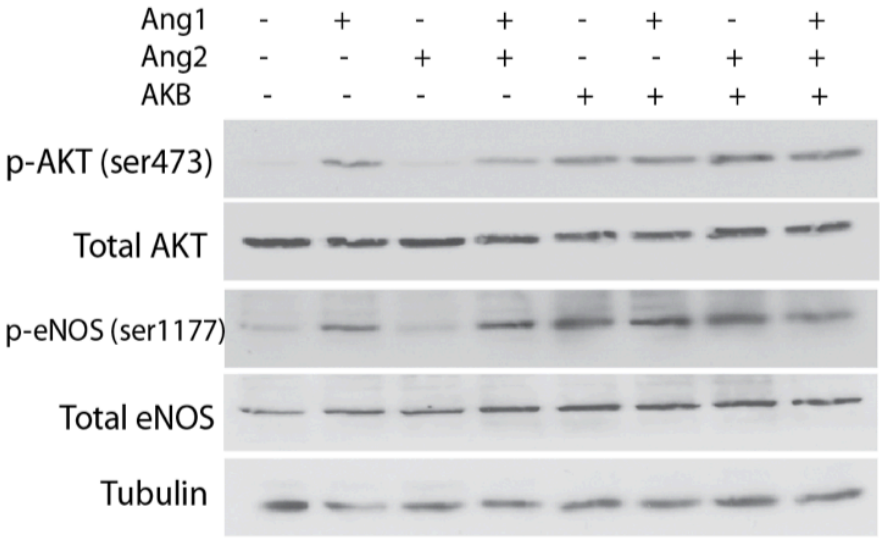

Figure 8: Levels of phosphorylated AKT (ser 473), total AKT, phosphorylated eNOS (ser 1177), and total eNOS in HUVEC lysates after 30 minutes' treatment with Ang-1, Ang-2, and/or AKB-9778. Experiments were performed in duplicate, with similar results.

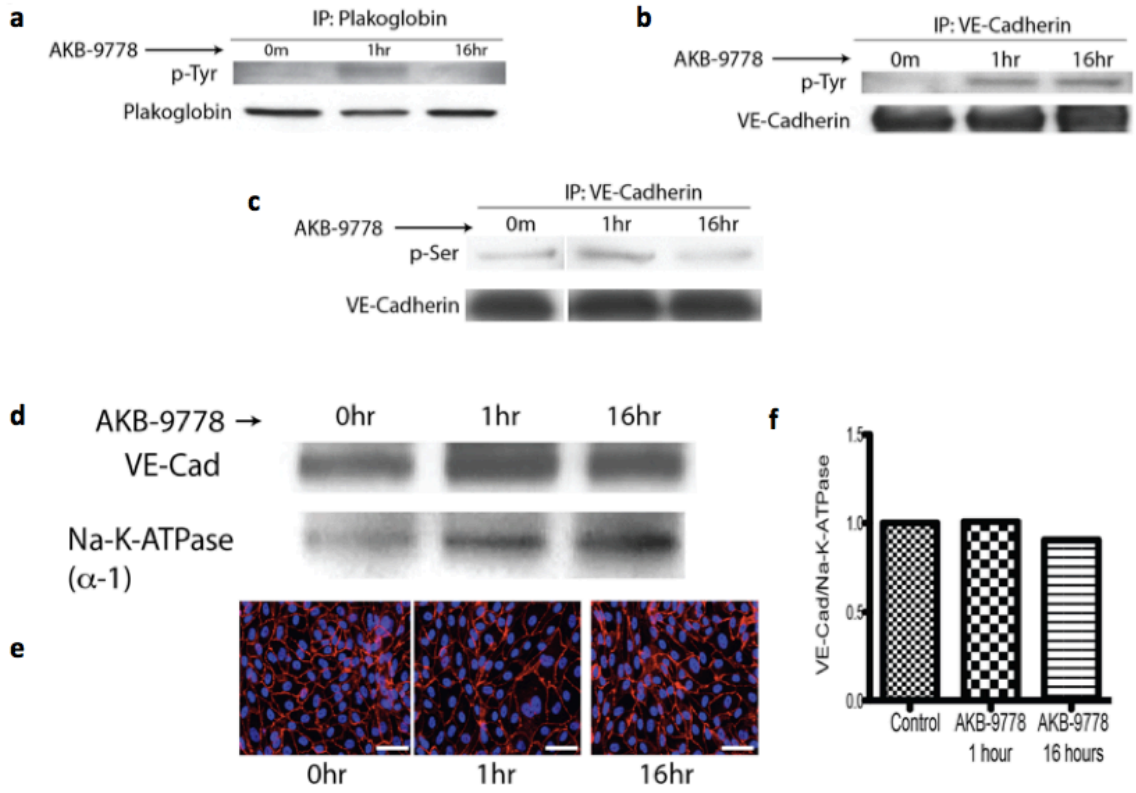

Figure 9: a) Western blot for phospho-tyrosine and total plakoglobin levels in HUVEC lysates after immunoprecipation for plakoglobin. b) Western blot for phospho-tyrosine and total VE-Cadherin levels in HUVEC lysates after immunoprecipation for VE-Cadherin. c) Western blot for phospho-serine and total VE-Cadherin levels in HUVEC lysates after immunoprecipation for VE-Cadherin (band densitometry ratios of p-ser:VE-Cad are 0.163, 0.276, and 0.142 for 0, 1, and 16h respectively). d) Confluent HUVECs were exposed to AKB-9778 *in vitro* for indicated time. Lysates were fractionated into cellular membrane and non-membrane fractions. Western blot shows total VE-Cadherin in membrane fraction (Na-K-ATPase as loading control). e) Immunofluorescence for VE-Cadherin in HUVECs after treatment with AKB-9778 over the same time course, scale bars 20 μm. f) Quantitative densitometry of Western blot in upper panel.

4 Chapter Four: The effects of AKB-9778 on embryonic angiogenesis

VE-PTP null mice are embryonically lethal due to severe defects in angiogenesis attributed to Tie-2 hyperactivation (Baumer et al., 2006, Dominguez et al., 2007). Because the VE-PTP phosphatase domains of *Danio rerio* (zebrafish) and *Mus musculus* have high sequence homology, we evaluated the effects of AKB-9778 on embryonic vessels in zebrafish. This was done in order to further characterize the activity of AKB-9778 as a VE-PTP inhibitor.

4.1 Impact of AKB-9778 on embryonic angiogenesis in *Danio rerio*

Flk1:GFP zebrafish demonstrate expression of green fluorescent protein (GFP) in endothelial cells, allowing clear visualization of blood vessels. *Flk1:GFP* zebrafish embryos were incubated in AKB-9778 and the developing vasculature was examined at 48h post-fertilization (hpf) under epifluorescence.

AKB-9778 induced specific defects in embryonic angiogenesis using this model (Fig 10). Of note, intersegmental vessels (ISVs) showed marked tortuosity and reduced sprouting. Furthermore, many ISVs had failed to reach the dorsal longitudinal anastomotic vessel (DLAV) by 48hpf, indicating impaired angiogenesis (Fig 10, middle and lower panels). When quantified, there was a statistically significant reduction in the number of ISVs making contact with the DLAV in the embryos incubated in AKB-9778 (Fig 11).

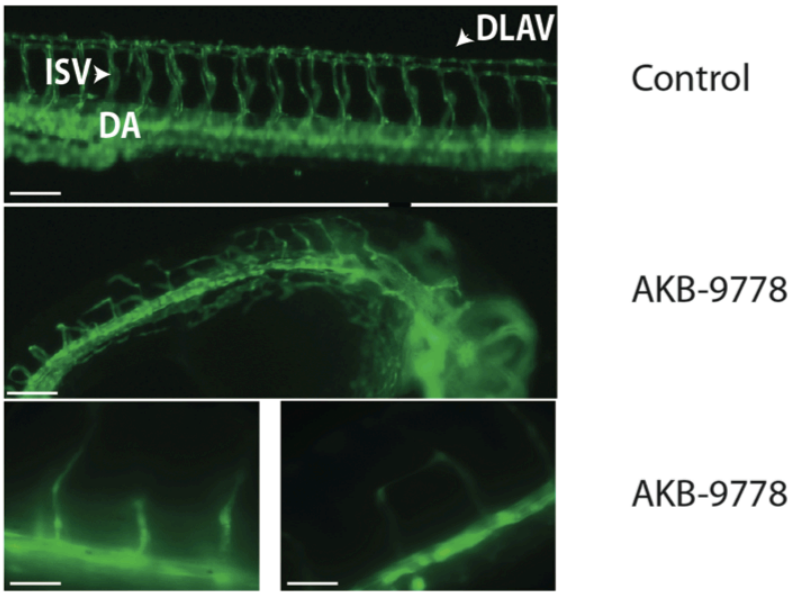

Figure 10: Representative epifluorescence micrographs of *Flk-1:GFP* zebrafish embryos treated with control vehicle (DMSO) (top panel) or AKB-9778 (middle panel) at 48h post-fertilization (hpf). Lower panels (left and right) show high-powered images of AKB-9778-treated embryos at 48 hpf. [DA = dosal aorta; ISV = intersegmental vessel; DLAV = dorsal longitudinal anastomotic vessel]. Scale bars: top panel = 100μm; middle = 75μm; bottom panels = 50μm.

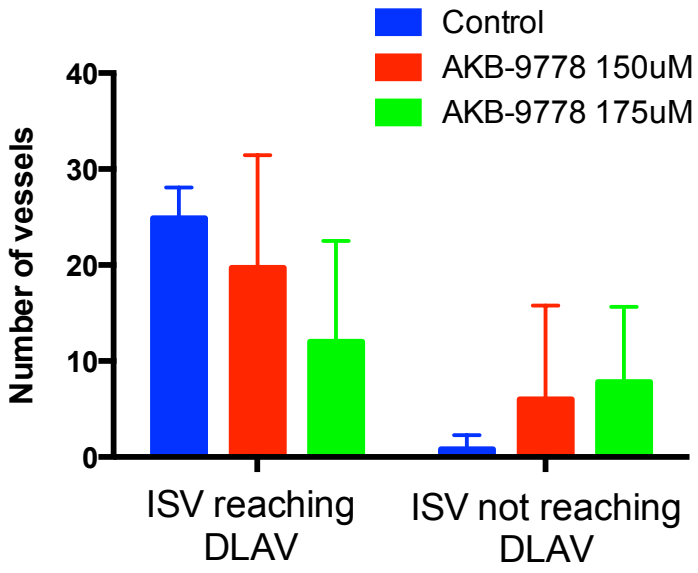

Figure 11: Percentage of vessels that sprouted from the dorsal aorta to reach the dorsal longitudinal anastomotic vessel in zebrafish embryos treated with control vehicle (DMSO) or AKB-9778 (*$p < 0.0001$ by Chi-squared test, n = 5-6 embryos per group).

4.2 Impact of AKB-9778 on angiogenesis in a *Danio rerio* xenograft model

A previously reported assay of tumour angiogenesis using zebrafish embryos (Nicoli and Presta, 2007) was then utilized to study the effects of AKB-9778 upon early tumour angiogenesis (in the context of an embryonic system). This assay was performed with the assistance of Dr Brian Walcott of the Massachusetts General Hospital, Boston MA (Fig 12). Murine mammary carcinoma cells expressing the dsRed fluorescent protein (4T1-dsRed) were implanted into the avascular perivitelline space of *Flk1:GFP* zebrafish embryos at 48hpf. Within 48h of implantation, a small tumour mass was visible (Fig 12, left). Using confocal microscopy, nascent vessels were observed sprouting into the tumour mass (Fig 12, centre). The degree of tumour angiogenesis was determined by dividing the total GFP-positive area within the tumour by the total tumour area (Figure 12, right). Consistent with the findings in the embryonic angiogenesis model, there was a reduction in the degree of tumour neoangiogenesis amongst those embryos incubated in AKB-9778 for 48h after tumour implantation (Figure 13).

Collectively, the data presented in Chapter Four show that as a VE-PTP inhibitor, AKB-9778 induces a failure of embryonic angiogenesis, akin to that previously reported in *VE-PTP* null mice. Moreover, AKB-9778 hinders tumour angiogenesis in the zebrafish embryo tumour xenograft assay.

The remainder of this thesis pertains to the consequences of VE-PTP inhibition with AKB-9778 in an adult mammalian model organism *(Mus musculus)*, with a specific focus on the solid tumour vasculature.

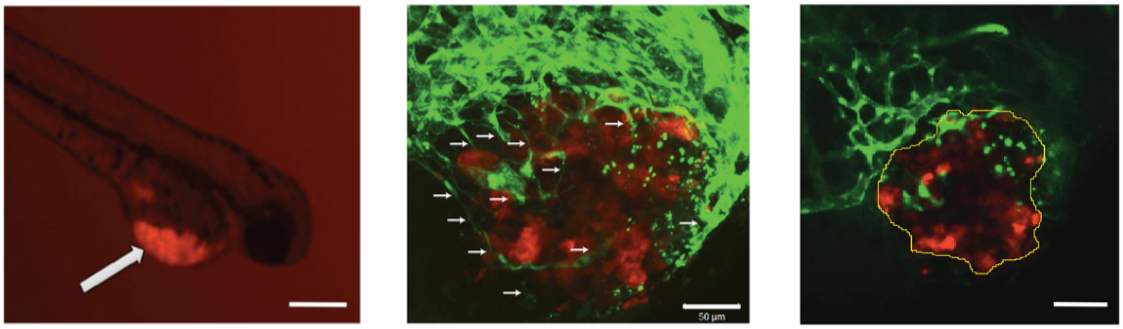

Figure 12: **Xenograft tumour growth and vascularization in the zebrafish perivitelline space**. Left, Confocal micrograph demonstrating growth of a 4T1-dsRed mammary carcinoma in the perivitelline space of a zebrafish embryo (white arrow indicates tumour, scale bar 270 μm). Centre, High power confocal micrograph demonstrating neovascularization of a 4T1-dsRed xenograft in a *Flk-1:GFP* zebrafish embryo. Nascent vessels (green) are indicated by white arrows (scale bar 50 μm). Right, Method for delineating tumour area for analysis of xenograft vessel density in zebrafish embryos. Area considered as "tumour area" is outlined by yellow-dashed line (scale bar 50 μm).

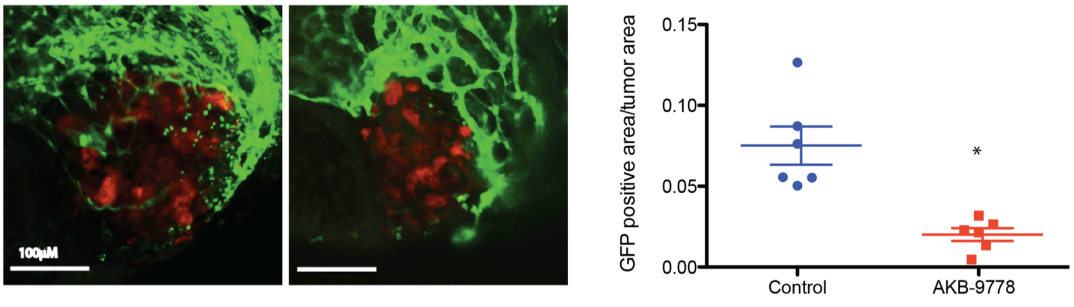

Figure 13: Left, 4T1-dsRed mammary carcinomas growing in *Flk-1:GFP* zebrafish embryos treated with control vehicle (left panel) or AKB-9778 (right panel). Right, Vessel density (determined as GFP-positive area/tumour area) from experiment in (c) (**p* = 0.001 by t-test, n = 6 embryos per group. Value for each embryo is determined as the mean of five individual micrographs taken throughout each tumour).

5 Chapter Five: The effects of AKB-9778 on murine mammary carcinoma

5.1 The effects of AKB-9778 on the early stages of primary tumour angiogenesis and growth

The effects of VE-PTP inhibition on the earliest phase of primary tumour development were studied next. During this time, tumour cells typically co-opt normal host ECs (Holash et al., 1999), leading them to overexpress Ang-2 and VE-PTP (Holash et al., 1999, Dominguez et al., 2007). This is in turn facilitates vascular destabilization, allowing for the onset of sprouting angiogenesis (Holash et al., 1999). Furthermore, abrogation of Ang-2 activity has been shown to specifically slow this earlier phase of tumour development, related at least in part to the prevention of early vessel destabilization (Nasarre et al., 2009).

5.1.1 Impact of AKB-9778 on the early phase of primary tumour growth

4T1 murine mammary carcinoma cells were implanted orthotopically into the mammary fat pads of female nude mice, and VE-PTP inhibition with AKB-9778 was initiated 24h later. AKB-9778 delayed the early phase of solid tumour growth (Fig 14, left) but had no impact on the later phases of tumour growth. Similar results were seen using the E0771 mammary carcinoma model in syngeneic C57Bl6/J mice (Fig 14, right). When growth curves from the 4T1 experiment are re-plotted using a logarithmic scale on the y-axis, it is clear that differences in primary tumour size are exclusively due to a delay in the early

phase of tumour growth (Fig 15). Of interest, these results mirror those seen when solid tumours are grown in Ang-2 deficient mice (Nasarre et al., 2009).

Of note, VE-PTP gene expression was not detectable in either cell line by RT-PCR, and AKB-9778 had virtually no cytotoxic effects on these cells in vitro (IC_{50} >300μM), suggesting that the our observations were not caused by a direct effect of AKB-9778 on tumour cell growth.

5.1.2 Impact of AKB-9778 upon vessel stability during early tumour growth

The vasculature of treated and untreated mammary tumours during the early phase of tumour growth was next examined. 4T1 cells were implanted orthotopically as before and AKB-9778 or control vehicle treatment begun after 24h. After 7-8 days (when tumour growth rates were discrepant, and tumour diameter was less than 1mm), tumours were resected and stained for NG2 (a marker of pericytes) and CD31 (a marker of ECs). After image analysis, it was noted that AKB-9778 treated tumours showed a significantly higher degree of EC coverage by pericytes. Furthermore, the mean distance between pericytes and EC's was significantly reduced in AKB-9778 treated tumours (Fig 16, 17).

Collectively, the data presented in section 5.1 shows that inhibition of VE-PTP hinders vascular destabilization during the early phase of tumour growth – evidenced by enhanced vascular pericyte coverage. This is also associated with a delay in the early, but not later, phase of tumour growth – an observation which phenocopies that seen for tumours grown in Ang-2 deficient mice, and is consistent with the known effects of Tie-2 activation.

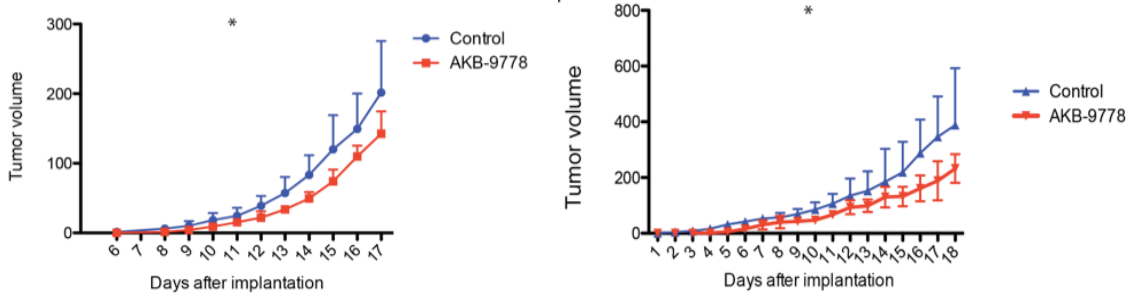

Figure 14: Left, Tumour growth curve for orthotopic 4T1 mammary carcinoma. Treatment with AKB-9778 or control vehicle was begun 24h after cell implantation. Curves show a delay in the early phase of primary tumour growth (*p < 0.01 by 2 way ANOVA, n = 6 per group). Right, Tumour growth curves for orthotopic E0771 mammary carcinoma. Treatment with AKB-9778 or control vehicle was begun immediately after cell implantation (*p < 0.01 by 2 way ANOVA, n = 6 per group). Note: in the first week of growth, AKB-9778 treated tumours grew as flat, ovoid discs whereas control tumours were spherical.

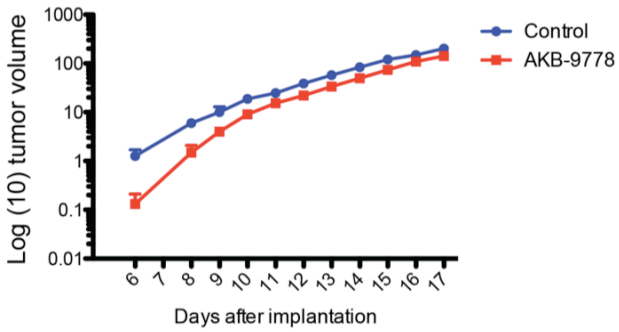

Figure 15: Data from Figure 14 (left panel) is plotted again with a log(10) scale on the y axis. Curves demonstrate that the difference in primary tumour size is due exclusively to a delay in the early phase of tumour growth.

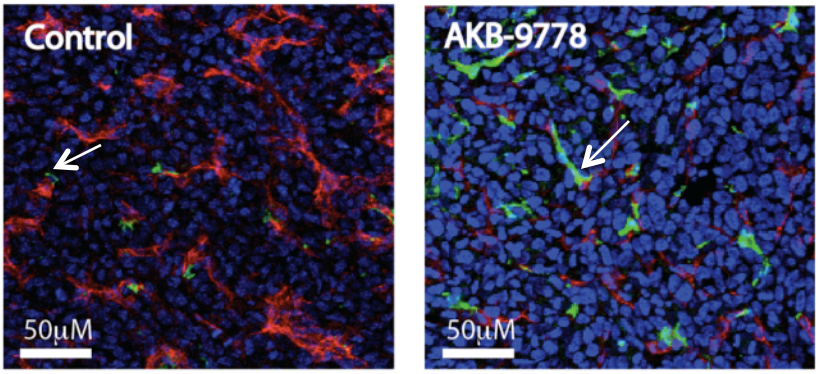

Figure 16: Representative fluorescent confocal micrographs of control treated (left panel) and AKB-9778 treated (right panel) tumours from the experiment depicted in Figure 17 (red, CD31; green, NG2; blue, DAPI). All error bars represent SD. Arrows exemplify the difference in pericyte-EC separation.

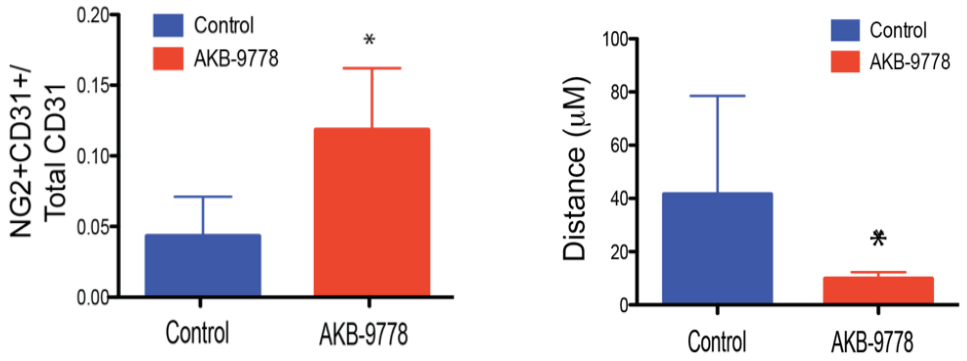

Figure 17: 4T1 mammary carcinoma was implanted orthotopically and treatment with AKB-9778 or control vehicle was begun 24 h later. After 7-8 days (when growth rates of AKB-9778 and control-treated tumours are discrepant), tumours were harvested. Left: Pericyte coverage in control and AKB-9778 tumours is shown (NG2 - pericyte marker; CD31 - endothelial cell marker; *p = 0.02 by 2-sided t-test, n = 5 per group). Right: Distance between pericytes and endothelial cells in the same tumours shows increased distance between these cell types in control-treated tumours (*p = 0.05 by 2 sided t-test, n=5 per group).

5.2 The effects of AKB-9778 on the growth of metastatic tumours

The earliest phase of primary tumour growth is not relevant to clinical oncology as patients only present once tumours are well established. At this time, however, there are often foci of disseminated tumour cells (micrometastases) that are clinically undetectable but may grow in subsequent years to form macrometastatic lesions. The rationale behind adjuvant therapy (systemic therapy given after resection of a primary tumour) is to prevent or delay the growth of these micrometastatic lesions.

When circulating tumour cells lodge in the vessels of distant organs, they induce EC overexpression of Ang-2 and therefore facilitate vascular destabilization, followed by tumour cell extravasation into distant organ parenchyma (Holash et al., 1999, Holopainen et al., 2012, Avraham et al., 2014). Given this, and the previous observation that VE-PTP inhibition with AKB-9778 delays the early phase of primary tumour growth, we next studied the effects of AKB-9778 on the early growth of metastatic lesions.

5.2.1 Impact of adjuvant AKB-9778 therapy on the spontaneous metastatic burden

A model of spontaneous 4T1 mammary carcinoma metastasis was used to specifically study the effects of VE-PTP inhibition on metastasis, (Figure 18). Through a series of pilot experiments performed in the Steele Laboratory, it was determined that micrometastatic clumps of tumour cells (less than 100 cells)

were typically first seen in the lungs of 4T1-tumour bearing mice once the primary tumour diameter reached 5mm (data not shown).

Therefore, 4T1 tumours were implanted orthotopically and allowed to grow to 5mm diameter before resection. At this stage, mice were likely to have several micrometastatic lesions. Mice were then randomly assigned to receive treatment with AKB-9778 or control vehicle, and sacrificed 3 weeks later.

At sacrifice, full necropsy was performed with macroscopic examination of lungs, liver, lymph nodes, and bones. AKB-9778 treated mice showed a reduction in the number of metastatic nodules in the lungs (Fig 19, left and Fig 20) and throughout the rest of the body including liver, lymph nodes, and bones (Fig 21). Furthermore, when the size of macroscopically detectable lung metastases was measured with stereomicroscopy, a shift towards smaller metastases in the lungs of AKB-9778 treated mice was seen (Fig 19, right). These results show that VE-PTP inhibition delays the growth of spontaneously arising micrometastatic lesions into macroscopic metastases, reducing the overall metastatic burden.

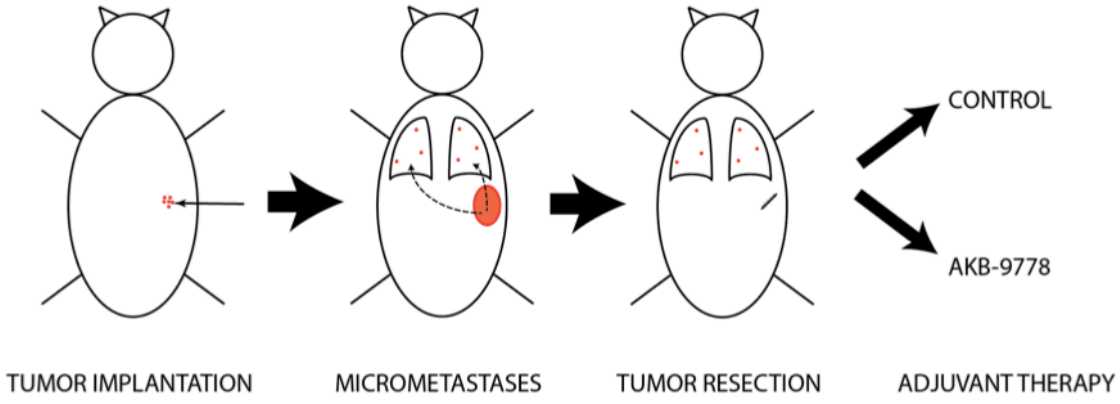

Figure 18: Schema demonstrating model for adjuvant AKB-9778 therapy. Tumours were resected at 5mm diameter.

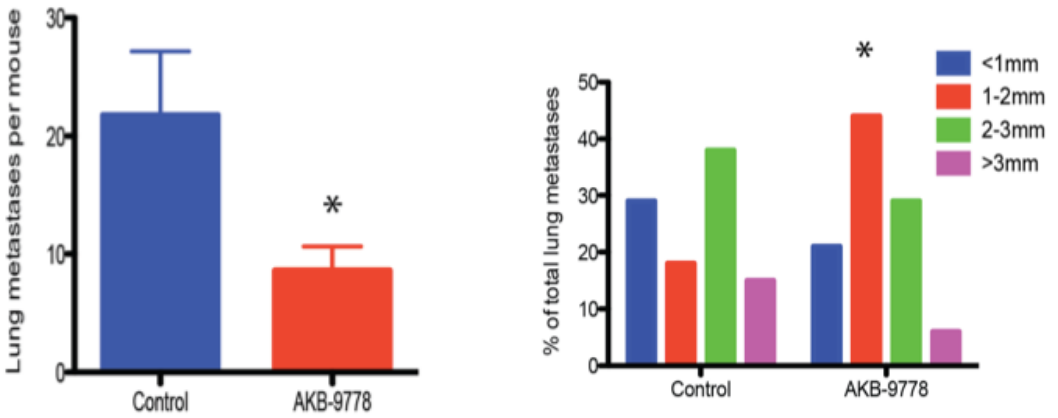

Figure 19: Left, Number of macroscopically detectable lung metastases in control vs. AKB-9778 treated mice (*p = 0.033 by t-test, n = 10 per group) after 3 weeks' treatment. Right, Distribution of size of macrometastatic lung nodules (*p < 0.001 by chi-squared test).

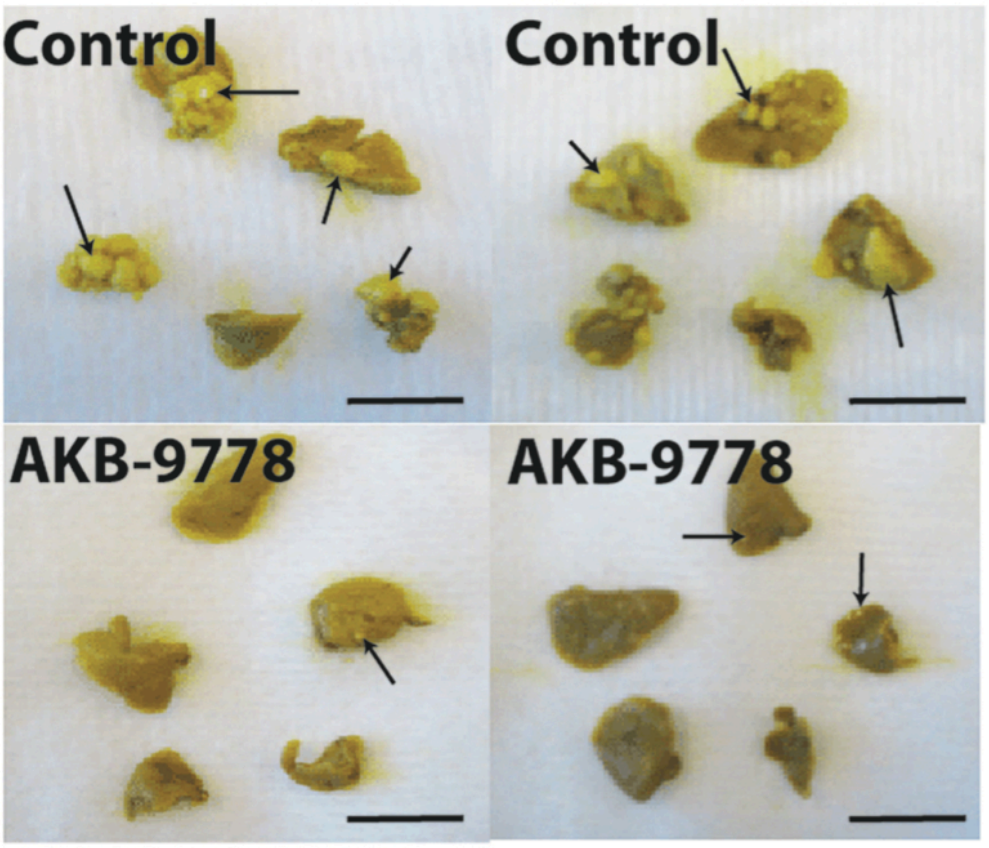

Figure 20: Representative images of lungs visualized after resection in control (upper panels) and AKB-9778 treated (lower panels) mice (from the same experiment depicted in Figure 19). Scale bars = 10mm.

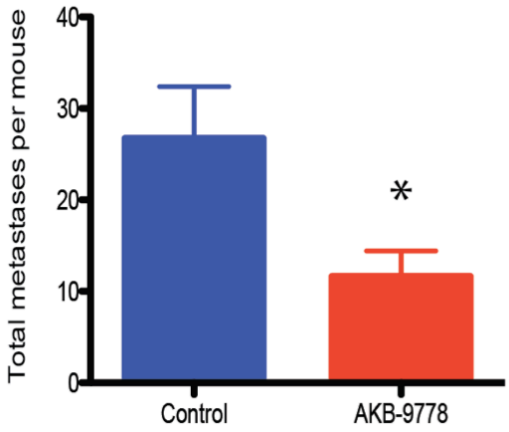

Figure 21: Total number of macroscopically detected metastases (including lung, liver, bone, lymph node, and soft tissue) (*p = 0.029, n = 10 per group, from the same experiment depicted in Figure 19).

5.2.2 The effects of adjuvant AKB-9778 therapy upon the growth of spontaneous micrometastases

To explore this finding in greater detail, the same experiment as described in Figure 18 was repeated, but lungs were resected after only 2 weeks of treatment. At this time point, macroscopic lung nodules were rarely seen. Multiple histologic sections were taken through each lobe of each lung (as detailed in Materials and Methods) and with the assistance of a trained pathologist, histologically detectable metastatic lesions were identified, counted, and measured in cross-sectional area using digital image analysis.

The number of mice in which metastatic lesions were observed was not significantly different between AKB-9978 and control-treated mice (Fig 22, left). However, there was a significant reduction in the average cross-sectional area of metastatic lesions observed in AKB-9778- treated mice (Fig 22, right and Fig 23).

These results are consistent with those from the immediately preceding experiment, and again show that VE-PTP inhibition slows the growth of micrometastatic lesions.

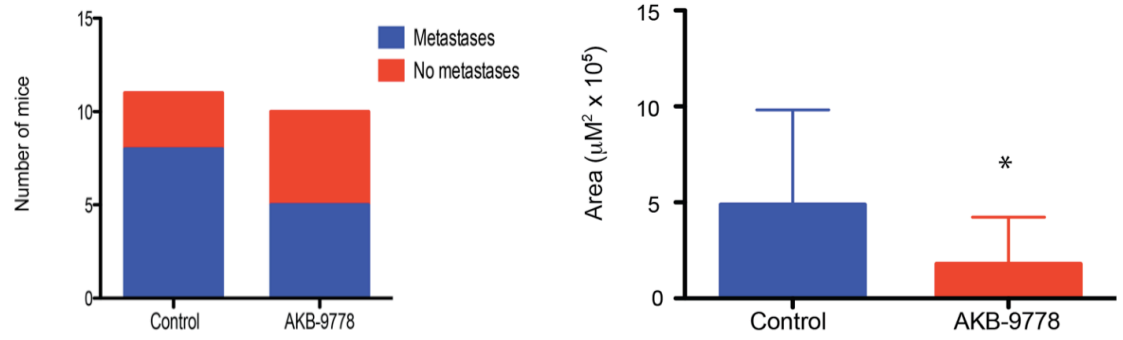

Figure 22: An adjuvant therapy model treating spontaneous metastasis was used as in Figure 18. Lungs were resected following 2 weeks of continuous treatment after primary tumour resection. Left, Number of mice with histologically detectable metastases (p = 0.38, two-sided Fisher's exact test). Right, Mean area of micrometastases (*p = 0.05 by two-sided t-test, n = 10-11 mice per group, 3 sections through each lobe analyzed. Data show all metastases pooled).

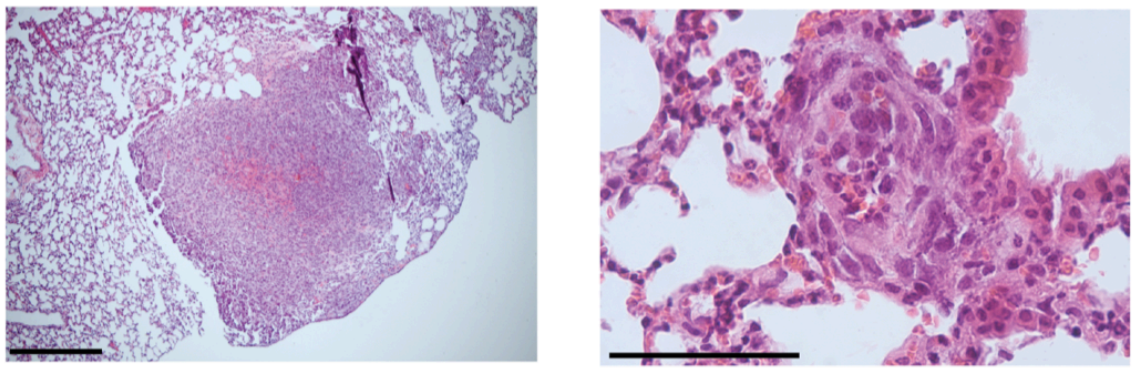

Figure 23: Representative histologic images of metastases in control (left panel, 40x original magnification) and AKB-9778 (right panel, 400x original magnification) treated lungs from the experiment depicted in Figure 22 (scale bars represent 500 μm in the left panel, 50 μm in the right panel).

5.2.3 Effect of adjuvant AKB-9778 on the extravasation of disseminated tumour cells into distant organ parenchyma

We hypothesized that the effect of AKB-9778 upon metastasis growth was specifically due to improved vessel stabilization via activation of Tie-2 signaling. Models of experimental metastasis, in which mammary carcinoma cells are injected intravenously and AKB-9778 treatment commenced 24h later, were used to test this hypothesis.

4T1 tumour cells metastatic to the lung are known to have a prolonged intravascular growth phase before extravasation into surrounding parenchyma (Wong et al., 2002). Here, 4T1 cells were injected intravenously and mice were treated for 8 days before resecting and analyzing lung tissue. The lungs of AKB-9778-treated mice showed significantly smaller micrometastases (Fig 24, left). Histologically, AKB-9778-treated mice showed clumps of micrometastatic cells lodged within alveolar vessels, while control vehicle-treated mice often showed cells that had extravasated into surrounding parenchyma (Fig 24, right). This finding was confirmed upon staining serial sections of lung metastases with hematoxylin and eosin, and collagen IV (a vascular basement membrane marker). AKB-9778 treated mice frequently showed tumour cells that had failed to breach the vascular basement membrane and enter the lung parenchyma (Fig 25).

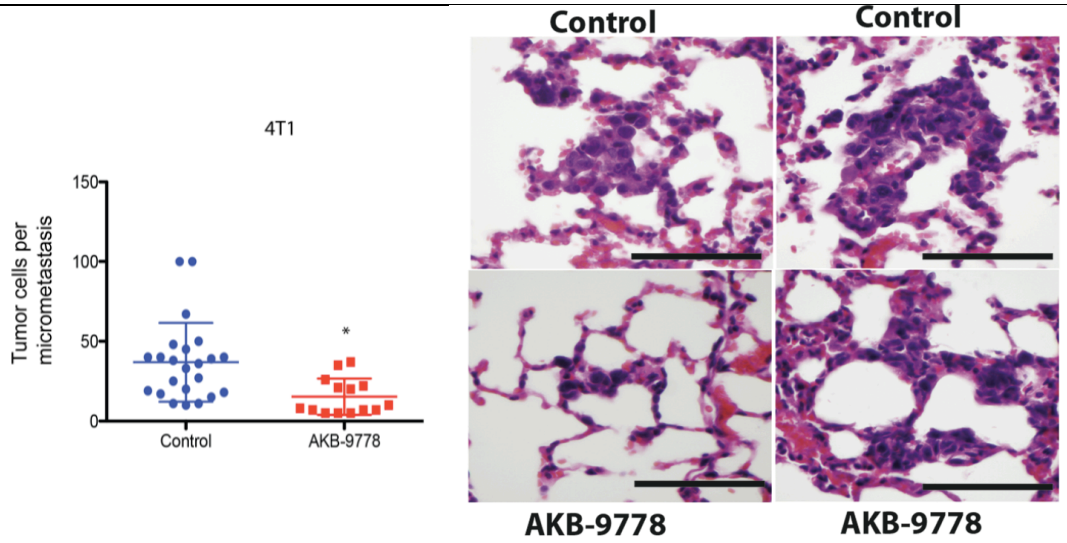

Figure 24: 4T1 tumour cells were injected intravenously and therapy with AKB-9778 or control commenced immediately. 9 days later lungs were resected and micrometastases identified histologically. Left, Data shows the number of tumour cells identified in hematoxylin and eosin stained sections of lung tissue. Each metastasis is represented by an individual data point. (*p < 0.01 by two-sided t-test, 6 mice per group, 3 sections of each lobe examined for each mouse). Right, Representative H&E stained sections of micrometastases. Control lungs (upper panels) show micrometastatic cells that have breached vascular boundaries and entered the alveolar airspace. AKB-9778 treated lungs (lower panels) show cells tracking within vessels, yet to extravasate. Scale bars = 100μm.

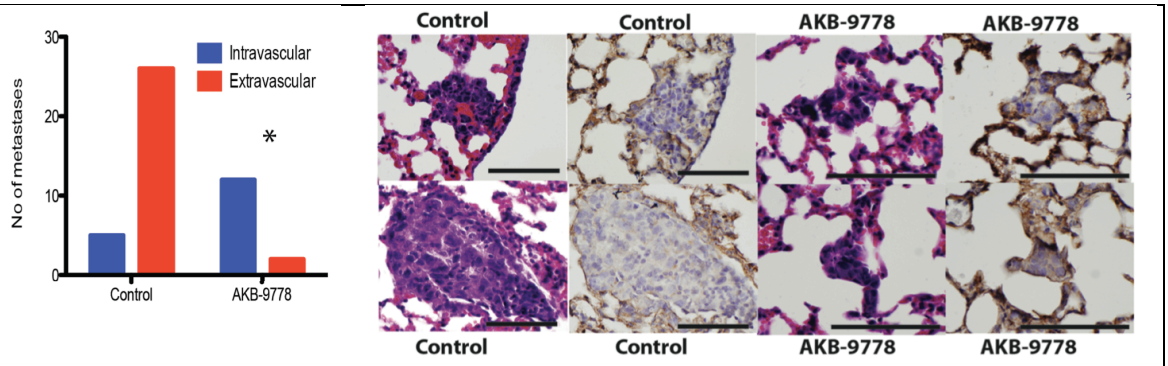

Figure 25: Left, Number of intra- versus extra-vascular micrometastases (*p < 0.0001, n = 6 mice per group) from the same experiment depicted in Figure 24. Right, Representative images of micrometastases. Images show H&E stained sections of micrometastases and serial sections (separated by 5um) showing the same metastasis stained for collagen IV (brown). Control mice show extravasation of tumour cells through the vascular basement membrane but AKB-9778 treated mice show tumour cells retained within vessels. Scale bar = 100μm.

Similar results were seen using an identical experimental system with E0771 mammary carcinoma cells (in syngeneic mice, Fig 26), as well as primary tumour cells derived from tumours that had spontaneously arisen *MMTV-PyVT* transgenic animals (Fig 27).

These results are consistent with those observed using the 4T1 model of spontaneous metastasis, and support the hypothesis that Tie-2 activation through VE-PTP inhibition increases vessel stability, preventing extravasation of metastatic tumour cells into the surrounding parenchymal tissue. This in turn slows the growth of these metastatic lesions.

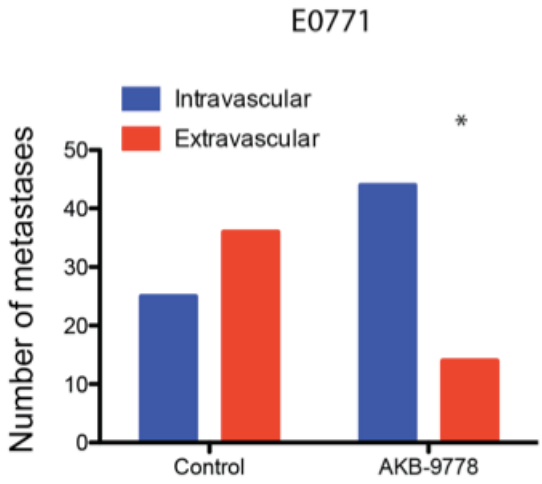

Figure 26: E0771 tumour cells were injected intravenously, therapy commenced, and lungs examined 5 days later. Graph shows ratio of intravascular to extravascular micrometastases (*p < 0.01 by Fisher's exact test, all metastases for each treatment group pooled). All error bars represent SD.

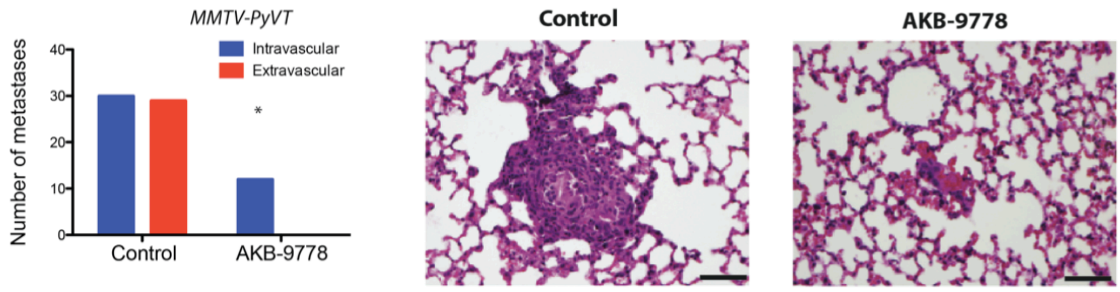

Figure 27: Tumour cells isolated from *MMTV:PyVT* tumours were injected intravenously, therapy commenced, and lungs examined 5 days later. Left, Graph shows ratio of intravascular to extravascular micrometastases (*p < 0.01 by two-sided Fisher's exact test, all metastases for each treatment group pooled). Right, Representative images (40 x H&E staining) of experimental *MMTV-PyVT* tumour cell micrometastases treated with control (left panel) or AKB-9778 (right panel). Scale bars = 100μm.

5.2.4 The impact of adding of AKB-9778 to adjuvant chemotherapy upon mouse survival

In clinical breast oncology, standard adjuvant therapy following surgery for high-risk primary breast cancer includes cytotoxic chemotherapy. Given the observation that VE-PTP inhibition delayed the growth of metastases in the adjuvant setting, we next tested whether the addition of AKB-9778 to standard chemotherapy would prove beneficial.

Using the same experimental design as outlined in Figure 18, mice were randomized to post-operative therapy with doxorubicin chemotherapy, with or without the addition of AKB-9778. Treatment was continued until animals met standard criteria for sacrifice. In this experiment, the addition of AKB-9778 to adjuvant chemotherapy significantly improved mouse survival (Fig 28).

Collectively, the data presented in section 5.2 show that pharmacological VE-PTP inhibition hinders the growth of micrometastases. This is due, at least in part, to the prevention of tumour cell extravasation, which likely relates to Tie-2 hyperactivation reducing vessel permeability. Finally, adjuvant VE-PTP inhibition improves mouse survival when added to standard chemotherapy.

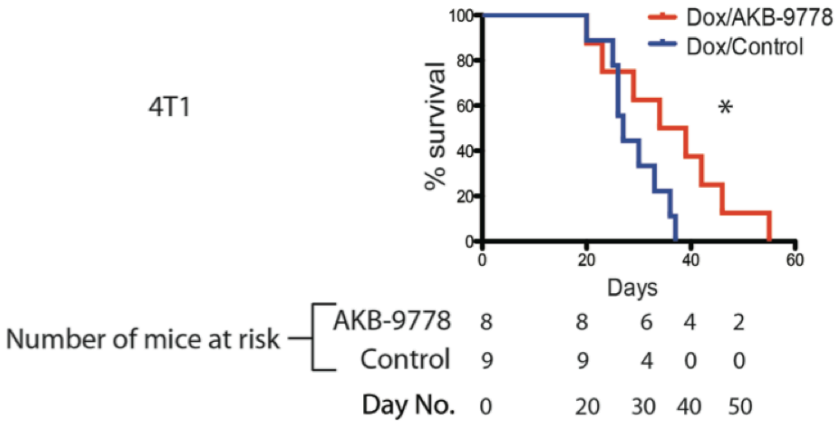

Figure 28: Mouse survival after adjuvant therapy with doxorubicin +/- AKB-9778. (*p = 0.05 using log-rank [Mantel-Cox] test, n = 8-9 mice per group) using a model of 4T1 spontaneous metastasis.

5.3 The effects of AKB-9778 on the structure of established primary tumour vessels

Having explored the consequences of VE-PTP inhibition on the early stages of both primary and metastatic tumour growth, the effects of AKB-9778 on more established primary tumours were studied next. For the purposes of these studies, "established" tumours are defined as tumours that have reached a diameter of 3mm. At this stage, they have passed through the "angiogenic switch" (Bergers and Benjamin, 2003), no longer rely solely upon the native host vasculature, and demonstrate robust angiogenesis with all the hallmarks of tumour vessels.

The effect of AKB-9778 therapy on the structure of blood vessels was examined first. We hypothesized that VE-PTP inhibition would enhance pericyte coverage, increase vessel diameter, and increase vessel density – all consistent with the effects of Tie-2 activation (Suri et al., 1998, Thurston et al., 1999)

5.3.1 Impact of AKB-9778 treatment of established primary tumours upon pericyte coverage of endothelial cells

4T1 mammary carcinoma cells were implanted into female mice and observed until tumours reached a diameter of 3mm. At this point, a 10-day treatment course with either AKB-9778 or control vehicle was initiated. Double immunofluorescent staining of resected tumours for pericyte (NG2 or desmin), and EC (CD31) markers was performed, and entire tumour cross sections were imaged by confocal microscopy and digitally analyzed. AKB-9778 therapy led to

more structurally mature vessels, evidenced by increased perivascular cell coverage (defined as the percentage of total CD31+ area showing co-localization for pericyte staining, Figures 29, 30). In addition, the mean distance between pericytes and ECs was significantly shorter in AKB-9778 treated tumours. Similar results were seen for E0771 mammary tumours, using an identical experimental design (Fig 31).

Sections from the 4T1 tumours in this experiment were also double-stained for the EC junctional protein VE-Cadherin, and CD31. Consistent with our *in vitro* data, total VE-Cadherin levels in tumour ECs were unchanged after nine days of AKB-9778 therapy (Fig 32).

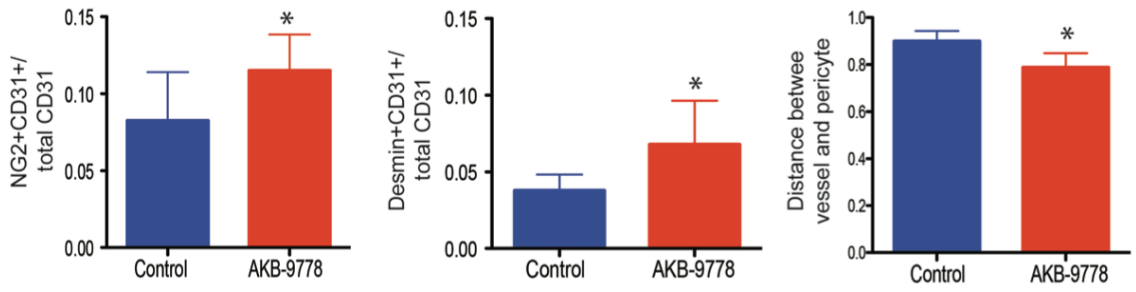

Figure 29: Left, Colocalization of CD31+ area (endothelial cells) and NG2+ area (perivascular cells) (*p=0.049 by t-test, n = 6 per group) in 4T1 tumours. Centre, Colocalization of CD31+ area (endothelial cells) and desmin+ area (perivascular cells) (*p = 0.014 by t-test, n = 6 per group) in 4T1 tumours. Right, Mean distance between desmin+ pericytes and CD31+ endothelial cells (*p = 0.004 by t-test, n = 6 per group) in 4T1 tumours.

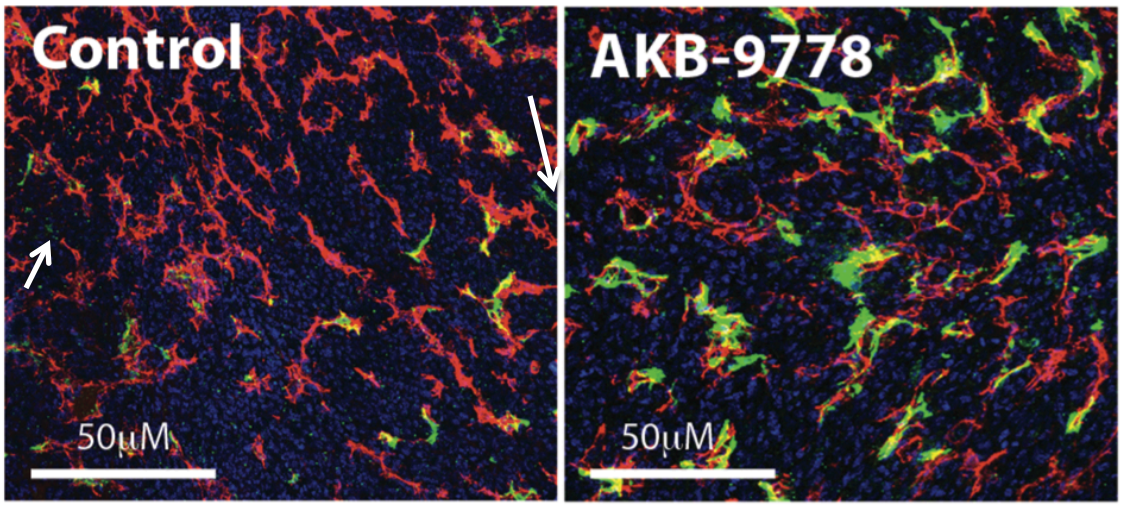

Figure 30: Enhanced vascular pericyte coverage in AKB-9778 treated 4T1 tumours (right panel) compared to control-treated tumours (left panel) (red = CD31, green = NG2, blue = DAPI). White arrows indicate pericytes in control treated tumours that are distant from endothelial cells.

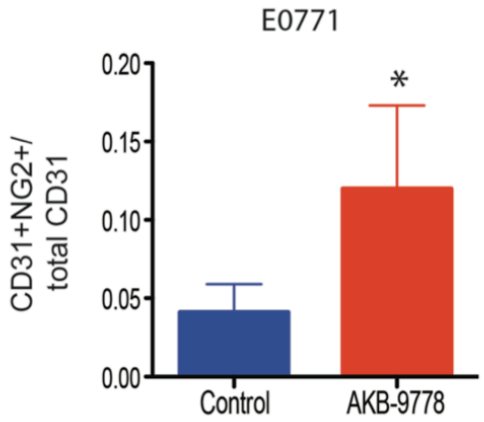

Figure 31: Colocalization of CD31+ area (endothelial cells) and NG2+ area (perivascular cells) (*p = 0.049 by t-test, n = 6 per group) in E0771 tumours (*p = 0.006, n=6 per group).

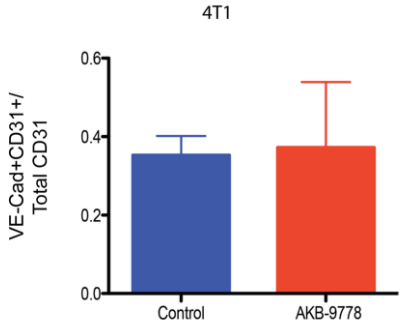

Figure 32: Orthotopic primary 4T1 breast tumours were treated with AKB-9778 or control once reaching diameter 3mm for 10 days. Graph depicts colocalization of VE-Cadherin and CD31 staining (p = 0.82 by two-sided t-test, n = 6 per group).

5.3.2 Impact of AKB-9778 treatment of established primary tumours upon vascular diameter

Whole tumour cross-sectional confocal micrographs from the experiments described in 5.3.1 were then analyzed to determine the mean vessel diameter in 4T1 and E0771 tumours. Using this algorithm, between 3000 and 10,000 vessel segments were analyzed for each individual tumour. In both models, there was a significant increase in vascular diameter in AKB-9778 treated tumours (Fig 33), by approximately 10 percent.

5.3.3 Impact of AKB-9778 treatment of established primary tumours upon vessel density

Finally, the mean microvessel density within tumours from the experiments described in 5.3.1 was determined. Detailed methodology is provided in the Materials and Methods chapter, but in brief a previously developed segmentation algorithm was used to delineate the entire vasculature into individual vessel segments. Vessel density was defined as the number of vessel segments per unit area. There was a statistically significant increase in tumour vessel density in both 4T1 and E0771 tumours treated with AKB-9778 (Fig 34).

Collectively, the results presented in section 5.3 show that pharmacologic VE-PTP inhibition within established primary mammary carcinomas enhances the structural maturity of vessels, and increases vascular diameter and density. These findings are consistent with the phenotype expected as a result of Tie-2 hyperactivation.

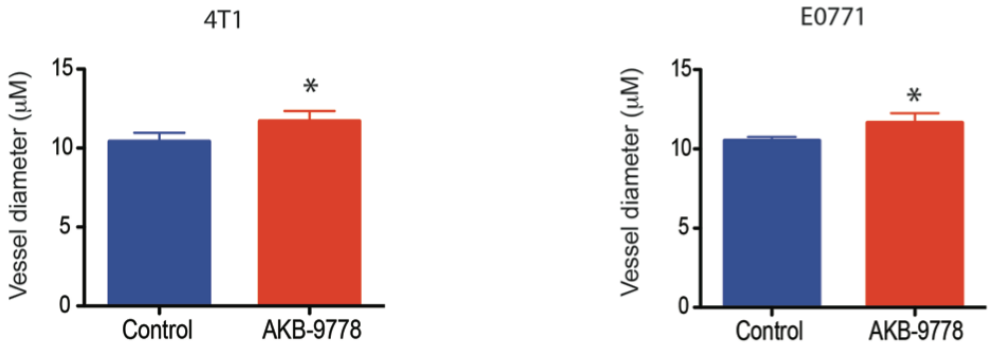

Figure 33: Vessel diameter in control versus AKB-9778 treated 4T1 (left) and E0771 (right) tumours (4T1: *p=0.0032 by t-test, n=6 per group; E0771: *p = 0.001, n = 6 per group).

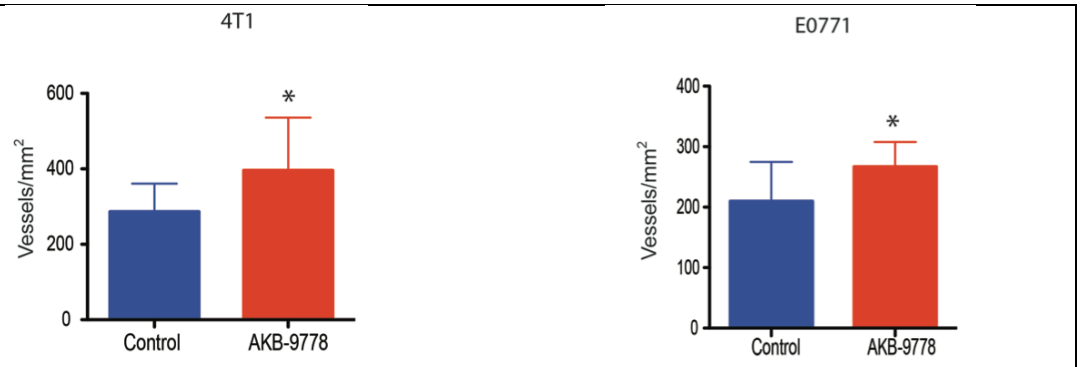

Figure 34: Vessel density in control versus AKB-9778 treated 4T1 (left) and E0771 (right) tumours (4T1: *p = 0.05 by t-test, n = 6 per group; E0771: *p = 0.05, n = 6 per group).

5.4 The effects of AKB-9778 on the function of established primary tumour vessels

Attention was next turned to changes in the function of established primary tumour vessels after treatment with AKB-9778. Given previous findings of enhanced pericyte coverage, increased vessel diameter, and increased vessel density after AKB-9778 treatment, and the known effects of enhanced Tie-2 activity (Suri et al., 1998, Thurston et al., 1999), we hypothesized that VE-PTP inhibition would result in reduced tumour vessel permeability, enhanced tumour perfusion by blood, and a reduction in tumour hypoxia.

5.4.1 Effect of AKB-9778 treatment of established primary tumours upon vascular permeability

To assess changes in tumour vessel permeability after VE-PTP inhibition, intravital microscopy of 4T1 tumours was performed, and the extravasation of intravenously injected bovine serum albumin was quantified at two time points – before initiation of therapy (tumour diameter 3-4mm) and again after 72h of therapy. As would be expected in a rapidly growing tumour with robust angiogenesis, control tumours showed an increase in tumour vessel permeability over time. This was entirely mitigated by AKB-9778 treatment (Fig 35).

5.4.2 Impact of AKB-9778 treatment of established primary tumours upon vascular perfusion

Changes in tumour blood perfusion after AKB-9778 treatment were next assayed in both the 4T1 and E0771 models. Treatment was begun once tumours

reached 3mm in size, and continued for 10 days. At this point, biotinylated lectin (a marker of perfused vessels) was injected intravenously and tumours were harvested 5 minutes later. Stained sections of tumour tissue were stained for CD31 and lectin, and the [lectin+ area/total tumour area] and [lectin+CD31+area/total tumour area] fractions were quantified. In both models, there was a significant increase in tumour perfusion with AKB-9778 treatment (Figs 36-38).

To further visualize changes in tumour perfusion after AKB-9778 therapy, we grew orthotopic 4T1 tumours under mammary fat pad windows and performed optical frequency domain imaging (OFDI) of the tumour vasculature before and after 4 days of AKB-9778 treatment. This imaging modality provides a detailed landscape of only vessels that are perfused, and that have a diameter 8-9μM or greater, to a depth of 800μM. Qualitative assessment showed a marked increase in tumour perfusion after 4 days of AKB-9778 therapy (Fig 39).

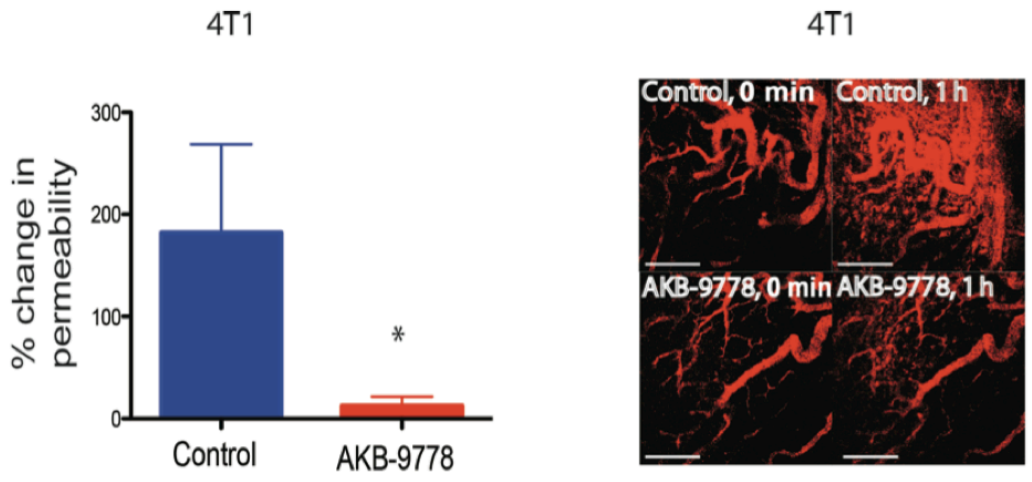

Figure 35: Left, Percentage change in permeability from baseline to after 72 h of treatment in control vs AKB-9778 treated 4T1 tumours (*p = 0.029 by t-test, n=3 per group). Right, Intravital micrographs taken 0 minutes and 1 hr after intravenous injection of fluorescent bovine serum albumin after treatment with control (top panels) or AKB-9778 (lower panels). Scale bar = 200uM.

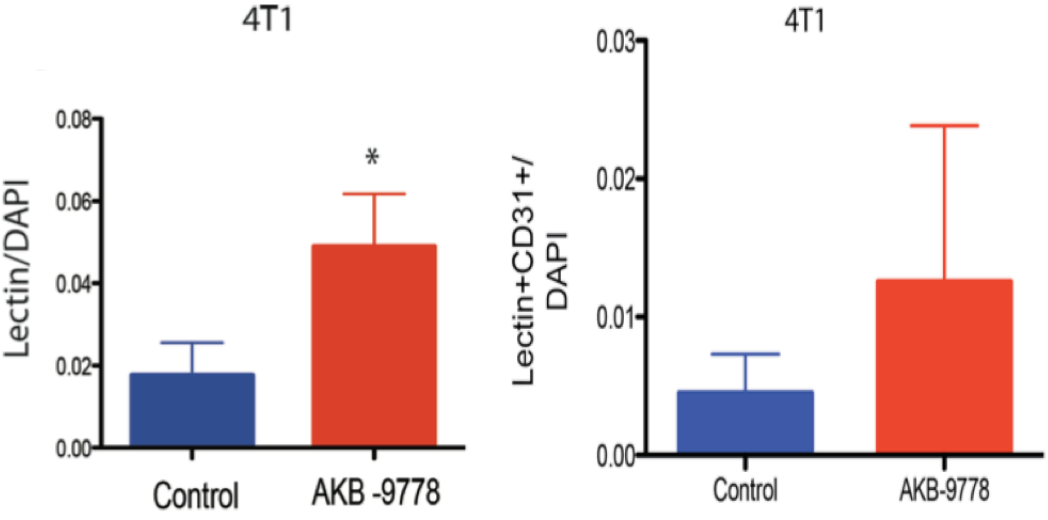

Figure 36: Established 4T1 orthotopic tumours were treated with AKB-9778 or control for 10 days and harvested 5 minutes after intravenous injection of lectin. Left, Lectin positive area in control versus AKB-9778 treated tumours (*p=0.029 by t-test, n=6 per group. Right, Graph depicts lectin-CD31 double positive area as a proportion of total tumour area (p = 0.12 by two-sided t-test, n = 6 per group).

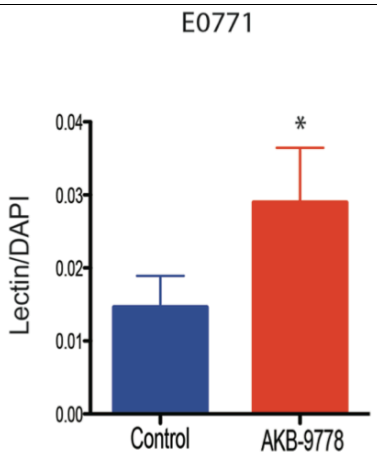

Figure 37: Lectin positive area in control versus AKB-9778 treated E0771 tumours (*p = 0.049, n = 5 per group).

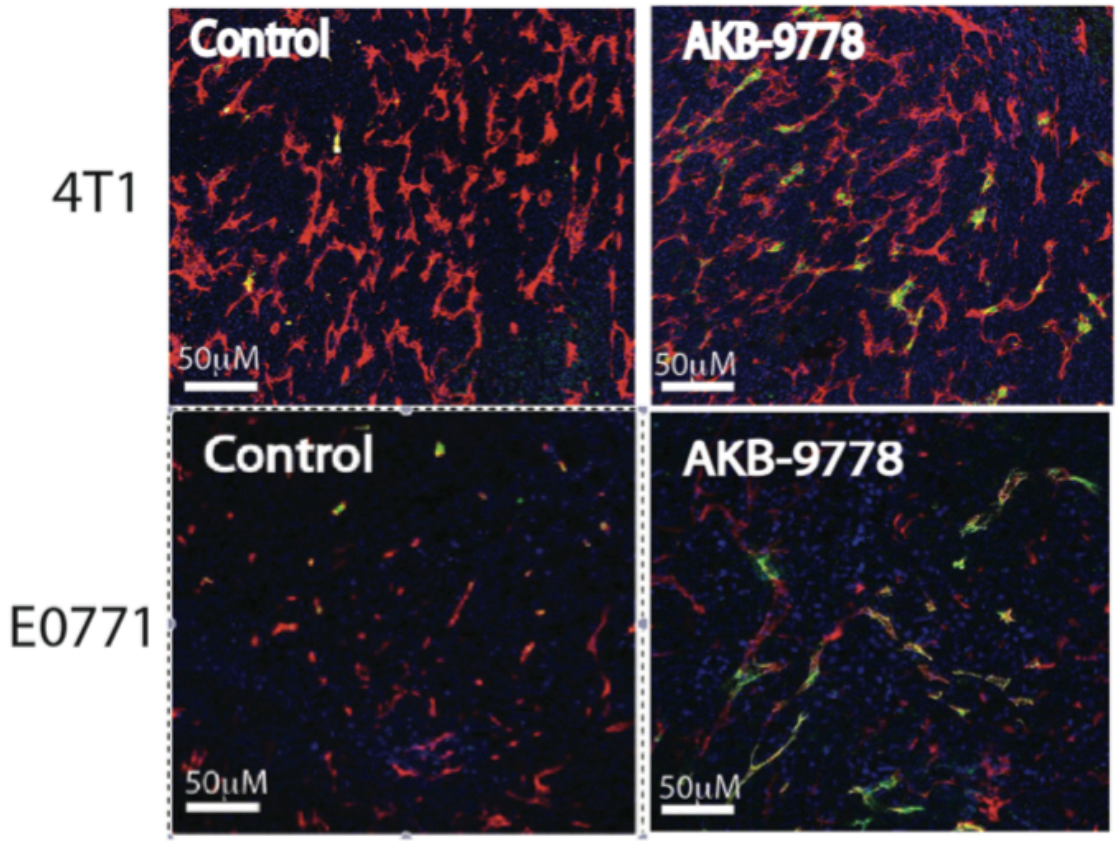

Figure 38: Enhanced vessel perfusion by lectin in AKB-9778 treated tumours compared to control (green = lectin, red = CD31, blue = DAPI).

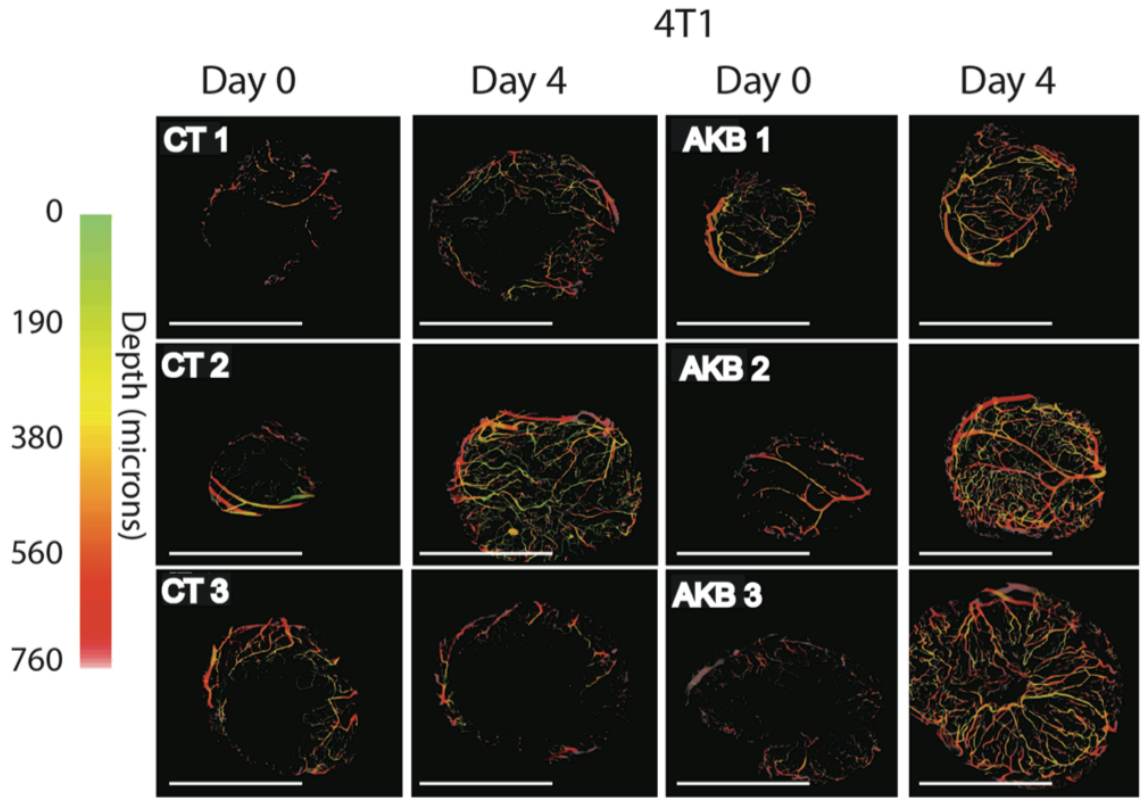

Figure 39: Intravital optical frequency domain imaging (OFDI) of 4T1 mammary carcinomas at baseline (Day 0, diameter 2-3mm) and after 4 days' treatment with AKB-9778 or control vehicle. Images show perfused vessels only. Scale bar represents 3mm.

5.4.3 Impact of AKB-9778 treatment of established primary tumours upon tumour hypoxia

We anticipated that improved perfusion within solid tumours after VE-PTP inhibition would lead to a reduction in tumour hypoxia. To test this hypothesis, experiments with an identical design to those described in 5.4.2 were performed. Instead of injecting lectin, mice were injected with pimonidazole 1h before sacrifice, and tumours were stained for redox markers as a measure of intratumoural hypoxia. In both models, there was a decrease in the hypoxic fraction in AKB-9778-treated tumours (Fig 40).

5.4.4 AKB-9778 treatment of established primary tumours does not alter their growth rate

Having observed several changes in vascular structure and function upon VE-PTP inhibition in established mammary tumours, we next asked if these were associated with any change in tumour growth rate. Data from 4 different tumour models, including the spontaneously arising *MMTV:PyVT* transgenic mouse model, showed that initiation of AKB-9778 treatment at a time when tumours measured 3mm in diameter had no impact upon the tumour growth rate (Fig 41).

5.4.5 AKB-9778 pre-treatment of established primary tumours potentiates the effect of external beam radiotherapy

Given the observed reduction in hypoxia (a known impediment to radiosensitivity), the effect of AKB-9778 pre-treatment on the efficacy of tumour radiotherapy was studied next. 4T1 mammary tumours were implanted

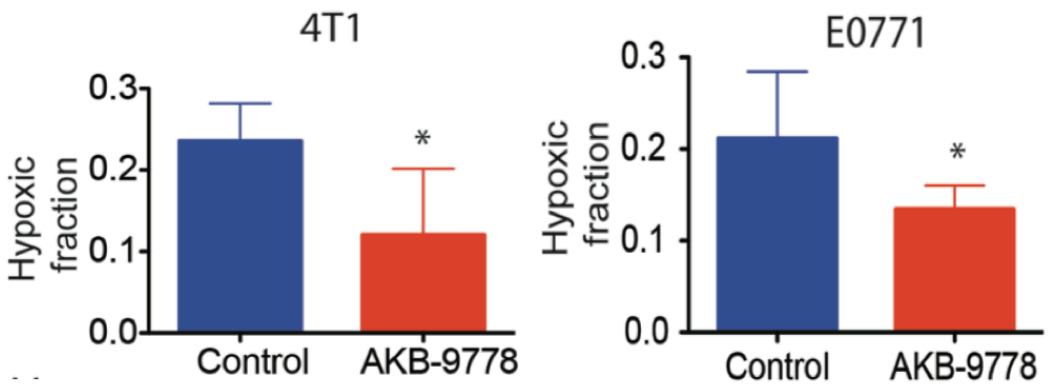

Figure 40: Relative hypoxic fraction assessed by pimonidazole staining in control vs AKB-9778 treated 4T1 (left) and E0771 (right) tumours (4T1: *p = 0.05, n = 10-13 per group; E0771: *p = 0.038, n = 9-10 per group).

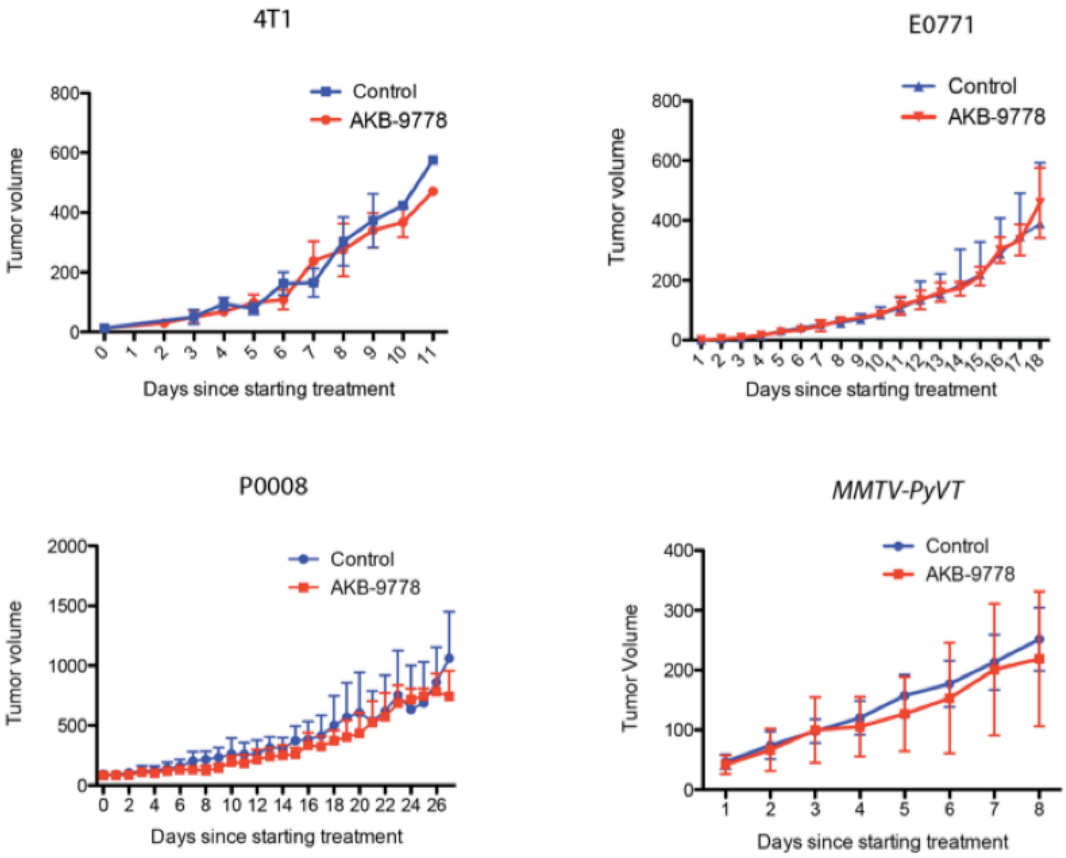

Figure 41: Effect of VE-PTP inhibition on the growth of established orthotopic primary tumours. For each experiment, treatment was commenced a tumour diameter 3mm. n = 6-8 mice per group). All error bars represent SD.

orthotopically, and at diameter 3mm were treated for 1 week with either AKB-9778 or control vehicle. Half of the mice from each treatment arm were then administered a single fraction of external beam radiation (20Gy) focused on the mammary tumour. As expected, AKB-9778 treatment alone had no impact upon tumour growth. However, pre-treatment with AKB-9778 significantly enhanced the efficacy of subsequently delivered radiation (Fig 42).

Collectively, the data presented in section 5.4 show that pharmacologic inhibition of VE-PTP reduces tumour vessel permeability, enhances perfusion, and reduces tumour hypoxia – effects which are all consistent with increased Tie-2 activity. These changes are not associated with an alteration of primary tumour growth per se, but do enhance the efficacy of radiotherapy, the efficacy of which is dependent on adequate tissue oxygenation.

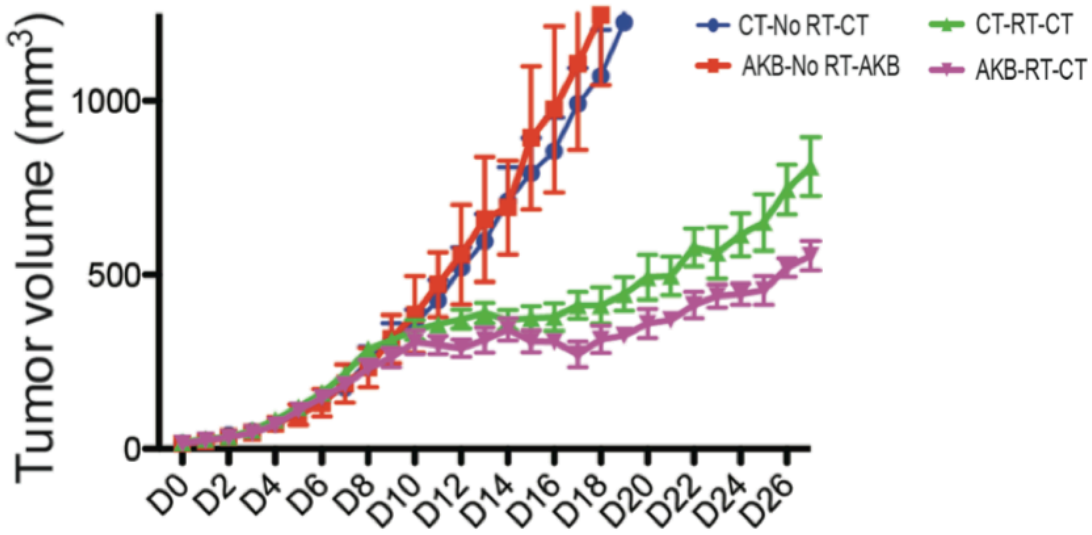

Figure 42: 4T1 tumour growth curves from combined AKB-9778 and radiotherapy. Treatment was begun at diameter 3mm, and radiotherapy given 1 week later. (*p < 0.001 comparing green and pink lines by ANOVA, n = 7 per group).

6 The effects of AKB-9778 on vessels within normal tissue

As a VE-PTP inhibitor, AKB-9778 is being moved into clinical trials for a variety of human diseases. Therefore in addition to assessing the efficacy of the compound in various tumour models, experiments were performed to assess the effects of AKB-9778 on normal host vessels, with the goal of obtaining preliminary insights into potential toxicities of the drug.

6.1 Impact of AKB-9778 on cutaneous vasculature permeability

Normal tissue vasculature has a basal level of permeability, which is essential for the maintenance of microenvironmental homeostasis (Nagy et al., 2008). To determine the effect of AKB-9778 on normal vessel permeability, non-tumour bearing adult mice were treated with AKB-9778 or control for 24h. A Miles assay was then performed – this is a well-established tool for measuring vascular permeability to molecules the size of albumin. In keeping with its capacity to activate Tie-2, AKB-9778 caused a reduction in cutaneous vascular permeability (Fig 43).

6.2 Impact of AKB-9778 on cutaneous vessel diameter and systemic blood pressure

The impact of AKB-9778 on cutaneous vessel diameter was assessed next. Healthy adult mice were treated for 48h and the mean vessel diameter (vessels

stained for CD31) in fragments of flank skin was quantified. There was a significant increase in mean cutaneous vessel diameter seen in treated animals (Fig 44, left). We expected that this might lead to a reduction in systemic vascular resistance and hence systemic blood pressure. Notably, 72h of AKB-9778 therapy did not significantly lower mean arterial pressure in healthy adult mice (Fig 44, right).

Collectively, the data presented in Chapter Six show that pharmacologic inhibition of VE-PTP invokes similar changes in the vessels of normal tissue (ie. increased diameter and reduced permeability) as those we previously observed in tumours. The phenotype is consistent with that observed with Tie-2 activation (Suri et al., 1998, Thurston et al., 1999).

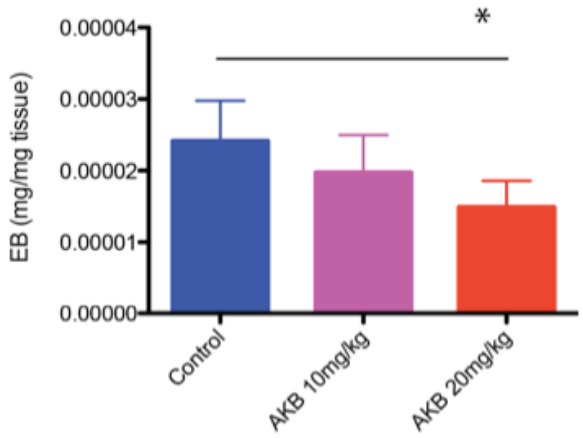

Figure 43: Miles assay demonstrating Evans Blue extravasation in skin of healthy mice pre-treated with control vehicle or AKB-9778 for 24h (*p < 0.01 by two-sided t-test, n = 4 per group).

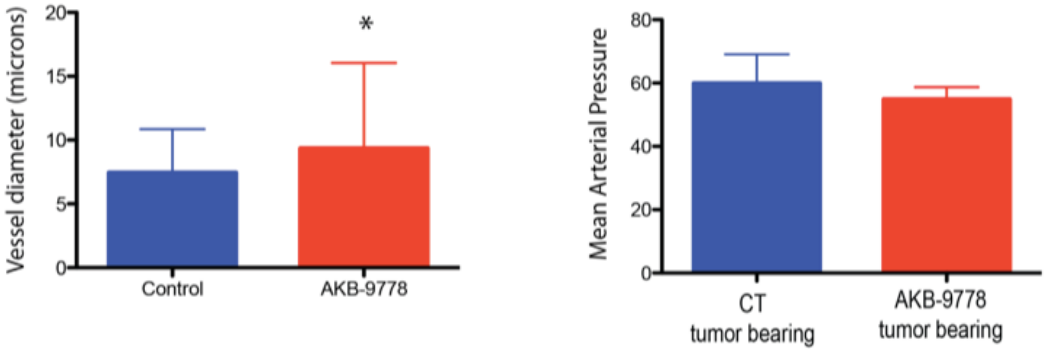

Figure 44: Left, Cutaneous vessel diameter in non-tumour bearing mice after 48h of treatment with control or AKB-9778 (*p = 0.04 by two-sided t-test, n = 3 per group). Right, Mean Arterial Pressure in tumour-bearing mice treated for 72h with AKB-9778 or control vehicle (p = 0.38 by two-sided t-test, n = 5 per group).

7 The role of endothelial nitric oxide synthase in mediating the effects of AKB-9778 on primary tumour vessels

In a non-tumour setting, Tie-2 mediated angiogenesis has been found to be dependent on the activity of endothelial nitric oxide synthase (eNOS) (Babaei et al., 2003). We had previously observed that by enhancing Tie-2 signaling, AKB-9778 induces activation of the endothelial nitric oxide synthase (eNOS), via phosphorylation at its ser1177 residue (Fig 4). Given this finding, we next explored whether VE-PTP inhibition increases EC production of nitric oxide (NO), and if so, whether eNOS-derived NO mediates the increases in tumour vessel density and diameter seen after VE-PTP inhibition with AKB-9778.

7.1 Impact of AKB-9778 on endothelial nitric oxide synthase activation and endothelial cell production of nitric oxide

In addition to its stimulatory ser1177 residue, eNOS activity can be inhibited by phosphorylation at its Thr495 residue. To further characterize the effects of AKB-9778 on eNOS in ECs, HUVECs were treated with AKB-9778 or Ang-1 (both Tie-2 activating stimuli). Neither enhanced phosphorylation at Thr495 (Fig 45). This suggests that VE-PTP inhibition alters eNOS phosphorylation patterns in a manner that increases its activity.

EC production of NO in response to AKB-9778 was assayed next using 4,5-diaminofluorescein diacetate (DAF-2 DA), an established marker of NO

production. AKB-9778 induced a marked increase in EC NO production (Fig 46). This effect could be suppressed with the use of the NOS inhibitor N^G-Monomethyl-L-arginine, showing that the increase in NO production is NOS-mediated.

7.2 The role of endothelial nitric oxide synthase as a mediator of AKB-9778-induced changes in tumour vessel diameter and density

Given our finding that AKB-9778 activates EC eNOS in a Tie-2 dependent manner, and that this in turn increases EC production of NO, we next asked whether the changes in tumour vessel phenotype observed after AKB-9778 treatment (increased vessel density and diameter) were mediated by eNOS activation. E0771 mammary carcinoma cells were implanted orthotopically into wild-type C57Bl6/J and *eNOS*$^{-/-}$ mice bred on a C57Bl6/J background.

When tumours reached 3mm in size, treatment was begun with either AKB-9778 or control vehicle. Firstly, when administered to eNOS-deficient mice, AKB-9778 therapy had no effect on tumour growth (Fig 47). Most notably, however, AKB-9778 therapy did not significantly increase vessel density or vessel diameter in *eNOS*$^{-/-}$ mice (Fig 48). These data stand in contrast to those seen in wild-type mice (Fig 33-34), and suggest that the changes in vessel density and diameter seen after AKB-9778 treatment are eNOS-dependent, at least in part.

Collectively, the data presented in Chapter Seven show that VE-PTP inhibition by AKB-9778 leads to activation of eNOS, which increases EC production of NO and in turn increases the number and size of tumour vessels.

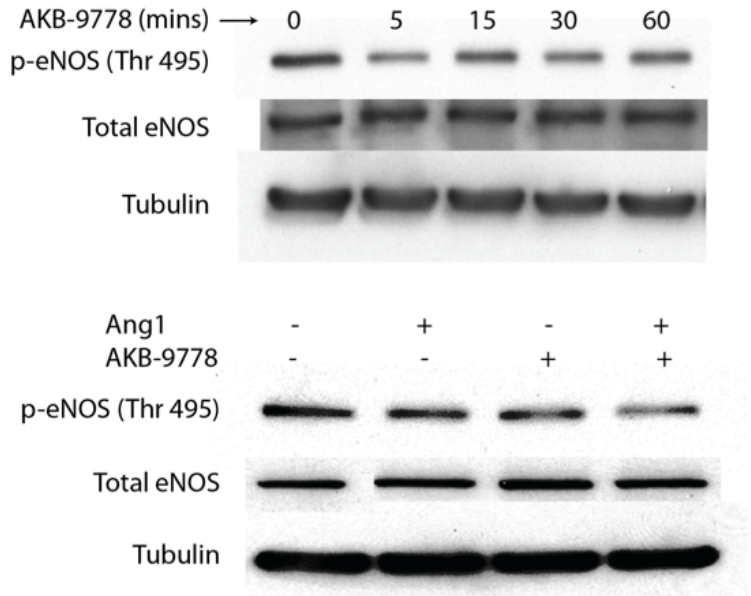

Figure 45: Top, eNOS phosphorylation (Thr495) and total eNOS in HUVEC lysates after AKB-9778 treatment. Bottom eNOS phosphorylation (Thr495) and total eNOS in HUVEC lysates after Angiopoietin-1 and/or AKB-9778 treatment for 30 minutes.

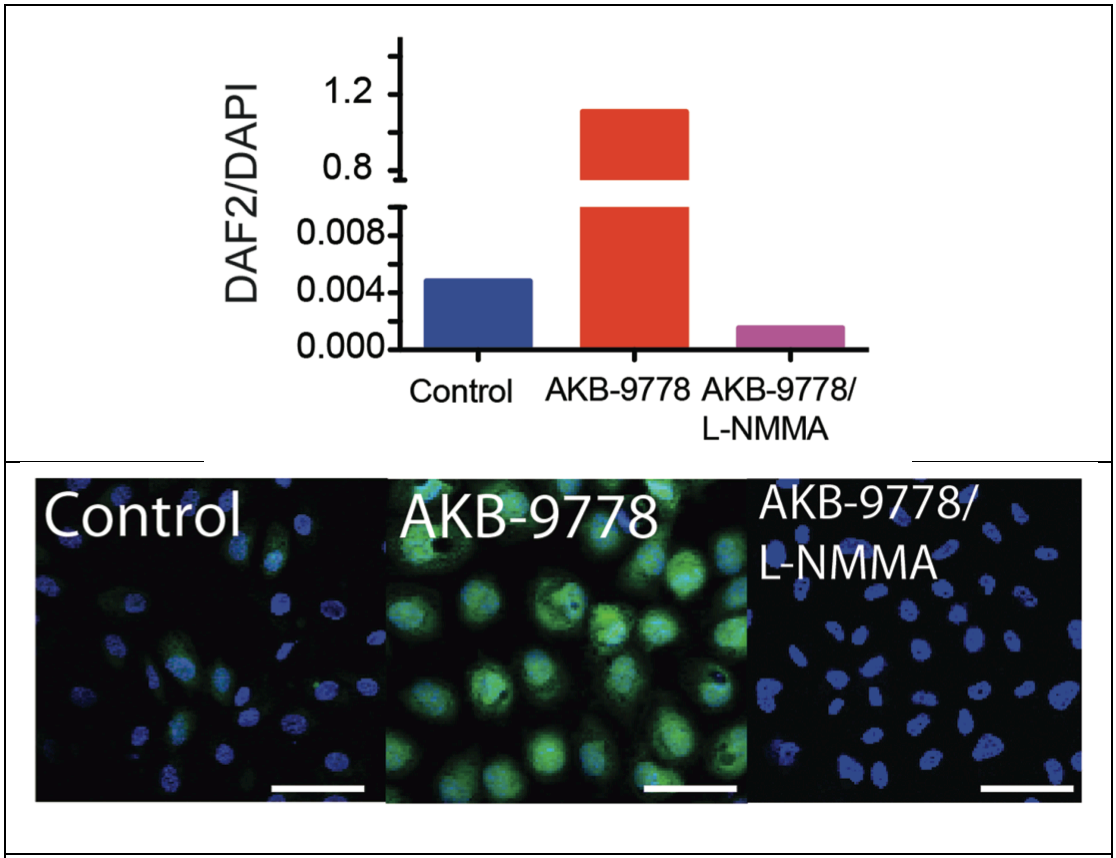

Figure 46: Top, HUVEC nitric oxide production *in vitro* after treatment with control, AKB-9778, or L-NMMA. Nitric oxide production was determined by quantification of the fluorescent signal from DAF-2T. Bottom, Representative images of DAF-2T fluorescence in HUVECs after treatment with control (left panel), AKB-9778 (center panel), or AKB-9778 and L-NMMA (right panel). Scale bar = 20μm.

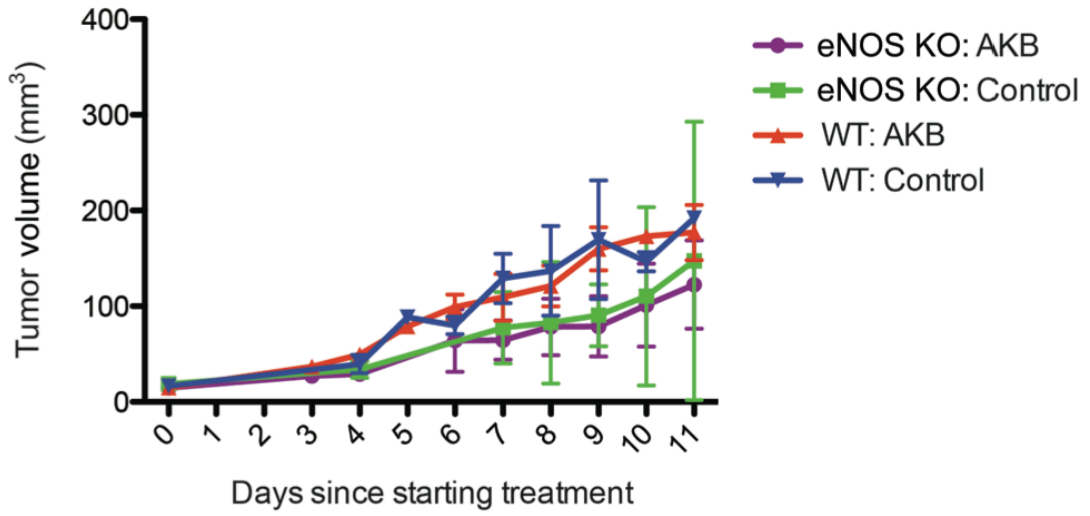

Figure 47: E0771 mammary carcinoma was implanted orthotopically into either wild-type (WT) C57Bl/6 mice or *eNOS*$^{-/-}$ mice (KO). At tumour diameter of 3mm, mice were treated with either AKB-9778 or control vehicle (n = 5 per group). Data show tumour growth curves.

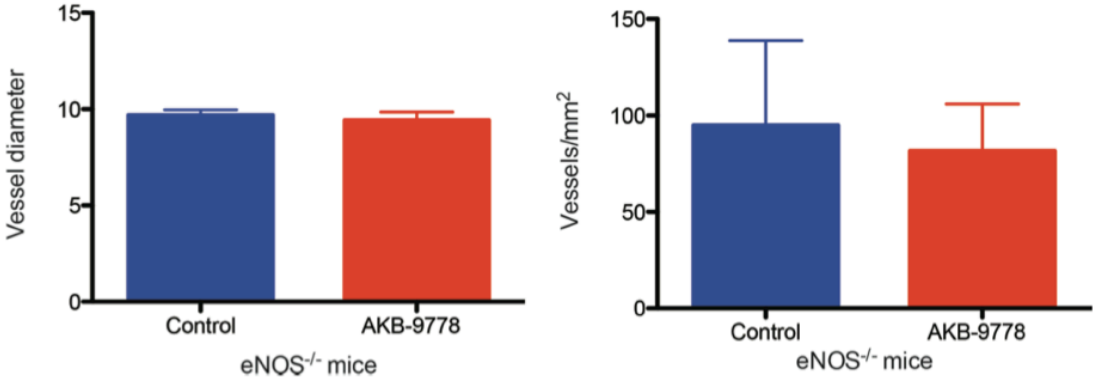

Figure 48: Left, Vessel diameter in E0771 orthotopic mammary carcinomas treated with AKB-9778 or control vehicle in *eNOS*$^{-/-}$ mice (p = 0.40, n = 5 per group). Right, Vessel density in E0771 orthotopic mammary carcinomas treated with AKB-9778 or control vehicle in *eNOS*$^{-/-}$ mice (p = 0.77, n = 5 per group).

8 Discussion

8.1 Introduction

The data presented within this dissertation and its publication in the peer-reviewed literature (Goel et al., 2013) are, to the best of our knowledge, the first to describe the effects of VE-PTP inhibition as a therapeutic strategy in any disease. We report that the novel, first-in-class VE-PTP inhibitor AKB-9778 is a potent activator of Tie-2 signaling within the endothelium, both *in vitro* and *in vivo*. AKB-9778 is the first small molecule inhibitor to activate Tie-2, and in doing so provides immense potential as a therapeutic agent in a number of disease settings where enhanced Tie-2 activity has conceivable beneficial effects.

Through a series of *in vitro* experiments, we show that AKB-9778 not only increases Tie-2 tyrosine phosphorylation, but also activates canonical signaling pathways downstream of Tie-2 (Augustin et al., 2009). Importantly, this occurs independently of the actions of Ang-1 and Ang-2. We then show in a number of mouse models of breast cancer that AKB-9778 therapy creates a more stable, mature vasculature characterized by a greater number of vessels which are also larger and relatively non-permeable. Although not conclusively proven in this study, this phenotype is likely a consequence Tie-2 activation.

In this chapter, we discuss the results of our experiments in detail, contextualizing them amongst other reports in the literature. We also discuss the limitations of this work, and suggest directions for future investigations into VE-PTP inhibition.

8.2 Vascular stability – a unifying theme

Within solid tumours, a large number of pro-angiogenic factors conspire to promote the formation of new blood vessels (Goel et al., 2011, Jain, 2001, Jain, 2005, Dvorak, 1986, Folkman, 1971, Kim et al., 1993, Holash et al., 1999, Yuan et al., 1996, Senger et al., 1983). Unlike in instances of physiologic angiogenesis (e.g. wound healing, ovulation), blood vessel growth in tumours occurs in a relentless, dysregulated fashion (Dvorak, 1986), primarily because the release of pro-angiogenic factors from tumour and stromal cells is not under tight control (Mazzone et al., 2009, Semenza, 2010b, Raza et al., 2010, Fukumura et al., 1998).

As a consequence of this excess in pro-angiogenic factors, vessels within solid tumours display a series of characteristic structural and functional abnormalities (Goel et al., 2011, Abramsson et al., 2003, Inai et al., 2004, Morikawa et al., 2002, Tong et al., 2004, Kamoun et al., 2009, Winkler et al., 2004). These abnormalities are well summarized by the terms “vascular immaturity” and “vascular instability”. Immature, unstable vessels are characterized by reduced perivascular cell coverage (Weis et al., 2004, Greenberg et al., 2008, Abramsson et al., 2003, Inai et al., 2004, Morikawa et al., 2002), a patchy basement membrane (Winkler et al., 2004, Kamoun et al., 2009), and hyperpermeability (Weis et al., 2004, Dvorak, 1990, Jain, 2003, Stohrer et al., 2000).

In the early phases of tumour development, vascular destabilization and loss of pericyte coverage facilitate the onset of sprouting angiogenesis, and hence

tumour growth (Holash et al., 1999, Nasarre et al., 2009). Within more established tumours, hyperpermeability increases interstitial fluid pressure, and chaotic blood flow promotes hypoxia – both of which exacerbate malignant traits and hinder the effectiveness of anti-cancer therapies (Goel et al., 2011, Tong et al., 2004, Winkler et al., 2004, Pennacchietti et al., 2003, Boucher et al., 1990, Boucher et al., 1991). Finally, the development of metastases relies upon local hyperpermeability in distant organ vessels, facilitating tumour cell extravasation (Holash et al., 1999, Holopainen et al., 2012, Wong et al., 2002, Weis et al., 2004, Avraham et al., 2014). For all of these reasons, strategies to reverse instability and immaturity in tumour vessels are theoretically very attractive.

The most concerted efforts to achieve this goal have relied upon pharmacologic blockade of the VEGF-A pathway. Such agents include the monoclonal antibody bevacizumab, a plethora of VEGF tyrosine kinase inhibitors, and the VEGF-trap aflibercept (Jain and Carmeliet, 2012). By inhibiting VEGF-driven abnormalities within vessels, such agents can transiently reverse some of their structural and functional abnormalities, a process coined “vascular normalization” (Jain, 2005, Goel et al., 2011). Unfortunately, pre-clinical studies suggest that this normalization is only a transient phenomenon, as prolonged inhibition of the VEGF pathway can eventually lead to vascular pruning and increased tumour hypoxia.

Manipulation of Tie-2 activity is a very attractive strategy to modulate vascular stability. Although the effects of individual ligands upon Tie-2 signaling are complex, it is clear that Tie-2 activation invokes a more mature, stable vascular

phenotype (Suri et al., 1998, Thurston et al., 1999, Gamble et al., 2000) and should not promote pruning of vessels. Theoretically, therefore, increasing Tie-2 activity within tumours could alleviate some of the negative consequences of vascular destabilization described above.

Given that VE-PTP can negatively regulate Tie-2 (Winderlich et al., 2009), we speculated that inhibition of VE-PTP activity might enhance vascular stability in tumours through enhancement of Tie-2 activity. Fortuitously, AKB-9778 was being introduced into preclinical studies at this time, and we therefore embarked upon the current study.

In each of the three phases of tumour progression (early primary tumour development, growth of established primary tumours, progression of metastatic lesions), we have shown that VE-PTP inhibition results in a more stable vascular phenotype (Goel et al., 2013, Kontos and Willett, 2013). This common theme unifies the results of our studies within solid tumours. In early primary tumour growth, the enforcement of perivascular cell coverage in host vessels was found to delay the early phases of tumour growth. In more established tumours, maintenance of vessel integrity improved perfusion, reduced hypoxia, and enhanced the efficacy of radiotherapy. Finally in developing metastatic lesions, inhibition of VE-PTP reduced circulating tumour cell extravasation into distant organs – in turn delaying the growth of metastases and prolonging mouse survival. The finding of our study and their relationship to vascular phenotype are summarized in Fig 49.

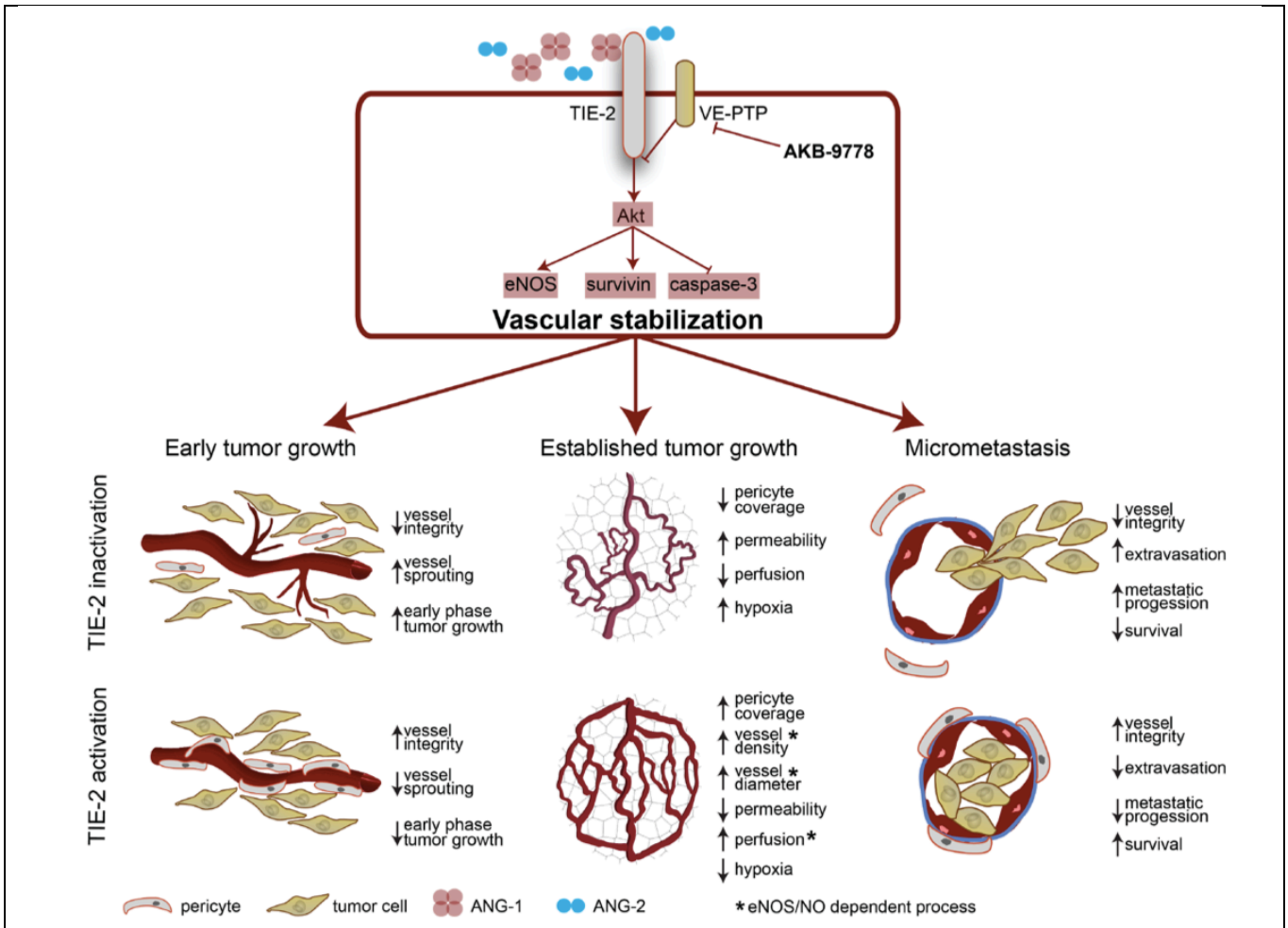

Fig 49: Inhibition of the VE-PTP phosphatase domain in endothelial cells activates Tie-2 signaling, in turn promoting a more stable vessel phenotype. In early tumour growth, this prevents early destabilization and hence slows the initial phase of tumour progression. In established tumours, vessels show structural and functional changes of normalization, resulting in improved tumour perfusion (which occurs due to an increased production of nitric oxide by endothelial eNOS). In the setting of micrometastasis, stabilization of distant organ vessels prevents extravasation of tumour cells, delaying micrometastatic progression and prolonging survival.

Note: some of the molecular pathways highlighted in this figure (ie. survivin and caspase-3 downstream of Tie-2) are extrapolated from the literature and not addressed in the current study.

Figure taken from Goel et al, 2013.

8.3 The mechanism of action for AKB-9778

AKB-9778 has been developed as a potent and selective inhibitor of VE-PTP through structural modifications of 1,2,3,4-tetrahydroisoquinolinyl sulfamic acids. These acids are phosphotyrosine mimetics, and act competitively to prevent phosphatases from dephosphorylating their endogenous targets. Coupling 1,2,3,4-tetrahydroisoquinolinyl sulfamic acids to a malonate template yields selective and potent inhibitors of VE-PTP (Amarasinghe et al., 2006). As detailed in the Introduction, AKB-9778 shows great potency and selectivity for VE-PTP.

Of interest, we found that AKB-9778 induced Tie-2 activation in a ligand-independent fashion. Endothelial cells grown in standard media, or in the presence of Ang-1 and/or Ang-2, all showed strong increases in p-AKT and p-eNOS after exposure to AKB-9778 *in vitro.* That is to say, we observed compound-induced Tie-2 activation in a ligand-independent fashion. Importantly, a second, independent report has been published since the completion of this work (Shen et al, 2014), which also reports identical findings after exposing endothelial cells in vitro to AKB-9778.

This finding is consistent with the notion that VE-PTP serves as a constant regulator of Tie-2, balancing Tie-2 activity within endothelial cells. Elegant studies from the laboratory of Vestweber have demonstrated that upon Tie-2 phosphorylation through Ang-1, VE-PTP serves to rapidly dephosphorylate Tie-2, serving as a constant negative feedback regulator of Tie-2 activation (Winderlich

et al., 2009). Given that there is always some basal level of Tie-2 phosphorylation within endothelial cells, it is certainly plausible that the continued presence of a VE-PTP inhibitor would allow for the accumulation of phosphorylated Tie-2 over time, regardless of the ligand context.

We also observed indirect evidence for the ligand-independent activity of AKB-9778 *in vivo*. As shown in Figure 7, AKB-9778 phosphorylated Tie-2 in both normal lung tissue (with low levels of Ang-2) and mammary tumour tissue (where Ang-2 levels are typically higher (Koh et al., 2010)).

This is an important point when drawing comparisons between VE-PTP inhibition and another pharmacologic strategy targeting the same pathway, namely Ang-2 inhibition. Firstly, inter- and intra-tumour levels of Ang-2 are highly variable (Sfiligoi et al., 2003) and anti-Ang-2 strategies can only be effective in tumours and regions that express sufficient levels of Ang-2. In contrast, we show that VE-PTP inhibition activates Tie-2 regardless of ligand context. Secondly, since tumours typically express higher levels of Ang-2 than Ang-1 (Koh et al., 2010), sequestering Ang-2 with monoclonal antibodies may not necessarily lead to Tie-2 activation in tumour ECs, as there is little Tie-2 agonist in the microenvironment. In contrast, VE-PTP inhibition consistently activates Tie-2, even in the presence of Ang-2, and its downstream effector pathways.

As such, one could speculate that Ang-2 blockade might induce a greater level of vascular regression (given that VEGF and Ang-2 act in concert to fuel angiogenesis), whereas VE-PTP inhibition might encourage vascular stabilization

without regression (as Tie-2 activation encourages the formation of mature, stable vessels). Unfortunately, we were unable to test these approaches directly given policies of pharmaceutical companies prohibiting head-to-head comparisons of investigational agents manufactured by different entities. Indeed, these concepts are consistent with observations in the published literature (Leow et al., 2012, Koh et al., 2010) and our own studies (Goel et al., 2013). VE-PTP inhibition therefore provides a unique opportunity to “hyperactivate” Tie-2 within solid tumours.

8.4 Other potential effects of VE-PTP inhibition

Of all the potential VE-PTP substrates, its interaction with Tie-2 in ECs is perhaps the best characterized and as is discussed in Chapter One, VE-PTP serves an important role as a negative feedback regulator of Tie-2 activity in normal cellular homeostasis (Winderlich et al., 2009). As such, we focused our initial *in vitro* studies upon the impact of AKB-9778 on Tie-2 activity within the endothelium.

However, the published literature regarding the function of VE-PTP in endothelial cells is more complex than this, and other potential binding partners have been identified (Kuppers et al., 2014). Indeed, although detailed exploration of other VE-PTP related pathways is outside the scope of this study, our relatively singular focus on Tie-2 activity is a limitation of this work.

Unlike the case for Tie-2, the precise interactions between VE-PTP and other potential substrates have not been clearly defined and it is therefore difficult to accurately predict how VE-PTP catalytic domain inhibition might affect these interactions and change the vascular phenotype. As is described in previous chapters, other potential interactors (either directly or indirectly) include the endothelial junctional proteins VE-Cadherin (Nawroth et al., 2002) and plakoglobin (Nottebaum et al., 2008), and possibly VEGFR2 (Hayashi et al., 2013).

The interaction between VE-PTP and VE-Cadherin is complex. It has been shown that these two molecules associate via their membrane-proximal

extracellular domains (Nawroth et al., 2002). In our studies, we found that inhibition of VE-PTP activity lead to reduced vessel permeability *in vivo*, consistent with increased Tie-2 activity. In contrast, *in vitro* studies by others have suggested that internalization and degradation of VE-PTP leads to increased tyrosine phosphorylation of VE-Cadherin and an associated *decrease* in endothelial barrier integrity (Nawroth et al., 2002). Although it may seem difficult to reconcile these findings, the latter study did report that this phenomenon was specifically dependent upon the extracellular binding between VE-PTP and VE-Cadherin, and not the VE-PTP catalytic domain. It is therefore conceivable that as a pure phosphatase inhibitor, AKB-9778 promotes Tie-2 activation (and hence reduced permeability) without disrupting VE-Cadherin/VE-PTP binding.

In keeping with this, we found that although AKB-9778 increased tyrosine phosphorylation of VE-Cadherin, there was no change in the total amount of VE-Cadherin at the cell membrane of endothelial cells treated with this compound.

Beyond VE-Cadherin, another report has implicated an interaction between VE-PTP and the endothelial junctional complex protein plakoglobin (otherwise known as gamma catenin) (Nottebaum et al., 2008). In this study, downregulation of VE-PTP caused tyrosine phosphorylation of plakoglobin and VE-Cadherin. This was again associated with a reduction in EC junctional integrity. However, the distinct roles of VE-PTP's extracellular and phosphatase domains in this process were not defined.

Importantly, we observed strong reductions in tumour vessel permeability with AKB-9778 treatment, consistent with Tie-2 activation and not with impaired EC junctional integrity. Collectively, these data suggest that the effects of pharmacological VE-PTP phosphatase domain inhibition are mediated primarily through increased Tie-2 kinase activity.

More recently, Hayashi et al reported a possible interaction between VE-PTP and VEGFR2. The investigators suggested that suppression of VE-PTP activity might indirectly increase VEGFR2 phosphorylation (and thus conceivably increase permeability and promote vascular immaturity) (Hayashi et al., 2013). At present, this remains an isolated report, and stands in contrast to data from the original study in which VE-PTP was first discovered (Fachinger et al., 1999). We did not study the status of VEGFR2 phosphorylation after AKB-9778 treatment in our studies, and this is an issue that warrants further clarification.

8.5 VE-PTP in embryonic angiogenesis

Like many key regulators of angiogenesis, VE-PTP is critical to successful embryogenesis and two different *VE-PTP* null mice both show an embryonic lethal phenotype (Baumer et al., 2006, Dominguez et al., 2007). The defects seen in these mice include dramatic enlargement of yolk sac vessels and a complete failure to elaborate the primitive vascular scaffold into higher-order branched arteries, veins, and capillaries. These changes have generally been attributed to Tie-2 hyperactivation (Dominguez et al., 2007).

We have utilized a different model of embryonic angiogenesis to assess the effects of pharmacologic VE-PTP inhibition, namely the zebrafish angiogenesis assay. It should be pointed out that there are several limitations with this approach. Firstly, due to the poor permeability of AKB-9778 into the zebrafish embryo, high concentrations are required within the fish water. It is therefore possible that some of the observed phenotype relates to non-specific or "off-target" effects. Secondly, the angiopoietin/Tie system in zebrafish is markedly distinct to that in mice or humans (Gjini et al., 2011), and it is not clear to what extent our findings are therefore applicable to mammalian systems.

It is worth noting that the discrepancy between the effects of AKB-9778 on embryonic angiogenesis (reduced sprouting and vessel density) and adult tumour vessels (increased vessel density) are not unexpected, and are in keeping with the distinct roles of several angiogenic factors in embryonic versus adult organisms (Maisonpierre et al., 1997, Suri et al., 1996, Dumont et al., 1994,

Carmeliet et al., 1996, Sato et al., 1995). Our zebrafish xenograft model, although looking at tumour angiogenesis, takes place in the context of embryogenesis, and as such the findings of reduced vessel density after AKB-9778 treatment in this experiment (Fig 13), cannot necessarily be compared with those seen in mouse tumours.

8.6 The role of VE-PTP in the early phase of tumour growth

In section 5.1, we show that AKB-9778 therapy delays the early phase of primary mammary tumour growth. Early in primary tumour development, cancer cells co-opt host vessels that then upregulate production of Ang-2 (Holash et al., 1999) and VE-PTP (Dominguez et al., 2007), presumably leading to Tie-2 deactivation, vessel destabilization, and sprouting angiogenesis (Holash et al., 1999).

We had hypothesized that VE-PTP inhibition during early tumour development would stabilize host vessels, delaying the onset of angiogenesis, and indeed found that the onset of vascular destabilization was delayed with AKB-9778 therapy. Collectively, these data show that VE-PTP inhibition delays the initial phase of tumour growth by upholding vascular maturity in host vessels.

These data are consistent with the results seen when growing tumours in *Ang2*$^{-/-}$ mice (Nasarre et al., 2009). However, one difference between our results and those published in *Ang2*$^{-/-}$ mice is that the latter study also observed a reduction in the diameters of intratumoural microvessels during this early growth phase. This discrepancy speaks further to the differences between Ang-2 blockade and VE-PTP inhibition, as discussed earlier.

8.7 The role of VE-PTP in the development and progression of metastases

Perhaps the most striking results of the present study are the findings that VE-PTP inhibition prevents the extravasation of circulating tumour cells into the parenchyma of distant organs, thus leading to a slowing in the growth of metastatic lesions and a prolonging of mouse survival. Indeed, clinical studies of vessel-targeted therapies in the “adjuvant” setting have been uniformly negative (Allegra et al., 2011, Cameron et al., 2013), and to our knowledge this is the first study – clinical or preclinical - to show a benefit from targeting the vasculature immediately after resection of a primary tumour.

The extravasation of tumour cells into distant organs is an important component of the metastatic cascade (Talmadge and Fidler, 2010). Critically, it requires an interaction between tumour cells and the endothelium, which results in endothelial production of Ang-2 (Holash et al., 1999). The consequent vessel destabilization and loss of perivascular cell coverage (Fuxe et al., 2011) facilitates the extravasation and colonization of cells in distant organs, and their subsequent growth into macroscopic metastases (Kienast et al., 2010, Weis et al., 2004). Once lodged in vessels, tumour cells may have a prolonged period of intravascular growth during which this vessel destabilization takes place, before they finally extravasate (Wong et al., 2002). Here, we show that VE-PTP inhibition attenuates this process, constraining metastatic tumour cells to the distant organ’s intravascular compartment and hence slowing metastatic progression.

Previous studies have shown a reduction in spontaneous metastasis using pharmacologic Ang-2 blockade (Koh et al., 2010, Holopainen et al., 2012). In these animal models, however, anti-Ang-2 therapy significantly delayed the growth of the primary tumours, which remained in situ through the study. This delay in primary tumour growth could in itself reduce metastasis (by virtue of a reduced primary tumour burden), and the results of these studies cannot confirm a specific role for Ang-2 blockade in hindering any step in the metastatic cascade. By using a spontaneous metastasis model where therapy was only begun after resection of the primary tumour, we confirm a specific influence of VE-PTP inhibition upon the metastatic process. Importantly, our experimental metastasis data (using 3 different tumour cell lines) provide evidence for enhanced vascular integrity as the mechanism behind these observations.

It is worth noting that as a part of this research, we attempted experiments to determine whether AKB-9978 therapy, by enhancing vessel integrity, reduces the shedding of cells from established primary tumours into the circulation. This observation has been previously made in transgenic mouse models of tumour vessel normalization (Mazzone et al., 2009). Unfortunately, our attempts to replicate these assays using identical methods were unsuccessful due to technical failure.

8.8 The effects of VE-PTP on the vasculature of established primary tumours

For decades after Folkman first proposed the notion of anti-angiogenic therapy for solid tumours (Folkman, 1971), the primary goal of the scientific community has been to inhibit the growth of vessels within established tumours, pruning them to a point that tumour cells are literally starved of nutrients. This effort has largely manifest through the development of anti-VEGF therapies.

Unfortunately, it is now clear that traditional anti-angiogenic therapies have not achieved this aim. For example, the anti-VEGF antibody bevacizumab invokes almost no meaningful responses in patients with breast, colorectal, or lung cancers when given as a monotherapy (reviewed in (Goel et al., 2011)). Furthermore, preclinical studies have shown that such therapies can actually prune vessels to the extent that tumour hypoxia increases, but tumours do not shrink. This may be in part because reduced tumour perfusion and increased tumour hypoxia are known determinants of aggressive behavior, insensitivity to chemo- and radiotherapy, and a poor prognosis (Suri et al., 1998, Sorensen et al., 2012, Wilson and Hay, 2011, Jain, 2005, Pennacchietti et al., 2003).

More recently, it appears that the goal posts for vessel-targeted therapies in solid tumours have moved. Pivotal studies using elegant genetic mouse models have suggested that more benefits may actually be realized through strategies that improve tumour perfusion and oxygenation (Hamzah et al., 2008, Mazzone et al., 2009). In these studies, a “normalized” vessel phenotype within tumours was

associated with improvements in perfusion, reductions in metastasis, improved oxygenation, and an enhanced anti-tumour immune infiltrate. Importantly, these studies did not report a slowing of tumour growth per se, but rather the improved efficacy of concomitant therapies (chemotherapy, radiation, immunotherapy), which rely on tumour perfusion and oxygenation in order to work (Hamzah et al., 2008, Mazzone et al., 2009, Jain, 2005). Finally, clinical data published recently also suggests that improvements in perfusion after vessel-targeted therapies may actually portend a better prognosis (Batchelor et al., 2013, Emblem et al., 2013).

To our knowledge, our data constitutes the first report where a similar vascular phenotype has been observed in response to a low molecular weight pharmacological agent. After treating tumour-bearing mice with AKB-9778, we observed structural and functional normalization of vessels with a phenotype entirely consistent with Tie-2 activation.

When therapy was commenced at tumour diameter 3mm (once robust angiogenesis is underway), we found that AKB-9778 therapy matured tumour vessel structure by enhancing pericyte coverage, and increased vessel diameter and density (also known effects of Tie-2 signaling). These changes were in turn associated with reduced vessel permeability, improved perfusion, and a consequent reduction in hypoxia. Of note, although the changes in vessel diameter that we observed were of the order of 10 percent, one would expect this to have a profound impact on perfusion (given Poiseuille's law stating that vascular resistance is inversely proportion to the radius to the fourth power).

With specific regard to our findings of enhanced vascular pericyte coverage, it is worth noting that our assessment of pericytes was performed using only two of an available suite of immunohistochemical markers for pericytes (NG2 and desmin). Pericytes express a number of markers of differentiation such as alpha smooth muscle actin (αSMA), desmin, chondroitin sulfate proteoglycan marker NG-2 (or high molecular weight melanoma antigen), PDGFRβ (platelet-derived growth factor receptorβ), aminopeptidases A and N and RGS5 (regulator of G-protein signaling). The regulation of marker expression is still largely not understood, and no single marker is able to identify all pericytes (Hall, 2006). For example, NG2 expression has been identified as a putative pericyte marker that has subsequently been found to be of more limited value, since its expression is restricted to arteriolar and capillary perivascular cells (vSMC and pericytes) and is absent on venular pericytes (Hall, 2006). It is thus not surprising that the absolute values obtained in experiments assaying pericyte coverage are different in experiments using NG2 as opposed to desmin as the pericyte marker.

Similarly, our data pertaining to effects of AKB-9778 on vascular permeability (both in skin and tumour vessels) is more accurately described as demonstrating a reduction in vascular leakage. Both the Miles assay (Fig 43) and measurement of BSA extravasation (Fig 35) can be affected not only by a reduction on permeability, but also by perfusion pressure and vessel surface area. Given our findings that AKB-9778 *increases* vessel density and has limited effect on systemic blood pressure, the most likely explanation for the reduced extravasation of Evan's Blue and BSA after AKB-9778 therapy is, however, a

direct attenuation of permeability – consistent with Tie-2 activation. Indeed although no single finding (enhanced pericyte coverage, increased vessel density or diameter, enhanced perfusion, reduced permeability) in our experiments serves as complete proof of a more mature, stable vasculature, the constellation of findings are collectively highly indicative of this phenotype.

Our results also support those of a previous study showing that *VE-PTP* gene silencing in embryonic stem cell derived tumours increases vessel diameter (Li et al., 2009), and also work suggesting that an increase in vessel diameter after loss of VE-PTP function is mediated by Tie-2 activity (Winderlich et al., 2009).

Importantly, by activating Tie-2 signaling, improving tumour perfusion, and ameliorating hypoxia, AKB-9778 therapy also improved radiotherapy efficacy. We note that these effects differ from those previously observed after anti-Ang2 therapies of solid tumours, which characteristically result in narrowed vessels with an increase in tumour hypoxia (Koh et al., 2010, Leow et al., 2012). Again, this may well relate to the previously discussed differences between anti-Ang2 therapy and VE-PTP inhibition on the state of Tie-2 activity.

8.9 eNOS as a mediator of Tie-2 activity in solid tumours

In our study, we report that particular changes in tumour vessels seen after VE-PTP inhibition – namely the increase in vessel diameter and density – are specifically related to the activity of the endothelial nitric oxide synthase (eNOS) (Goel et al., 2013). These findings are to some extent not surprising, and are in keeping with much of the published literature relating to Tie-2, eNOS, and vascular phenotype. Indeed, previous work has demonstrated that the pro-angiogenic effects of Tie-2 in a non-tumour setting are, at least in part, eNOS-dependent (Babaei et al., 2003).

In the setting of solid tumours, the situation is more complex. Nitric oxide within solid tumours can be synthesized by endothelial cells (by eNOS), but also by tumour cells (by inducible NOS, iNOS, and neuronal NOS, nNOS) and stromal cells (nNOS) (Fukumura et al., 2006). In each tumour, there exists a “nitric oxide gradient” between vessels and surrounding tissue. In tumours with high levels of tumour and/or stromal NO production, the NO gradient is away from the vessel. Conversely, in tumours with low levels of tumour and/or stromal NO production, the NO gradient is towards the vessel.

Two reports have previously demonstrated that concentrating intra-tumoural nitric oxide around the endothelial compartment normalizes tumour vessel structure and function, improving perfusion and reducing hypoxia (Kashiwagi et al., 2005, Kashiwagi et al., 2008). Given that eNOS activation is known to lie downstream of Tie-2 in ECs, we speculated that AKB-9778-treated ECs would increase NO

production by eNOS, in turn concentrating NO gradients around vessels – improving perfusion and reducing hypoxia.

Importantly, and in contrast to a previous report (Oubaha and Gratton, 2009), we not only found an increase in eNOS phosphorylation at the stimulatory ser1177 residue after VE-PTP inhibition, but also found no increase in phosphorylation at the inhibitory Thr495 residue. This finding is in keeping with eNOS biology, where counter-regulatory residues are typically phosphorylated and dephosphorylated in a manner that yields a unidirectional effect on enzyme activity. By comparing the effects of AKB-9778 in wild-type and eNOS-deficient mice, we next demonstrated that eNOS activity in the host-organism mediates the vessel density and diameter increases seen after AKB-9778 therapy.

Further studies are required to fully understand involvement of eNOS in AKB-9778's effects on blood vessels, tumour progression and dissemination. Other downstream effects of Tie-2 signaling include upregulation of survivin (mitigating EC apoptosis) and inhibition of EC cleaved caspase 3 (having the same effect) (Huang et al., 2010). It is conceivable that these mediators, by preventing EC death, may also play a significant role in increasing vessel density after VE-PTP inhibition.

8.10 Limitations of the current study

Our study has a number of important limitations, which must be acknowledged to properly contextualize and interpret the data.

Firstly, the models used within our experiments have a number of limitations. As discussed earlier, the use of a zebrafish model to study the effects of AKB-9778 upon embryonic angiogenesis might have little relevance to the mammalian situation, as the angiopoietin/Tie system in zebrafish bears many major differences to that in humans or mice. As such, the results of these studies should be considered hypothesis generating.

Furthermore, the mouse models employed also have various limitations. When studying the early phases of tumour growth, we injected tumour cells directly into the mammary fat pads of mice. This model is clearly distinct from the clinical reality, in which tumours develop slowly over time, and gradually develop regions of hypoxia and new vessel formation. To this end, we must acknowledge that the early stages of neoangiogenesis within our models may not accurately reflect the role of VE-PTP in the vessels of spontaneously arising tumours.

We also acknowledge that our study contains no information relating to the function or presence of VE-PTP in human tumours. Firstly, all of the mouse models utilize murine mammary carcinoma cells. While these have the advantage of being implanted into syngeneic mice with competent immune systems, there are fundamental differences between human and murine cancers

that limit the generalizability of our results. Furthermore, we have yet to perform studies examining the presence or role of VE-PTP in human tumour specimens.

In addition, our studies of the effects of VE-PTP inhibition upon normal tissues are somewhat limited. Our findings of an increase in cutaneous vessel diameter and a reduction in permeability may well have significant implications for the development of AKB-9778 as a therapeutic, in terms of toxicity. As such, more comprehensive toxicity data is urgently needed – in particular an examination of the effects of AKB-9778 on the vasculature of other organs, and on the capacity of the cardiovascular system to respond appropriately to changes in systemic blood pressure.

Most importantly, we acknowledge that the understanding of VE-PTP biology, its substrates, and interactions is a very young and emerging field. Our study focused almost exclusively on the interaction between VE-PTP and Tie-2, its best characterized substrate. Although the vessel phenotype we observed in our mouse tumour models is certainly consistent with a Tie-2 effect, we must acknowledge that other key players in the endothelial cell (including VE-Cadherin and VEGFR2) may also have direct and indirect interactions with VE-PTP. We have not explored the effects of VE-PTP inhibition on either of these targets in any detail, as this was felt to lie beyond the scope of this study. Nevertheless, it is entirely possible that some of our *in vivo* experimental results are in fact related to some of these other complex interactions that VE-PTP has.

-

8.11 Significance of the current findings, and future directions

VE-PTP was first isolated in 1999, and over the last 15 years, only a small number of laboratories worldwide have attempted to characterize its distribution, binding partners, and catalytic functions. This work has been almost exclusively conducted within *in vitro* systems, or in mouse models of embryogenesis (Fachinger et al., 1999, Baumer et al., 2006, Hayashi et al., 2013, Nottebaum et al., 2008, Winderlich et al., 2009). Given the overwhelming evidence that VE-PTP acts as a negative regulator of Tie-2 activity, its potential has a therapeutic target for diseases characterized by vascular immaturity has only recently been realized.

In this regard, we understand that our study presents the first data examining the prospective utility of VE-PTP as a therapeutic target (Goel et al., 2013). By studying the effects of AKB-9778 within solid tumours, our findings offer two major advances.

First, we show that the *in vivo* vascular phenotype observed after inhibition of VE-PTP's catalytic domain is one most consistent with Tie-2 activation – that is, one characterized by an increased number of mature, functional vessels with reduced permeability. There are now multiple conflicting reports on the potential effect of VE-PTP on endothelial barrier integrity (Hayashi et al., 2013, Nottebaum et al., 2008, Nawroth et al., 2002), relating to its interaction with different binding partners. While our translational approach does not allow for precise dissection of each of these pathways individually, we do demonstrate that the net result of

VE-PTP phosphatase inhibition in the tumour setting is one of reduced permeability and increased vessel stability. Indeed as discussed earlier, future studies must carefully determine the precise role of VE-PTP's catalytic and extracellular domains, and their relationship to VE-Cadherin, plakoglobin, and VEGFR2.

Second, our results are encouraging for the further development of VE-PTP inhibitors as a potential therapy for solid tumours. From a translational perspective, our most exciting results are the enhancement of radiation response in tumours pre-treated with AKB-9778, and the improvement of mouse survival after adjuvant AKB-9778 therapy. Of course, these results are preliminary, and should be replicated by other groups. We suggest that future studies should examine the effects of AKB-9778 in a variety of other solid tumour types (eg. colorectal carcinoma, renal cell carcinoma, ovarian carcinoma) where pathologic angiogenesis and vascular hyperpermeability are significant clinical problems.

In addition to its effects on tumour vessels, we suggest that future studies also examine the impact of AKB-9778 on the immune cell infiltrate within solid tumours. Tie-2 activation is known to serve an anti-inflammatory function (Gamble et al., 2000, Huang et al., 2010), in part mediated by downregulation of endothelial adhesion molecules E-selectin, Vascular cell adhesion protein 1 (VCAM-1), and Intercellular Adhesion Molecule 1 (ICAM-1). It is thus conceivable that AKB-9778 could invoke an "anti-inflammatory phenotype" within solid tumours, which may or may not prove advantageous depending on precisely which immune cell population levels are modified, and in which direction. In

addition, it is possible that AKB-9778, through reduction in tumour hypoxia, could have other beneficial effects on the tumour immune microenvironment, such as a shift from “pro-tumour” M2 macrophages to “anti-tumour” M1 macrophages (Huang et al., 2013, Rolny et al., 2011).

Other future studies in solid tumours should also determine the expression and possible function of VE-PTP in human tumours. Initially, confirming the presence of VE-PTP in the human tumour endothelium is needed to verify its candidacy as a therapeutic target. Furthermore, to gain preliminary insights into a possible functional role for VE-PTP in human cancer, it would be valuable to quantify the expression level of VE-PTP and phospho-Tie-2 (quantified by immunohistochemistry) in a series of breast cancer specimens, and to determine if these parameters are correlated with either tumour vessel phenotype or clinical outcome. The latter could easily be determined using one of a large number of commercially available tissue microarray resources, which come with patient outcome data attached.

Finally, future preclinical work should begin to explore the effects of combined therapy with a VE-PTP inhibitor such as AKB-9778 and more established vessel-targeted therapies such as VEGF inhibitors. AKB-9778 has recently been found to specifically inhibit the vascular leak induced by excessive VEGF levels (Shen et al., 2014). Furthermore, work from the De Palma laboratory has now revealed a specific role for excessive Ang-2 activity (and hence Tie-2 antagonism) in resistance to VEGF blockade. (Rigamonti et al., 2014). In this light, it is conceivable that the administration of AKB-9778 together with anti-VEGF therapy

could, by opposing the effects of Ang-2, prevent this resistance to VEGF blockade. Furthermore, one could speculate that the more durable vascular stabilizing effects of AKB-9778 might mitigate excessive vascular regression sometimes seen after anti-VEGF therapy, potentially further enhancing the effects of anti-VEGF agents as “normalizers” of the tumour vasculature.

At the time of writing, AKB-9778 has now entered early phase clinical trials. Based on unpublished data from the drug’s manufacturer, together with our findings, the compound will be tested in a variety of disease characterized by excessive vascular leak, including sepsis and diabetic macular edema. The initial phase 1 study was conducted in patients with macular edema secondary to diabetes mellitus, where pathologic angiogenesis and vascular leak are responsible for deterioration in vision. The results of this study showed that AKB-9778 was well tolerated by patients, and resulted in a meaningful reduction in retinal edema in a proportion of patients (Aerpio Therapeutics, 2014). This observation is consistent with our observation that VE-PTP inhibition enhances vascular integrity *in vivo.* If our findings are replicated in other mouse models, phase 1 trials of AKB-9778 in cancer patients are anticipated. Initially, these will focus on dose-finding and pharmacokinetic parameters.

In more general terms, our study is also a timely reminder regarding the potential of phosphatase inhibition as a therapeutic tool in cancer. The human tyrosine phosphatome contains a variety of enzymes that dephosphorylate target proteins and balance the effects of tyrosine kinases (Julien et al., 2011). As the growth of most tumour cells is driven by kinase activity, drug development has focused

almost exclusively on tyrosine kinase inhibitors. However, certain tyrosine phosphatases can also act as oncoproteins, or promote deleterious tumour behavior (such as VE-PTP), and inhibiting their catalytic activity could open up a wide range of new therapeutic strategies.

References

ABRAMSSON, A., LINDBLOM, P. & BETSHOLTZ, C. 2003. Endothelial and nonendothelial sources of PDGF-B regulate pericyte recruitment and influence vascular pattern formation in tumours. *J Clin Invest,* 112**,** 1142-51.

AERPIO THERAPEUTICS, I. 2014. *Aerpio Therapeutics Presents Full Results from Phase 1b/2a Study of AKB-9778 for the Treatment of Diabetic Macular Edema at ARVO Annual Meeting* [Online]. Available: http://www.aerpio.com/news/Aerpio-ARVO-2014-Data.pdf [Accessed September 26 2014].

ALGIRE, G. H. & CHALKLEY, H. W. 1945. Vascular reactions of normal and malignant tissues in vivo. I. Vascular reactions of mice to wounds and to normal and neoplastic transplants. *J Natl Cancer Inst USA,* 6**,** 73-85.

ALLEGRA, C. J., YOTHERS, G., O'CONNELL, M. J., SHARIF, S., PETRELLI, N. J., COLANGELO, L. H., ATKINS, J. N., SEAY, T. E., FEHRENBACHER, L., GOLDBERG, R. M., O'REILLY, S., CHU, L., AZAR, C. A., LOPA, S. & WOLMARK, N. 2011. Phase III trial assessing bevacizumab in stages II and III carcinoma of the colon: results of NSABP protocol C-08. *J Clin Oncol,* 29**,** 11-6.

AMARASINGHE, K. K., EVDOKIMOV, A. G., XU, K., CLARK, C. M., MAIER, M. B., SRIVASTAVA, A., COLSON, A. O., GERWE, G. S., STAKE, G. E., HOWARD, B. W., POKROSS, M. E., GRAY, J. L. & PETERS, K. G. 2006. Design and synthesis of potent, non-peptidic inhibitors of HPTPbeta. *Bioorg Med Chem Lett,* 16**,** 4252-6.

AUGUSTIN, H. G., KOH, G. Y., THURSTON, G. & ALITALO, K. 2009. Control of vascular morphogenesis and homeostasis through the angiopoietin-Tie system. *Nat Rev Mol Cell Biol,* 10**,** 165-77.

AVRAHAM, H. K., JIANG, S., FU, Y., NAKSHATRI, H., OVADIA, H. & AVRAHAM, S. 2014. Angiopoietin-2 mediates blood-brain barrier impairment and colonization of triple-negative breast cancer cells in brain. *J Pathol,* 232**,** 369-81.

BABAEI, S., TEICHERT-KULISZEWSKA, K., ZHANG, Q., JONES, N., DUMONT, D. J. & STEWART, D. J. 2003. Angiogenic actions of angiopoietin-1 require endothelium-derived nitric oxide. *Am J Pathol,* 162**,** 1927-36.

BAISH, J. W. & JAIN, R. K. 2000. Fractals and cancer. *Cancer Res,* 60**,** 3683-8.

BAISH, J. W., STYLIANOPOULOS, T., LANNING, R. M., KAMOUN, W. S., FUKUMURA, D., MUNN, L. L. & JAIN, R. K. 2011. Scaling rules for diffusive drug delivery in tumour and normal tissues. *Proc Natl Acad Sci U S A,* 108**,** 1799-1803.

BARKER, A. D., SIGMAN, C. C., KELLOFF, G. J., HYLTON, N. M., BERRY, D. A. & ESSERMAN, L. J. 2009. I-SPY 2: an adaptive breast cancer trial design in the setting of neoadjuvant chemotherapy. *Clin Pharmacol Ther,* 86**,** 97-100.

BATCHELOR, T. T., GERSTNER, E. R., EMBLEM, K. E., DUDA, D. G., KALPATHY-CRAMER, J., SNUDERL, M., ANCUKIEWICZ, M., POLASKOVA, P., PINHO, M. C., JENNINGS, D., PLOTKIN, S. R., CHI, A. S., EICHLER, A. F., DIETRICH, J., HOCHBERG, F. H., LU-EMERSON, C., IAFRATE, A. J., IVY, S. P., ROSEN, B. R., LOEFFLER, J. S., WEN, P. Y., SORENSEN, A. G. & JAIN, R. K. 2013. Improved tumour oxygenation and survival in glioblastoma patients who show increased blood perfusion after cediranib and chemoradiation. *Proc Natl Acad Sci U S A,* 110**,** 19059-64.

BAUM, O., SUTER, F., GERBER, B., TSCHANZ, S. A., BUERGY, R., BLANK, F., HLUSHCHUK, R. & DJONOV, V. 2010. VEGF-A promotes intussusceptive angiogenesis in the developing chicken chorioallantoic membrane. *Microcirculation,* 17**,** 447-57.

BAUMER, S., KELLER, L., HOLTMANN, A., FUNKE, R., AUGUST, B., GAMP, A., WOLBURG, H., WOLBURG-BUCHHOLZ, K., DEUTSCH, U. & VESTWEBER, D. 2006. Vascular endothelial cell-specific phosphotyrosine phosphatase (VE-PTP) activity is required for blood vessel development. *Blood,* 107**,** 4754-62.

BERGERS, G. & BENJAMIN, L. E. 2003. Tumourigenesis and the angiogenic switch. *Nat Rev Cancer,* 3**,** 401-10.

BO, W. J., MERCURI, M., TUCKER, R. & BOND, M. G. 1992. The human carotid atherosclerotic plaque stimulates angiogenesis on the chick chorioallantoic membrane. *Atherosclerosis,* 94**,** 71-8.

BOCCI, G., FRANCIA, G., MAN, S., LAWLER, J. & KERBEL, R. S. 2003. Thrombospondin 1, a mediator of the antiangiogenic effects of low-dose metronomic chemotherapy. *Proc Natl Acad Sci U S A,* 100**,** 12917-22.

BOTTARO, D. P. & LIOTTA, L. A. 2003. Cancer: Out of air is not out of action. *Nature,* 423**,** 593-5.

BOUCHER, Y., BAXTER, L. T. & JAIN, R. K. 1990. Interstitial pressure gradients in tissue-isolated and subcutaneous tumours: implications for therapy. *Cancer Res,* 50**,** 4478-84.

BOUCHER, Y., KIRKWOOD, J. M., OPACIC, D., DESANTIS, M. & JAIN, R. K. 1991. Interstitial hypertension in superficial metastatic melanomas in humans. *Cancer Res,* 51**,** 6691-4.

BOUCHER, Y., SALEHI, H., WITWER, B., HARSH, G. R. T. & JAIN, R. K. 1997. Interstitial fluid pressure in intracranial tumours in patients and in rodents. *Br J Cancer,* 75**,** 829-36.

BROERMANN, A., WINDERLICH, M., BLOCK, H., FRYE, M., ROSSAINT, J., ZARBOCK, A., CAGNA, G., LINNEPE, R., SCHULTE, D., NOTTEBAUM, A. F. & VESTWEBER, D. 2011. Dissociation of VE-PTP from VE-cadherin is required for leukocyte extravasation and for VEGF-induced vascular permeability in vivo. *J Exp Med,* 208**,** 2393-401.

BROWN, E., MCKEE, T., DITOMASO, E., PLUEN, A., SEED, B., BOUCHER, Y. & JAIN, R. K. 2003. Dynamic imaging of collagen and its modulation in tumours in vivo using second-harmonic generation. *Nat Med,* 9**,** 796-800.

BROWN, J. L., CAO, Z. A., PINZON-ORTIZ, M., KENDREW, J., REIMER, C., WEN, S., ZHOU, J. Q., TABRIZI, M., EMERY, S., MCDERMOTT, B., PABLO, L., MCCOON, P., BEDIAN, V. & BLAKEY, D. C. 2010. A human monoclonal anti-ANG2 antibody leads to broad antitumour activity in combination with VEGF inhibitors and chemotherapy agents in preclinical models. *Mol Cancer Ther,* 9**,** 145-56.

BRUFSKY, A. M., HURVITZ, S., PEREZ, E., SWAMY, R., VALERO, V., O'NEILL, V. & RUGO, H. S. 2011. RIBBON-2: a randomized, double-blind, placebo-controlled, phase III trial evaluating the efficacy and safety of bevacizumab in combination with chemotherapy for second-line treatment of human epidermal growth factor receptor 2-negative metastatic breast cancer. *J Clin Oncol,* 29**,** 4286-93.

CAMERON, D., BROWN, J., DENT, R., JACKISCH, C., MACKEY, J., PIVOT, X., STEGER, G. G., SUTER, T. M., TOI, M., PARMAR, M., LAEUFLE, R., IM, Y. H., ROMIEU, G., HARVEY, V., LIPATOV, O., PIENKOWSKI, T., COTTU, P., CHAN, A., IM, S. A., HALL, P. S., BUBUTEISHVILI-PACAUD, L., HENSCHEL, V., DEURLOO, R. J., PALLAUD, C. & BELL, R. 2013. Adjuvant bevacizumab-containing therapy in triple-negative breast cancer (BEATRICE): primary results of a randomised, phase 3 trial. *Lancet Oncol,* 14**,** 933-42.

CARMELIET, P., FERREIRA, V., BREIER, G., POLLEFEYT, S., KIECKENS, L., GERTSENSTEIN, M., FAHRIG, M., VANDENHOECK, A., HARPAL, K., EBERHARDT, C., DECLERCQ, C., PAWLING, J., MOONS, L., COLLEN, D., RISAU, W. & NAGY, A. 1996. Abnormal blood vessel development and lethality in embryos lacking a single VEGF allele. *Nature,* 380**,** 435-9.

CARMELIET, P. & JAIN, R. K. 2000. Angiogenesis in cancer and other diseases. *Nature,* 407**,** 249-57.

CERNIGLIA, G. J., PORE, N., TSAI, J. H., SCHULTZ, S., MICK, R., CHOE, R., XING, X., DURDURAN, T., YODH, A. G., EVANS, S. M., KOCH, C. J., HAHN, S. M., QUON, H., SEHGAL, C. M., LEE, W. M. & MAITY, A. 2009. Epidermal growth factor receptor inhibition modulates the microenvironment by vascular normalization to improve chemotherapy and radiotherapy efficacy. *PLoS One,* 4**,** e6539.

CHAE, S. S., KAMOUN, W. S., FARRAR, C. T., KIRKPATRICK, N. D., NIEMEYER, E., DE GRAAF, A. M., SORENSEN, A. G., MUNN, L. L., JAIN, R. K. & FUKUMURA, D. 2010. Angiopoietin-2 interferes with anti-VEGFR2-induced vessel normalization and survival benefit in mice bearing gliomas. *Clin Cancer Res,* 16**,** 3618-27.

CHUNG, A. S., LEE, J. & FERRARA, N. 2010. Targeting the tumour vasculature: insights from physiological angiogenesis. *Nat Rev Cancer,* 10**,** 505-14.

COBLEIGH, M. A., LANGMUIR, V. K., SLEDGE, G. W., MILLER, K. D., HANEY, L., NOVOTNY, W. F., REIMANN, J. D. & VASSEL, A. 2003. A phase I/II dose-escalation trial of bevacizumab in previously treated metastatic breast cancer. *Semin Oncol,* 30**,** 117-24.

DALY, C., PASNIKOWSKI, E., BUROVA, E., WONG, V., ALDRICH, T. H., GRIFFITHS, J., IOFFE, E., DALY, T. J., FANDL, J. P., PAPADOPOULOS,

N., MCDONALD, D. M., THURSTON, G., YANCOPOULOS, G. D. & RUDGE, J. S. 2006. Angiopoietin-2 functions as an autocrine protective factor in stressed endothelial cells. *Proc Natl Acad Sci U S A,* 103**,** 15491-6.

DECLERCK, K. & ELBLE, R. C. 2010. The role of hypoxia and acidosis in promoting metastasis and resistance to chemotherapy. *Front Biosci,* 15**,** 213-25.

DEJANA, E., TOURNIER-LASSERVE, E. & WEINSTEIN, B. M. 2009. The control of vascular integrity by endothelial cell junctions: molecular basis and pathological implications. *Dev Cell,* 16**,** 209-21.

DOMINGUEZ, M. G., HUGHES, V. C., PAN, L., SIMMONS, M., DALY, C., ANDERSON, K., NOGUERA-TROISE, I., MURPHY, A. J., VALENZUELA, D. M., DAVIS, S., THURSTON, G., YANCOPOULOS, G. D. & GALE, N. W. 2007. Vascular endothelial tyrosine phosphatase (VE-PTP)-null mice undergo vasculogenesis but die embryonically because of defects in angiogenesis. *Proc Natl Acad Sci U S A,* 104**,** 3243-8.

DUMONT, D. J., GRADWOHL, G., FONG, G. H., PURI, M. C., GERTSENSTEIN, M., AUERBACH, A. & BREITMAN, M. L. 1994. Dominant-negative and targeted null mutations in the endothelial receptor tyrosine kinase, tek, reveal a critical role in vasculogenesis of the embryo. *Genes Dev,* 8**,** 1897-909.

DUYVERMAN, A. M., KOHNO, M., ROBERGE, S., FUKUMURA, D., DUDA, D. G. & JAIN, R. K. 2012. An isolated tumour perfusion model in mice. *Nat Protoc,* 7**,** 749-55.

DVORAK, H. F. 1986. Tumours: wounds that do not heal. Similarities between tumour stroma generation and wound healing. *N Engl J Med,* 315**,** 1650-9.

DVORAK, H. F. 1990. Leaky tumour vessels: consequences for tumour stroma generation and for solid tumour therapy. *Prog Clin Biol Res,* 354A**,** 317-30.

EHRMANN, R. L. & KNOTH, M. 1968. Choriocarcinoma: transfilter stimulation of vasoproliferation in the hamster cheek pouch studied by light and electron microscopy. *J Natl Cancer Inst,* 41**,** 1329-1341.

EMBLEM, K. E., MOURIDSEN, K., BJORNERUD, A., FARRAR, C. T., JENNINGS, D., BORRA, R. J., WEN, P. Y., IVY, P., BATCHELOR, T. T., ROSEN, B. R., JAIN, R. K. & SORENSEN, A. G. 2013. Vessel architectural imaging identifies cancer patient responders to anti-angiogenic therapy. *Nat Med,* 19**,** 1178-83.

FACHINGER, G., DEUTSCH, U. & RISAU, W. 1999. Functional interaction of vascular endothelial-protein-tyrosine phosphatase with the angiopoietin receptor Tie-2. *Oncogene,* 18**,** 5948-53.

FALCON, B. L., HASHIZUME, H., KOUMOUTSAKOS, P., CHOU, J., BREADY, J. V., COXON, A., OLINER, J. D. & MCDONALD, D. M. 2009. Contrasting actions of selective inhibitors of angiopoietin-1 and angiopoietin-2 on the normalization of tumour blood vessels. *Am J Pathol,* 175**,** 2159-70.

FERRARA, N. 2002. VEGF and the quest for tumour angiogenesis factors. *Nat Rev Cancer,* 2**,** 795-803.

FOLBERG, R., RUMMELT, V., PARYS-VAN GINDERDEUREN, R., HWANG, T., WOOLSON, R. F., PE'ER, J. & GRUMAN, L. M. 1993. The prognostic value of tumour blood vessel morphology in primary uveal melanoma. *Ophthalmology,* 100**,** 1389-98.

FOLKMAN, J. 1971. Tumour angiogenesis: therapeutic implications. *N Engl J Med,* 285**,** 1182-6.

FUKUMURA, D., DUDA, D. G., MUNN, L. L. & JAIN, R. K. 2010. Tumour microvasculature and microenvironment: novel insights through intravital imaging in pre-clinical models. *Microcirculation,* 17**,** 206-25.

FUKUMURA, D., KASHIWAGI, S. & JAIN, R. K. 2006. The role of nitric oxide in tumour progression. *Nat Rev Cancer,* 6**,** 521-34.

FUKUMURA, D., XAVIER, R., SUGIURA, T., CHEN, Y., PARK, E. C., LU, N., SELIG, M., NIELSEN, G., TAKSIR, T., JAIN, R. K. & SEED, B. 1998. Tumour induction of VEGF promoter activity in stromal cells. *Cell,* 94**,** 715-25.

FUXE, J., TABRUYN, S., COLTON, K., ZAID, H., ADAMS, A., BALUK, P., LASHNITS, E., MORISADA, T., LE, T., O'BRIEN, S., EPSTEIN, D. M., KOH, G. Y. & MCDONALD, D. M. 2011. Pericyte requirement for anti-leak action of angiopoietin-1 and vascular remodeling in sustained inflammation. *Am J Pathol,* 178**,** 2897-909.

GAMBLE, J. R., DREW, J., TREZISE, L., UNDERWOOD, A., PARSONS, M., KASMINKAS, L., RUDGE, J., YANCOPOULOS, G. & VADAS, M. A. 2000. Angiopoietin-1 is an antipermeability and anti-inflammatory agent in vitro and targets cell junctions. *Circ Res,* 87**,** 603-7.

GANSS, R., ARNOLD, B. & HAMMERLING, G. J. 2004. Mini-review: overcoming tumour-intrinsic resistance to immune effector function. *Eur J Immunol,* 34**,** 2635-41.

GAZIT, Y., BAISH, J. W., SAFABAKHSH, N., LEUNIG, M., BAXTER, L. T. & JAIN, R. K. 1997. Fractal characteristics of tumour vascular architecture during tumour growth and regression. *Microcirculation,* 4**,** 395-402.

GIANTONIO, B. J., CATALANO, P. J., MEROPOL, N. J., O'DWYER, P. J., MITCHELL, E. P., ALBERTS, S. R., SCHWARTZ, M. A. & BENSON, A. B., 3RD 2007. Bevacizumab in combination with oxaliplatin, fluorouracil, and leucovorin (FOLFOX4) for previously treated metastatic colorectal cancer: results from the Eastern Cooperative Oncology Group Study E3200. *J Clin Oncol,* 25**,** 1539-44.

GJINI, E., HEKKING, L. H., KUCHLER, A., SAHARINEN, P., WIENHOLDS, E., POST, J. A., ALITALO, K. & SCHULTE-MERKER, S. 2011. Zebrafish Tie-2 shares a redundant role with Tie-1 in heart development and regulates vessel integrity. *Dis Model Mech,* 4**,** 57-66.

GOEL, S., DUDA, D. G., XU, L., MUNN, L. L., BOUCHER, Y., FUKUMURA, D. & JAIN, R. K. 2011. Normalization of the vasculature for treatment of cancer and other diseases. *Physiol Rev,* 91**,** 1071-121.

GOEL, S., GUPTA, N., WALCOTT, B. P., SNUDERL, M., KESLER, C. T., KIRKPATRICK, N. D., HEISHI, T., HUANG, Y., MARTIN, J. D., AGER, E., SAMUEL, R., WANG, S., YAZBEK, J., VAKOC, B. J., PETERSON, R. T.,

PADERA, T. P., DUDA, D. G., FUKUMURA, D. & JAIN, R. K. 2013. Effects of vascular-endothelial protein tyrosine phosphatase inhibition on breast cancer vasculature and metastatic progression. *J Natl Cancer Inst,* 105**,** 1188-201.

GREENBERG, J. I., SHIELDS, D. J., BARILLAS, S. G., ACEVEDO, L. M., MURPHY, E., HUANG, J., SCHEPPKE, L., STOCKMANN, C., JOHNSON, R. S., ANGLE, N. & CHERESH, D. A. 2008. A role for VEGF as a negative regulator of pericyte function and vessel maturation. *Nature,* 456**,** 809-13.

GREENBLATT, M. & SHUBIK, P. 1968. Tumour angiogenesis: transfilter diffusion studies in the hamster by the transparent chamber technique. *J Natl Cancer Inst,* 41**,** 111-124.

GULLINO, P. M. 1978. Angiogenesis and oncogenesis. *J Natl Cancer Inst,* 61**,** 639-43.

GUNAJE, J. J., BAHRAMI, A. J., SCHWARTZ, S. M., DAUM, G. & MAHONEY, W. M., JR. 2011. PDGF-dependent regulation of regulator of G protein signaling-5 expression and vascular smooth muscle cell functionality. *Am J Physiol Cell Physiol,* 301**,** C478-89

HALL, A. P. 2006. Review of the pericyte during angiogenesis and its role in cancer and diabetic retinopathy. *Toxicol Pathol,* 34**,** 763-75.

HAMMERSEN, F., ENDRICH, B. & MESSMER, K. 1985. The fine structure of tumour blood vessels. I. Participation of non-endothelial cells in tumour angiogenesis. *Int J Microcirc Clin Exp,* 4**,** 31-43.

HAMZAH, J., JUGOLD, M., KIESSLING, F., RIGBY, P., MANZUR, M., MARTI, H. H., RABIE, T., KADEN, S., GRONE, H. J., HAMMERLING, G. J., ARNOLD, B. & GANSS, R. 2008. Vascular normalization in Rgs5-deficient tumours promotes immune destruction. *Nature,* 453**,** 410-4.

HANSEN-ALGENSTAEDT, N., STOLL, B. R., PADERA, T. P., DOLMANS, D. E., HICKLIN, D. J., FUKUMURA, D. & JAIN, R. K. 2000. Tumor oxygenation in hormone-dependent tumors during vascular endothelial growth factor receptor-2 blockade, hormone ablation, and chemotherapy. *Cancer Res,* 60**,** 4556-60.

HARRIS, A. L. 2002. Hypoxia--a key regulatory factor in tumour growth. *Nat Rev Cancer,* 2**,** 38-47.

HASHIZUME, H., BALUK, P., MORIKAWA, S., MCLEAN, J. W., THURSTON, G., ROBERGE, S., JAIN, R. K. & MCDONALD, D. M. 2000. Openings between defective endothelial cells explain tumour vessel leakiness. *Am J Pathol,* 156**,** 1363-80.

HAYASHI, M., MAJUMDAR, A., LI, X., ADLER, J., SUN, Z., VERTUANI, S., HELLBERG, C., MELLBERG, S., KOCH, S., DIMBERG, A., KOH, G. Y., DEJANA, E., BELTING, H. G., AFFOLTER, M., THURSTON, G., HOLMGREN, L., VESTWEBER, D. & CLAESSON-WELSH, L. 2013. VE-PTP regulates VEGFR2 activity in stalk cells to establish endothelial cell polarity and lumen formation. *Nat Commun,* 4**,** 1672.

HELMLINGER, G., YUAN, F., DELLIAN, M. & JAIN, R. K. 1997. Interstitial pH and pO2 gradients in solid tumours in vivo: high-resolution measurements reveal a lack of correlation. *Nat Med,* 3**,** 177-82.

HOBBS, S. K., MONSKY, W. L., YUAN, F., ROBERTS, W. G., GRIFFITH, L., TORCHILIN, V. P. & JAIN, R. K. 1998. Regulation of transport pathways in tumour vessels: role of tumour type and microenvironment. *Proc Natl Acad Sci U S A,* 95**,** 4607-12.
HOCKEL, M., SCHLENGER, K., HOCKEL, S. & VAUPEL, P. 1999. Hypoxic cervical cancers with low apoptotic index are highly aggressive. *Cancer Res,* 59**,** 4525-8.
HOCKEL, M. & VAUPEL, P. 2001. Tumour hypoxia: definitions and current clinical, biologic, and molecular aspects. *J Natl Cancer Inst,* 93**,** 266-76.
HOLASH, J., MAISONPIERRE, P. C., COMPTON, D., BOLAND, P., ALEXANDER, C. R., ZAGZAG, D., YANCOPOULOS, G. D. & WIEGAND, S. J. 1999. Vessel cooption, regression, and growth in tumours mediated by angiopoietins and VEGF. *Science,* 284**,** 1994-8.
HOLOPAINEN, T., SAHARINEN, P., D'AMICO, G., LAMPINEN, A., EKLUND, L., SORMUNEN, R., ANISIMOV, A., ZARKADA, G., LOHELA, M., HELOTERA, H., TAMMELA, T., BENJAMIN, L. E., YLA-HERTTUALA, S., LEOW, C. C., KOH, G. Y. & ALITALO, K. 2012. Effects of angiopoietin-2-blocking antibody on endothelial cell-cell junctions and lung metastasis. *J Natl Cancer Inst,* 104**,** 461-75.
HUANG, H., BHAT, A., WOODNUTT, G. & LAPPE, R. 2010. Targeting the ANGPT-TIE2 pathway in malignancy. *Nat Rev Cancer,* 10**,** 575-85.
HUANG, H., LAI, J. Y., DO, J., LIU, D., LI, L., DEL ROSARIO, J., DOPPALAPUDI, V. R., PIRIE-SHEPHERD, S., LEVIN, N., BRADSHAW, C., WOODNUTT, G., LAPPE, R. & BHAT, A. 2011. Specifically targeting angiopoietin-2 inhibits angiogenesis, tie2-expressing monocyte infiltration, and tumour growth. *Clin Cancer Res,* 17**,** 1001-11.
HUANG, P., DUDA, D. G., JAIN, R. K. & FUKUMURA, D. 2008. Histopathologic findings and establishment of novel tumour lines from spontaneous tumours in FVB/N mice. *Comp Med,* 58**,** 253-63.
HUANG, Y., GOEL, S., DUDA, D. G., FUKUMURA, D. & JAIN, R. K. 2013. Vascular normalization as an emerging strategy to enhance cancer immunotherapy. *Cancer Res,* 73**,** 2943-8.
HURWITZ, H., FEHRENBACHER, L., NOVOTNY, W., CARTWRIGHT, T., HAINSWORTH, J., HEIM, W., BERLIN, J., BARON, A., GRIFFING, S., HOLMGREN, E., FERRARA, N., FYFE, G., ROGERS, B., ROSS, R. & KABBINAVAR, F. 2004. Bevacizumab plus irinotecan, fluorouracil, and leucovorin for metastatic colorectal cancer. *N Engl J Med,* 350**,** 2335-42.
IDE, A. G., BAKER, N. H. & WARREN, S. L. 1939. Vascularization of the Brown-Pearce rabbit epithelioma transplant as seen in the transparent ear chamber. *Am J Radiol,* 42**,** 891-899.
IZUMI, Y., XU, L., DI TOMASO, E., FUKUMURA, D. & JAIN, R. K. 2002. Tumour biology: herceptin acts as an anti-angiogenic cocktail. *Nature,* 416**,** 279-80.
INAI, T., MANCUSO, M., HASHIZUME, H., BAFFERT, F., HASKELL, A., BALUK, P., HU-LOWE, D. D., SHALINSKY, D. R., THURSTON, G., YANCOPOULOS, G. D. & MCDONALD, D. M. 2004. Inhibition of vascular

endothelial growth factor (VEGF) signaling in cancer causes loss of endothelial fenestrations, regression of tumour vessels, and appearance of basement membrane ghosts. *Am J Pathol,* 165**,** 35-52.
JAIN, R. K. 1988. Determinants of tumour blood flow: a review. *Cancer Res,* 48**,** 2641-58.
JAIN, R. K. 1989. Delivery of novel therapeutic agents in tumours: physiological barriers and strategies. *J Natl Cancer Inst,* 81**,** 570-6.
JAIN, R. K., SAFABAKHSH, N., SCKELL, A., CHEN, Y., JIANG, P., BENJAMIN, L., YUAN, F. & KESHET, E. 1998. Endothelial cell death, angiogenesis, and microvascular function after castration in an androgen-dependent tumor: role of vascular endothelial growth factor. *Proc Natl Acad Sci U S A,* 95**,** 10820-5.
JAIN, R. K. 2001. Normalizing tumour vasculature with anti-angiogenic therapy: a new paradigm for combination therapy. *Nat Med,* 7**,** 987-9.
JAIN, R. K. 2003. Molecular regulation of vessel maturation. *Nat Med,* 9**,** 685-93.
JAIN, R. K. 2005. Normalization of tumour vasculature: an emerging concept in antiangiogenic therapy. *Science,* 307**,** 58-62.
JAIN, R. K. & CARMELIET, P. 2012. SnapShot: Tumour angiogenesis. *Cell,* 149**,** 1408-1408 e1.
JAIN, R. K., DUDA, D. G., CLARK, J. W. & LOEFFLER, J. S. 2006. Lessons from phase III clinical trials on anti-VEGF therapy for cancer. *Nat Clin Pract Oncol,* 3**,** 24-40.
JAIN, R. K., FINN, A. V., KOLODGIE, F. D., GOLD, H. K. & VIRMANI, R. 2007. Antiangiogenic therapy for normalization of atherosclerotic plaque vasculature: a potential strategy for plaque stabilization. *Nature Clinical Practice Cardiovascular Medicine,* 4**,** 491-502.
JULIEN, S. G., DUBE, N., HARDY, S. & TREMBLAY, M. L. 2011. Inside the human cancer tyrosine phosphatome. *Nat Rev Cancer,* 11**,** 35-49.
KAMOUN, W. S., LEY, C. D., FARRAR, C. T., DUYVERMAN, A. M., LAHDENRANTA, J., LACORRE, D. A., BATCHELOR, T. T., DI TOMASO, E., DUDA, D. G., MUNN, L. L., FUKUMURA, D., SORENSEN, A. G. & JAIN, R. K. 2009. Edema control by cediranib, a vascular endothelial growth factor receptor-targeted kinase inhibitor, prolongs survival despite persistent brain tumour growth in mice. *Journal of Clinical Oncology,* 27**,** 2542-52.
KASHIWAGI, S., IZUMI, Y., GOHONGI, T., DEMOU, Z. N., XU, L., HUANG, P. L., BUERK, D. G., MUNN, L. L., JAIN, R. K. & FUKUMURA, D. 2005. NO mediates mural cell recruitment and vessel morphogenesis in murine melanomas and tissue-engineered blood vessels. *J Clin Invest,* 115**,** 1816-27.
KASHIWAGI, S., TSUKADA, K., XU, L., MIYAZAKI, J., KOZIN, S. V., TYRRELL, J. A., SESSA, W. C., GERWECK, L. E., JAIN, R. K. & FUKUMURA, D. 2008. Perivascular nitric oxide gradients normalize tumour vasculature. *Nat Med,* 14**,** 255-7.

KECK, P. J., HAUSER, S. D., KRIVI, G., SANZO, K., WARREN, T., FEDER, J. & CONNOLLY, D. T. 1989. Vascular permeability factor, an endothelial cell mitogen related to PDGF. *Science,* 246**,** 1309-12.

KIENAST, Y., VON BAUMGARTEN, L., FUHRMANN, M., KLINKERT, W. E., GOLDBRUNNER, R., HERMS, J. & WINKLER, F. 2010. Real-time imaging reveals the single steps of brain metastasis formation. *Nat Med,* 16**,** 116-22.

KIM, K. J., LI, B., WINER, J., ARMANINI, M., GILLETT, N., PHILLIPS, H. S. & FERRARA, N. 1993. Inhibition of vascular endothelial growth factor-induced angiogenesis suppresses tumour growth in vivo. *Nature,* 362**,** 841-4.

KIM, K. T., CHOI, H. H., STEINMETZ, M. O., MACO, B., KAMMERER, R. A., AHN, S. Y., KIM, H. Z., LEE, G. M. & KOH, G. Y. 2005. Oligomerization and multimerization are critical for angiopoietin-1 to bind and phosphorylate Tie2. *J Biol Chem,* 280**,** 20126-31.

KIM, P., CHUNG, E., YAMASHITA, H., HUNG, K. E., MIZOGUCHI, A., KUCHERLAPATI, R., FUKUMURA, D., JAIN, R. K. & YUN, S. H. 2010. In vivo wide-area cellular imaging by side-view endomicroscopy. *Nat Methods,* 7**,** 303-5.

KOH, Y. J., KIM, H. Z., HWANG, S. I., LEE, J. E., OH, N., JUNG, K., KIM, M., KIM, K. E., KIM, H., LIM, N. K., JEON, C. J., LEE, G. M., JEON, B. H., NAM, D. H., SUNG, H. K., NAGY, A., YOO, O. J. & KOH, G. Y. 2010. Double antiangiogenic protein, DAAP, targeting VEGF-A and angiopoietins in tumour angiogenesis, metastasis, and vascular leakage. *Cancer Cell,* 18**,** 171-84.

KONTOS, C. D. & WILLETT, C. G. 2013. Inhibiting the inhibitor: targeting vascular endothelial protein tyrosine phosphatase to promote tumour vascular maturation. *J Natl Cancer Inst,* 105**,** 1163-5.

KUPPERS, V., VOCKEL, M., NOTTEBAUM, A. F. & VESTWEBER, D. 2014. Phosphatases and kinases as regulators of the endothelial barrier function. *Cell Tissue Res*.

LEE, C. G., HEIJN, M., DI TOMASO, E., GRIFFON-ETIENNE, G., ANCUKIEWICZ, M., KOIKE, C., PARK, K. R., FERRARA, N., JAIN, R. K., SUIT, H. D. & BOUCHER, Y. 2000. Anti-Vascular endothelial growth factor treatment augments tumour radiation response under normoxic or hypoxic conditions. *Cancer Res,* 60**,** 5565-70.

LEIBOVICH, S. J., POLVERINI, P. J., SHEPARD, H. M., WISEMAN, D. M., SHIVELY, V. & NUSEIR, N. 1987. Macrophage-induced angiogenesis is mediated by tumour necrosis factor-alpha. *Nature,* 329**,** 630-2.

LEOW, C. C., COFFMAN, K., INIGO, I., BREEN, S., CZAPIGA, M., SOUKHAREV, S., GINGLES, N., PETERSON, N., FAZENBAKER, C., WOODS, R., JALLAL, B., RICKETTS, S. A., LAVALLEE, T., COATS, S. & CHANG, Y. 2012. MEDI3617, a human anti-angiopoietin 2 monoclonal antibody, inhibits angiogenesis and tumour growth in human tumour xenograft models. *Int J Oncol,* 40**,** 1321-30.

LESS, J. R., POSNER, M. C., BOUCHER, Y., BOROCHOVITZ, D., WOLMARK, N. & JAIN, R. K. 1992. Interstitial hypertension in human breast and colorectal tumours. *Cancer Res,* 52**,** 6371-4.

LESS, J. R., POSNER, M. C., SKALAK, T. C., WOLMARK, N. & JAIN, R. K. 1997. Geometric resistance and microvascular network architecture of human colorectal carcinoma. *Microcirculation,* 4**,** 25-33.

LESS, J. R., SKALAK, T. C., SEVICK, E. M. & JAIN, R. K. 1991. Microvascular architecture in a mammary carcinoma: branching patterns and vessel dimensions. *Cancer Res,* 51**,** 265-73.

LEUNG, D. W., CACHIANES, G., KUANG, W. J., GOEDDEL, D. V. & FERRARA, N. 1989. Vascular endothelial growth factor is a secreted angiogenic mitogen. *Science,* 246**,** 1306-9.

LEUNIG, M., YUAN, F., MENGER, M. D., BOUCHER, Y., GOETZ, A. E., MESSMER, K. & JAIN, R. K. 1992. Angiogenesis, microvascular architecture, microhemodynamics, and interstitial fluid pressure during early growth of human adenocarcinoma LS174T in SCID mice. *Cancer Res,* 52**,** 6553-60.

LI, Z., HUANG, H., BOLAND, P., DOMINGUEZ, M. G., BURFEIND, P., LAI, K. M., LIN, H. C., GALE, N. W., DALY, C., AUERBACH, W., VALENZUELA, D., YANCOPOULOS, G. D. & THURSTON, G. 2009. Embryonic stem cell tumour model reveals role of vascular endothelial receptor tyrosine phosphatase in regulating Tie2 pathway in tumour angiogenesis. *Proc Natl Acad Sci U S A,* 106**,** 22399-404.

MAISONPIERRE, P. C., SURI, C., JONES, P. F., BARTUNKOVA, S., WIEGAND, S. J., RADZIEJEWSKI, C., COMPTON, D., MCCLAIN, J., ALDRICH, T. H., PAPADOPOULOS, N., DALY, T. J., DAVIS, S., SATO, T. N. & YANCOPOULOS, G. D. 1997. Angiopoietin-2, a natural antagonist for Tie2 that disrupts in vivo angiogenesis. *Science,* 277**,** 55-60.

MAKHOUL, I., GRIFFIN, R. J., SIEGEL, E., LEE, J., DHAKAL, I., RAJ, V., JAMSHIDI-PARSIAN, A., KLIMBERG, S., HUTCHINS, L. F. & KADLUBAR, S. 2014. High-circulating Tie2 is Associated With Pathologic Complete Response to Chemotherapy and Antiangiogenic Therapy in Breast Cancer. *Am J Clin Oncol*.

MAZZONE, M., DETTORI, D., LEITE DE OLIVEIRA, R., LOGES, S., SCHMIDT, T., JONCKX, B., TIAN, Y. M., LANAHAN, A. A., POLLARD, P., RUIZ DE ALMODOVAR, C., DE SMET, F., VINCKIER, S., ARAGONES, J., DEBACKERE, K., LUTTUN, A., WYNS, S., JORDAN, B., PISACANE, A., GALLEZ, B., LAMPUGNANI, M. G., DEJANA, E., SIMONS, M., RATCLIFFE, P., MAXWELL, P. & CARMELIET, P. 2009. Heterozygous deficiency of PHD2 restores tumour oxygenation and inhibits metastasis via endothelial normalization. *Cell,* 136**,** 839-51.

MILES, D. W., CHAN, A., DIRIX, L. Y., CORTES, J., PIVOT, X., TOMCZAK, P., DELOZIER, T., SOHN, J. H., PROVENCHER, L., PUGLISI, F., HARBECK, N., STEGER, G. G., SCHNEEWEISS, A., WARDLEY, A. M., CHLISTALLA, A. & ROMIEU, G. 2010. Phase III study of bevacizumab plus docetaxel compared with placebo plus docetaxel for the first-line

treatment of human epidermal growth factor receptor 2-negative metastatic breast cancer. *J Clin Oncol,* 28**,** 3239-47.
MILES, D., HARBECK, N., ESCUDIER, B., HURWITZ, H., SALTZ, L., VAN CUTSEM, E., CASSIDY, J., MUELLER, B. & SIRZEN, F. 2011. Disease course patterns after discontinuation of bevacizumab: pooled analysis of randomized phase III trials. *J Clin Oncol,* 29**,** 83-8.
MILLAUER, B., WIZIGMANN-VOOS, S., SCHNURCH, H., MARTINEZ, R., MOLLER, N. P., RISAU, W. & ULLRICH, A. 1993. High affinity VEGF binding and developmental expression suggest Flk-1 as a major regulator of vasculogenesis and angiogenesis. *Cell,* 72**,** 835-46.
MILLER, K., WANG, M., GRALOW, J., DICKLER, M., COBLEIGH, M., PEREZ, E. A., SHENKIER, T., CELLA, D. & DAVIDSON, N. E. 2007. Paclitaxel plus bevacizumab versus paclitaxel alone for metastatic breast cancer. *N Engl J Med,* 357**,** 2666-76.
MORFOISSE, F., KUCHNIO, A., FRAINAY, C., GOMEZ-BROUCHET, A., DELISLE, M. B., MARZI, S., HELFER, A. C., HANTELYS, F., PUJOL, F., GUILLERMET-GUIBERT, J., BOUSQUET, C., DEWERCHIN, M., PYRONNET, S., PRATS, A. C., CARMELIET, P. & GARMY-SUSINI, B. 2014. Hypoxia induces VEGF-C expression in metastatic tumor cells via a HIF-1alpha-independent translation-mediated mechanism. *Cell Rep,* 6**,** 155-67.
MORIKAWA, S., BALUK, P., KAIDOH, T., HASKELL, A., JAIN, R. K. & MCDONALD, D. M. 2002. Abnormalities in pericytes on blood vessels and endothelial sprouts in tumours. *Am J Pathol,* 160**,** 985-1000.
NAGY, J. A., BENJAMIN, L., ZENG, H., DVORAK, A. M. & DVORAK, H. F. 2008. Vascular permeability, vascular hyperpermeability and angiogenesis. *Angiogenesis,* 11**,** 109-19.
NAGY, J. A., CHANG, S. H., DVORAK, A. M. & DVORAK, H. F. 2009. Why are tumour blood vessels abnormal and why is it important to know? *Br J Cancer,* 100**,** 865-9.
NAGY, J. A., VASILE, E., FENG, D., SUNDBERG, C., BROWN, L. F., DETMAR, M. J., LAWITTS, J. A., BENJAMIN, L., TAN, X., MANSEAU, E. J., DVORAK, A. M. & DVORAK, H. F. 2002. Vascular permeability factor/vascular endothelial growth factor induces lymphangiogenesis as well as angiogenesis. *J Exp Med,* 196**,** 1497-506.
NASARRE, P., THOMAS, M., KRUSE, K., HELFRICH, I., WOLTER, V., DEPPERMANN, C., SCHADENDORF, D., THURSTON, G., FIEDLER, U. & AUGUSTIN, H. G. 2009. Host-derived angiopoietin-2 affects early stages of tumour development and vessel maturation but is dispensable for later stages of tumour growth. *Cancer Res,* 69**,** 1324-33.
NAWROTH, R., POELL, G., RANFT, A., KLOEP, S., SAMULOWITZ, U., FACHINGER, G., GOLDING, M., SHIMA, D. T., DEUTSCH, U. & VESTWEBER, D. 2002. VE-PTP and VE-cadherin ectodomains interact to facilitate regulation of phosphorylation and cell contacts. *EMBO J,* 21**,** 4885-95.

NICOLI, S. & PRESTA, M. 2007. The zebrafish/tumour xenograft angiogenesis assay. *Nat Protoc,* 2**,** 2918-23.

NOTTEBAUM, A. F., CAGNA, G., WINDERLICH, M., GAMP, A. C., LINNEPE, R., POLASCHEGG, C., FILIPPOVA, K., LYCK, R., ENGELHARDT, B., KAMENYEVA, O., BIXEL, M. G., BUTZ, S. & VESTWEBER, D. 2008. VE-PTP maintains the endothelial barrier via plakoglobin and becomes dissociated from VE-cadherin by leukocytes and by VEGF. *J Exp Med,* 205**,** 2929-45.

ORLANDI, C., DUNN, C. J. & CUTSHAW, L. G. 1988. Evaluation of angiogenesis in chronic inflammation by laser-Doppler flowmetry. *Clin Sci (Lond),* 74**,** 119-21.

OUBAHA, M. & GRATTON, J. P. 2009. Phosphorylation of endothelial nitric oxide synthase by atypical PKC zeta contributes to angiopoietin-1-dependent inhibition of VEGF-induced endothelial permeability in vitro. *Blood,* 114**,** 3343-51.

PADERA, T. P., KUO, A. H., HOSHIDA, T., LIAO, S., LOBO, J., KOZAK, K. R., FUKUMURA, D. & JAIN, R. K. 2008. Differential response of primary tumour versus lymphatic metastasis to VEGFR-2 and VEGFR-3 kinase inhibitors cediranib and vandetanib. *Mol Cancer Ther,* 7**,** 2272-9.

PADERA, T. P., STOLL, B. R., TOOREDMAN, J. B., CAPEN, D., DI TOMASO, E. & JAIN, R. K. 2004. Pathology: cancer cells compress intratumour vessels. *Nature,* 427**,** 695.

PATAN, S., MUNN, L. L. & JAIN, R. K. 1996. Intussusceptive microvascular growth in a human colon adenocarcinoma xenograft: a novel mechanism of tumour angiogenesis. *Microvasc Res,* 51**,** 260-72.

PENNACCHIETTI, S., MICHIELI, P., GALLUZZO, M., MAZZONE, M., GIORDANO, S. & COMOGLIO, P. M. 2003. Hypoxia promotes invasive growth by transcriptional activation of the met protooncogene. *Cancer Cell,* 3**,** 347-61.

PRIES, A. R., CORNELISSEN, A. J., SLOOT, A. A., HINKELDEY, M., DREHER, M. R., HOPFNER, M., DEWHIRST, M. W. & SECOMB, T. W. 2009. Structural adaptation and heterogeneity of normal and tumour microvascular networks. *PLoS Comput Biol,* 5**,** e1000394.

PRIES, A. R., HOPFNER, M., LE NOBLE, F., DEWHIRST, M. W. & SECOMB, T. W. 2010. The shunt problem: control of functional shunting in normal and tumour vasculature. *Nat Rev Cancer,* 10**,** 587-93.

QAYUM, N., MUSCHEL, R. J., IM, J. H., BALATHASAN, L., KOCH, C. J., PATEL, S., MCKENNA, W. G. & BERNHARD, E. J. 2009. Tumor vascular changes mediated by inhibition of oncogenic signaling. *Cancer Res,* 69**,** 6347-54.

QU, H., NAGY, J. A., SENGER, D. R., DVORAK, H. F. & DVORAK, A. M. 1995. Ultrastructural localization of vascular permeability factor/vascular endothelial growth factor (VPF/VEGF) to the abluminal plasma membrane and vesiculovacuolar organelles of tumour microvascular endothelium. *J Histochem Cytochem,* 43**,** 381-9.

RAZA, A., FRANKLIN, M. J. & DUDEK, A. Z. 2010. Pericytes and vessel maturation during tumour angiogenesis and metastasis. *Am J Hematol,* 85**,** 593-8.

RECK, M., VON PAWEL, J., ZATLOUKAL, P., RAMLAU, R., GORBOUNOVA, V., HIRSH, V., LEIGHL, N., MEZGER, J., ARCHER, V., MOORE, N. & MANEGOLD, C. 2009. Phase III trial of cisplatin plus gemcitabine with either placebo or bevacizumab as first-line therapy for nonsquamous non-small-cell lung cancer: AVAil. *J Clin Oncol,* 27**,** 1227-34.

RELF, M., LEJEUNE, S., SCOTT, P. A., FOX, S., SMITH, K., LEEK, R., MOGHADDAM, A., WHITEHOUSE, R., BICKNELL, R. & HARRIS, A. L. 1997. Expression of the angiogenic factors vascular endothelial cell growth factor, acidic and basic fibroblast growth factor, tumour growth factor beta-1, platelet-derived endothelial cell growth factor, placenta growth factor, and pleiotrophin in human primary breast cancer and its relation to angiogenesis. *Cancer Res,* 57**,** 963-9.

RICCI-VITIANI, L., PALLINI, R., BIFFONI, M., TODARO, M., INVERNICI, G., CENCI, T., MAIRA, G., PARATI, E. A., STASSI, G., LAROCCA, L. M. & DE MARIA, R. 2010. Tumour vascularization via endothelial differentiation of glioblastoma stem-like cells. *Nature,* 468**,** 824-8.

RIGAMONTI, N., KADIOGLU, E., KEKLIKOGLOU, I., WYSER RMILI, C., LEOW, C. C. & DE PALMA, M. 2014. Role of angiopoietin-2 in adaptive tumor resistance to VEGF signaling blockade. *Cell Rep,* 8**,** 696-706.

ROBERT, N. J., DIERAS, V., GLASPY, J., BRUFSKY, A. M., BONDARENKO, I., LIPATOV, O. N., PEREZ, E. A., YARDLEY, D. A., CHAN, S. Y., ZHOU, X., PHAN, S. C. & O'SHAUGHNESSY, J. 2011. RIBBON-1: randomized, double-blind, placebo-controlled, phase III trial of chemotherapy with or without bevacizumab for first-line treatment of human epidermal growth factor receptor 2-negative, locally recurrent or metastatic breast cancer. *J Clin Oncol,* 29**,** 1252-60.

RODRIGUEZ, P. L., JIANG, S., FU, Y., AVRAHAM, S. & AVRAHAM, H. K. 2014. The proinflammatory peptide substance P promotes blood-brain barrier breaching by breast cancer cells through changes in microvascular endothelial cell tight junctions. *Int J Cancer,* 134**,** 1034-44.

ROH, H. D., BOUCHER, Y., KALNICKI, S., BUCHSBAUM, R., BLOOMER, W. D. & JAIN, R. K. 1991. Interstitial hypertension in carcinoma of uterine cervix in patients: possible correlation with tumour oxygenation and radiation response. *Cancer Res,* 51**,** 6695-8.

ROLNY, C., MAZZONE, M., TUGUES, S., LAOUI, D., JOHANSSON, I., COULON, C., SQUADRITO, M. L., SEGURA, I., LI, X., KNEVELS, E., COSTA, S., VINCKIER, S., DRESSELAER, T., AKERUD, P., DE MOL, M., SALOMAKI, H., PHILLIPSON, M., WYNS, S., LARSSON, E., BUYSSCHAERT, I., BOTLING, J., HIMMELREICH, U., VAN GINDERACHTER, J. A., DE PALMA, M., DEWERCHIN, M., CLAESSON-WELSH, L. & CARMELIET, P. 2011. HRG inhibits tumour growth and metastasis by inducing macrophage polarization and vessel normalization through downregulation of PlGF. *Cancer Cell,* 19**,** 31-44.

SALTZ, L. B., CLARKE, S., DIAZ-RUBIO, E., SCHEITHAUER, W., FIGER, A., WONG, R., KOSKI, S., LICHINITSER, M., YANG, T. S., RIVERA, F., COUTURE, F., SIRZEN, F. & CASSIDY, J. 2008. Bevacizumab in combination with oxaliplatin-based chemotherapy as first-line therapy in metastatic colorectal cancer: a randomized phase III study. *J Clin Oncol,* 26**,** 2013-9.

SANDLER, A., GRAY, R., PERRY, M. C., BRAHMER, J., SCHILLER, J. H., DOWLATI, A., LILENBAUM, R. & JOHNSON, D. H. 2006. Paclitaxel-carboplatin alone or with bevacizumab for non-small-cell lung cancer. *N Engl J Med,* 355**,** 2542-50.

SATO, T. N., TOZAWA, Y., DEUTSCH, U., WOLBURG-BUCHHOLZ, K., FUJIWARA, Y., GENDRON-MAGUIRE, M., GRIDLEY, T., WOLBURG, H., RISAU, W. & QIN, Y. 1995. Distinct roles of the receptor tyrosine kinases Tie-1 and Tie-2 in blood vessel formation. *Nature,* 376**,** 70-4.

SCHNELL, C. R., STAUFFER, F., ALLEGRINI, P. R., O'REILLY, T., MCSHEEHY, P. M., DARTOIS, C., STUMM, M., COZENS, R., LITTLEWOOD-EVANS, A., GARCIA-ECHEVERRIA, C. & MAIRA, S. M. 2008. Effects of the dual phosphatidylinositol 3-kinase/mammalian target of rapamycin inhibitor NVP-BEZ235 on the tumor vasculature: implications for clinical imaging. *Cancer Res,* 68**,** 6598-607.

SEMENZA, G. L. 2010a. Defining the role of hypoxia-inducible factor 1 in cancer biology and therapeutics. *Oncogene,* 29**,** 625-34.

SEMENZA, G. L. 2010b. HIF-1: upstream and downstream of cancer metabolism. *Curr Opin Genet Dev,* 20**,** 51-6.

SENGER, D. R., GALLI, S. J., DVORAK, A. M., PERRUZZI, C. A., HARVEY, V. S. & DVORAK, H. F. 1983. Tumour cells secrete a vascular permeability factor that promotes accumulation of ascites fluid. *Science,* 219**,** 983-5.

SFILIGOI, C., DE LUCA, A., CASCONE, I., SORBELLO, V., FUSO, L., PONZONE, R., BIGLIA, N., AUDERO, E., ARISIO, R., BUSSOLINO, F., SISMONDI, P. & DE BORTOLI, M. 2003. Angiopoietin-2 expression in breast cancer correlates with lymph node invasion and short survival. *Int J Cancer,* 103**,** 466-74.

SHEN, J., FRYE, M., LEE, B. L., REINARDY, J. L., MCCLUNG, J. M., DING, K., KOJIMA, M., XIA, H., SEIDEL, C., SILVA, R. L., DONG, A., HACKETT, S. F., WANG, J., HOWARD, B. W., VESTWEBER, D., KONTOS, C. D., PETERS, K. G. & CAMPOCHIARO, P. A. 2014. Targeting VE-PTP activates TIE2 and stabilizes the ocular vasculature. *J Clin Invest*.

SIDKY, Y. A. & AUERBACH, R. 1975. Lymphocyte-induced angiogenesis: a quantitative and sensitive assay of the graft-vs.-host reaction. *J Exp Med,* 141**,** 1084-1100.

SORENSEN, A. G., EMBLEM, K. E., POLASKOVA, P., JENNINGS, D., KIM, H., ANCUKIEWICZ, M., WANG, M., WEN, P. Y., IVY, P., BATCHELOR, T. T. & JAIN, R. K. 2012. Increased survival of glioblastoma patients who respond to antiangiogenic therapy with elevated blood perfusion. *Cancer Res,* 72**,** 402-7.

STARLING, E. H. 1896. On the Absorption of Fluids from the Connective Tissue Spaces. *J Physiol,* 19**,** 312-26.
STOHRER, M., BOUCHER, Y., STANGASSINGER, M. & JAIN, R. K. 2000. Oncotic pressure in solid tumours is elevated. *Cancer Res,* 60**,** 4251-5.
SURI, C., JONES, P. F., PATAN, S., BARTUNKOVA, S., MAISONPIERRE, P. C., DAVIS, S., SATO, T. N. & YANCOPOULOS, G. D. 1996. Requisite role of angiopoietin-1, a ligand for the TIE2 receptor, during embryonic angiogenesis. *Cell,* 87**,** 1171-80.
SURI, C., MCCLAIN, J., THURSTON, G., MCDONALD, D. M., ZHOU, H., OLDMIXON, E. H., SATO, T. N. & YANCOPOULOS, G. D. 1998. Increased vascularization in mice overexpressing angiopoietin-1. *Science,* 282**,** 468-71.
TABRUYN, S. P., COLTON, K., MORISADA, T., FUXE, J., WIEGAND, S. J., THURSTON, G., COYLE, A. J., CONNOR, J. & MCDONALD, D. M. 2010. Angiopoietin-2-driven vascular remodeling in airway inflammation. *Am J Pathol,* 177**,** 3233-43.
TALMADGE, J. E. & FIDLER, I. J. 2010. AACR centennial series: the biology of cancer metastasis: historical perspective. *Cancer Res,* 70**,** 5649-69.
TEBBUTT, N. C., WILSON, K., GEBSKI, V. J., CUMMINS, M. M., ZANNINO, D., VAN HAZEL, G. A., ROBINSON, B., BROAD, A., GANJU, V., ACKLAND, S. P., FORGESON, G., CUNNINGHAM, D., SAUNDERS, M. P., STOCKLER, M. R., CHUA, Y., ZALCBERG, J. R., SIMES, R. J. & PRICE, T. J. 2010. Capecitabine, bevacizumab, and mitomycin in first-line treatment of metastatic colorectal cancer: results of the Australasian Gastrointestinal Trials Group Randomized Phase III MAX Study. *J Clin Oncol,* 28**,** 3191-8.
TEICHER, B. A. 1996. A systems approach to cancer therapy. (Antioncogenics + standard cytotoxics-->mechanism(s) of interaction). *Cancer Metastasis Rev,* 15**,** 247-72.
TERMAN, B. I., DOUGHER-VERMAZEN, M., CARRION, M. E., DIMITROV, D., ARMELLINO, D. C., GOSPODAROWICZ, D. & BOHLEN, P. 1992. Identification of the KDR tyrosine kinase as a receptor for vascular endothelial cell growth factor. *Biochem Biophys Res Commun,* 187**,** 1579-86.
THURSTON, G., RUDGE, J. S., IOFFE, E., ZHOU, H., ROSS, L., CROLL, S. D., GLAZER, N., HOLASH, J., MCDONALD, D. M. & YANCOPOULOS, G. D. 2000. Angiopoietin-1 protects the adult vasculature against plasma leakage. *Nature Medicine,* 6**,** 460-3.
THURSTON, G., SURI, C., SMITH, K., MCCLAIN, J., SATO, T. N., YANCOPOULOS, G. D. & MCDONALD, D. M. 1999. Leakage-resistant blood vessels in mice transgenically overexpressing angiopoietin-1. *Science,* 286**,** 2511-4.
TONG, R. T., BOUCHER, Y., KOZIN, S. V., WINKLER, F., HICKLIN, D. J. & JAIN, R. K. 2004. Vascular normalization by vascular endothelial growth factor receptor 2 blockade induces a pressure gradient across the

vasculature and improves drug penetration in tumours. *Cancer Research,* 64**,** 3731-6.
VAKOC, B. J., LANNING, R. M., TYRRELL, J. A., PADERA, T. P., BARTLETT, L. A., STYLIANOPOULOS, T., MUNN, L. L., TEARNEY, G. J., FUKUMURA, D., JAIN, R. K. & BOUMA, B. E. 2009. Three-dimensional microscopy of the tumour microenvironment in vivo using optical frequency domain imaging. *Nat Med,* 15**,** 1219-23.
WARREN, R. S., YUAN, H., MATLI, M. R., GILLETT, N. A. & FERRARA, N. 1995. Regulation by vascular endothelial growth factor of human colon cancer tumourigenesis in a mouse model of experimental liver metastasis. *J Clin Invest,* 95**,** 1789-97.
WATNICK, R. S., CHENG, Y. N., RANGARAJAN, A., INCE, T. A. & WEINBERG, R. A. 2003. Ras modulates Myc activity to repress thrombospondin-1 expression and increase tumour angiogenesis. *Cancer Cell,* 3**,** 219-31.
WEIS, S., CUI, J., BARNES, L. & CHERESH, D. 2004. Endothelial barrier disruption by VEGF-mediated Src activity potentiates tumour cell extravasation and metastasis. *J Cell Biol,* 167**,** 223-9.
WELCH, S., SPITHOFF, K., RUMBLE, R. B. & MAROUN, J. 2010. Bevacizumab combined with chemotherapy for patients with advanced colorectal cancer: a systematic review. *Ann Oncol,* 21**,** 1152-62.
WESSEL, F., WINDERLICH, M., HOLM, M., FRYE, M., RIVERA-GALDOS, R., VOCKEL, M., LINNEPE, R., IPE, U., STADTMANN, A., ZARBOCK, A., NOTTEBAUM, A. F. & VESTWEBER, D. 2014. Leukocyte extravasation and vascular permeability are each controlled in vivo by different tyrosine residues of VE-cadherin. *Nat Immunol,* 15**,** 223-30.
WILDIERS, H., GUETENS, G., DE BOECK, G., VERBEKEN, E., LANDUYT, B., LANDUYT, W., DE BRUIJN, E. A. & VAN OOSTEROM, A. T. 2003. Effect of antivascular endothelial growth factor treatment on the intratumoural uptake of CPT-11. *Br J Cancer,* 88**,** 1979-86.
WILLETT, C. G., BOUCHER, Y., DI TOMASO, E., DUDA, D. G., MUNN, L. L., TONG, R. T., CHUNG, D. C., SAHANI, D. V., KALVA, S. P., KOZIN, S. V., MINO, M., COHEN, K. S., SCADDEN, D. T., HARTFORD, A. C., FISCHMAN, A. J., CLARK, J. W., RYAN, D. P., ZHU, A. X., BLASZKOWSKY, L. S., CHEN, H. X., SHELLITO, P. C., LAUWERS, G. Y. & JAIN, R. K. 2004. Direct evidence that the VEGF-specific antibody bevacizumab has antivascular effects in human rectal cancer. *Nat Med,* 10**,** 145-7.
WILLETT, C. G., DUDA, D. G., DI TOMASO, E., BOUCHER, Y., ANCUKIEWICZ, M., SAHANI, D. V., LAHDENRANTA, J., CHUNG, D. C., FISCHMAN, A. J., LAUWERS, G. Y., SHELLITO, P., CZITO, B. G., WONG, T. Z., PAULSON, E., POLESKI, M., VUJASKOVIC, Z., BENTLEY, R., CHEN, H. X., CLARK, J. W. & JAIN, R. K. 2009. Efficacy, safety, and biomarkers of neoadjuvant bevacizumab, radiation therapy, and fluorouracil in rectal cancer: a multidisciplinary phase II study. *J Clin Oncol,* 27**,** 3020-6.
WILSON, W. R. & HAY, M. P. 2011. Targeting hypoxia in cancer therapy. *Nat Rev Cancer,* 11**,** 393-410.

WINDERLICH, M., KELLER, L., CAGNA, G., BROERMANN, A., KAMENYEVA, O., KIEFER, F., DEUTSCH, U., NOTTEBAUM, A. F. & VESTWEBER, D. 2009. VE-PTP controls blood vessel development by balancing Tie-2 activity. *J Cell Biol,* 185**,** 657-71.

WINKLER, F., KOZIN, S. V., TONG, R. T., CHAE, S. S., BOOTH, M. F., GARKAVTSEV, I., XU, L., HICKLIN, D. J., FUKUMURA, D., DI TOMASO, E., MUNN, L. L. & JAIN, R. K. 2004. Kinetics of vascular normalization by VEGFR2 blockade governs brain tumour response to radiation: role of oxygenation, angiopoietin-1, and matrix metalloproteinases. *Cancer Cell,* 6**,** 553-63.

WONG, A. L., HAROON, Z. A., WERNER, S., DEWHIRST, M. W., GREENBERG, C. S. & PETERS, K. G. 1997. Tie2 expression and phosphorylation in angiogenic and quiescent adult tissues. *Circ Res,* 81**,** 567-74.

WONG, C. W., SONG, C., GRIMES, M. M., FU, W., DEWHIRST, M. W., MUSCHEL, R. J. & AL-MEHDI, A. B. 2002. Intravascular location of breast cancer cells after spontaneous metastasis to the lung. *Am J Pathol,* 161**,** 749-53.

WOUTERS, B. G. & BROWN, J. M. 1997. Cells at intermediate oxygen levels can be more important than the "hypoxic fraction" in determining tumour response to fractionated radiotherapy. *Radiat Res,* 147**,** 541-50.

YUAN, F., CHEN, Y., DELLIAN, M., SAFABAKHSH, N., FERRARA, N. & JAIN, R. K. 1996. Time-dependent vascular regression and permeability changes in established human tumour xenografts induced by an anti-vascular endothelial growth factor/vascular permeability factor antibody. *Proc Natl Acad Sci U S A,* 93**,** 14765-70.

ZHENG, W., NURMI, H., APPAK, S., SABINE, A., BOVAY, E., KORHONEN, E. A., ORSENIGO, F., LOHELA, M., D'AMICO, G., HOLOPAINEN, T., LEOW, C. C., DEJANA, E., PETROVA, T. V., AUGUSTIN, H. G. & ALITALO, K. 2014. Angiopoietin 2 regulates the transformation and integrity of lymphatic endothelial cell junctions. *Genes Dev,* 28**,** 1592-603.

Acknowledgements

1. First and foremost, I offer my heartfelt thanks to Professor Jennifer Gamble (University of Sydney) and Professor Rakesh Jain (Harvard Medical School), who served as inspiring and supportive mentors throughout my doctoral work. Their relentless support, encouragement, and enthusiasm allowed me to make the transition from a clinical oncologist to a clinician-scientist with joy.
2. I also extend my gratitude to Associate Professor Dai Fukumura, Associate Professor Dan Duda, Assistant Professor Timothy Padera, and Assistant Professor Peigen Huang (Harvard Medical School) for their mentorship, guidance, and support.
3. I also offer thanks to Professor Randall Peterson (Harvard Medical School) who provided the resources and facilities for me to perform the zebrafish experiments.
4. For their technical assistance in the laboratory, I thank Ms Sylvie Roberge, Ms Eve Smith, and Ms Carolyn Smith.
5. For their daily guidance, support, and above all friendship, I thank Dr Nathaniel Kirkpatrick, Dr Walid Kamoun, Dr David Kodack, Dr Eleanor Ager, Dr Yuhui Huang, and Mr John Martin.
6. I thank Ms Nisha Gupta, Ms Shuhan Wang, and Mr John Yazbek – as my students, they have taught me as much about myself as they have about science.

I sincerely thank Dr Jane Beith. As my primary mentor in clinical oncology, her unyielding support, encouragement, friendship, and belief in my potential have provided me the confidence to reach beyond my expectations. I have no doubt that this has had a much more profound impact upon me than I yet realize.

Finally I thank my mother Meera, Aarti, Karim, and Sage. Without you, nothing I have done would be possible.

I dedicate this work, and my career, to my father Dr Ashok Goel.

Appendices

Works published in peer-reviewed journals that are relevant to the content of this thesis are included as the following Appendices:

1. Goel S, Gupta N, Walcott B, Snuderl M, Kirkpatrick ND, Heishi T, Huang YH, Kesler CT, Martin JD, Ager E, Samuel R, Wang S, Yazbek J, Vakoc B, Peterson R, Duda DG, Fukumura D, Jain RK. Tie-2 activation by a vascular-endothelial protein tyrosine phosphatase inhibitor normalizes breast cancer vasculature. **Journal of the National Cancer Institute**. 2013 Aug 21;105(16):1188-201 [PMID: 23899555].
2. Goel S, Duda DG, Xu L, Munn LL, Boucher Y, Fukumura D, Jain RK. Normalization of the vasculature in cancer and other diseases. **Physiological Reviews.** 2011 Jul;91(3):1071-121. [PMID: 21742796]
3. Goel S, Wong AH, Jain RK. Vascular normalization as a therapeutic strategy for malignant and nonmalignant disease. **Cold Spring Harbor Perspectives in Medicine**. 2012 Mar;2(3):a006486. [PMID: 22393532].
4. Goel S, Fukumura D, Jain RK. Normalization of the tumour vasculature through oncogenic inhibition: an emerging paradigm in tumour biology. **Proceedings of the National Academy of Sciences of the United States of America**. 2012 May 1. [PMID: 22550180]
5. Huang Y, Goel S, Duda DG, Fukumura D, Jain R.K. Vascular normalization as an emerging strategy to enhance cancer immunotherapy. **Cancer Research.** 2013 May 15;73(10):2943-8. [PMID 23440326].